ZETA POTENTIAL OF REVERSE OSMOSIS MEMBRANES:

IMPLICATIONS FOR MEMBRANE PERFORMANCE

Water Treatment Technology Program Report No. 10

December 1996

U.S. DEPARTMENT OF THE INTERIOR
Bureau of Reclamation
Denver Office
Technical Service Center
Environmental Resources Team
Water Treatment Engineering and Research Group

REPORT DOCUMENTATION PAGE

Form Approved
OMB No. 0704-0188

1. AGENCY USE ONLY (Leave Blank)	2. REPORT DATE	3. REPORT TYPE AND DATES COVERED
	December 1996	Final

4. TITLE AND SUBTITLE
Zeta Potential of Reverse Osmosis Membranes: Implications for Membrane Performance

5. FUNDING NUMBERS
Contract No.
1425-4-CR-81-19290

6. AUTHOR(S)
Menachem Elimelech and Amy E. Childress

7. PERFORMING ORGANIZATION NAME(S) AND ADDRESS(ES)
Department of Civil and Environmental Engineering
University of California
Los Angeles CA 90024-1593

8. PERFORMING ORGANIZATION REPORT NUMBER
None

9. SPONSORING/MONITORING AGENCY NAME(S) AND ADDRESS(ES)
Bureau of Reclamation
Denver Federal Center
PO Box 25007
Denver CO 80225-0007

10. SPONSORING/MONITORING AGENCY REPORT NUMBER
Water Treatment Technology Program Report No. 10

11. SUPPLEMENTARY NOTES
Hard copy available at the Technical Service Center, Denver, Colorado

12a. DISTRIBUTION/AVAILABILITY STATEMENT
Available from the National Technical Information Service, Operations Division, 5285 Port Royal Road, Springfield, Virginia 22161

12b. DISTRIBUTION CODE

13. ABSTRACT (Maximum 200 words)

The Bureau of Reclamation sponsored this report, which presents data and analysis of the streaming potentials of four different types of membranes measured using an electrokinetic analyzer. Three reverse osmosis membranes and one thin film composite nanofiltration membrane were analyzed. The reverse osmosis membranes consisted of an asymmetric cellulose acetate blend, a fully aromatic polyamide thin-film composite, and a thin film composite with enhanced rejection. Zeta potentials were calculated from the measured streaming potential using the Helmholtz-Smoluchowski equation. Results show that all membranes display an iso-electric point at an acidic pH; the zeta potential is negatively charged at pH values above the iso-electric point and is positively charged at lower pH. Measurements were also made in the presence of divalent ions and humic substances.

14. SUBJECT TERMS	15. NUMBER OF PAGES
-desalination/ membranes/ reverse osmosis/ nanofiltration/ zeta potential/ streaming potential./	71
	16. PRICE CODE

17. SECURITY CLASSIFICATION OF REPORT	18. SECURITY CLASSIFICATION OF THIS PAGE	19. SECURITY CLASSIFICATION OF ABSTRACT	20. LIMITATION OF ABSTRACT
UL	UL	UL	UL

CONTENTS

TABLES

CONTENTS-CONTINUED

FIGURES

ABSTRACT

The streaming potentials of four different types of membranes have been analyzed using an electrokinetic analyzer (BI-EKA, Brookhaven Instruments Corp., Holtsville, New York). Three of the membranes are reverse osmosis membranes, including an asymmetric cellulose acetate blended membrane, a fully aromatic polyamide thin-film composite membrane, and a thin-film composite membrane with enhanced rejection. The fourth membrane is a thin-film composite nanofiltration membrane. The streaming potentials of the membranes were determined over a wide range of pH using test solutions of inorganic salts (sodium chloride, calcium chloride, and sodium sulfate), humic acid, and surfactant.

Prior to the measurements of streaming potential, several steps were taken to ensure maximum repeatability of the measurements. First, templates, spacers, and formers were fabricated so that variations in the location and shape of the flow channel were minimized. Second, tests were performed to determine the maximum variation in the measured value of streaming potential with different samples of the same membrane and with different equilibration times after solution adjustments. Third, based on the equilibration tests, a procedure for preparing the membranes and performing the measurements was developed.

Zeta potentials were calculated from the measured streaming potential using the Helmholtz-Smoluchowski equation. Results show that all membranes display an i.e.p. (iso-electric point) at an acidic pH; the zeta potential is negatively charged at pH values above the i.e.p. and is positively charged at lower pH. In general, the surface charge of the thin-film composite RO membranes becomes more negative with increasing sodium chloride concentrations. This change is attributed to the close approach of co-ions. When calcium chloride is added to the solution, all of the membranes acquire a more positive zeta potential, most likely because of specific adsorption of the divalent cations (Ca^{2+}). On the other hand, when sodium sulfate is added to the solution, the effect of the divalent anion (SO_4^{2-}) is not as noticeable. Results for the experiments with Suwannee River humic acid show that with only a small concentration of hurnic acid in the solution, the membranes become more negatively charged over the entire pH range (3 to 10). The negatively charged functional groups of the humics dominate the surface charge of the membrane. The experiments with (SDS) sodium dodecyl sulfate also resulted in more negative zeta potentials over the entire pH range. This result is attributed to the negatively charged sulfate functional groups of the adsorbed surfactant molecules.

1. INTRODUCTION

Reverse osmosis (RO) membranes were originally developed for the purpose of sea water and brackish water desalination. However, since their development, the applications of RO membranes -have expanded to wastewater and process water reclamation, drinking water treatment, and numerous other areas (Mulder, 1991; Morin, 1994). Currently, the application of RO is being evaluated for the removal of specific drinking water contaminants, such as arsenic (e.g., Waypa et al., 1995). As drinking water regulations become more stringent, more research efforts are being put into RO membrane technologies. These technologies offer solutions to a diverse array of drinking water problems, and these solutions will not become obsolete as regulations become even more stringent.

The major advantage of membrane treatment is the superior quality of the product water. This quality is attained with the addition of fewer chemicals than conventional water treatment processes (Yoo et al., 1995). In addition to requiring fewer chemicals, membrane processes have other advantages. First, membrane plants can be much smaller than conventional water treatment plants (Yoo et al., 1995) because of the modular configuration of membranes and the possible elimination of other processes (e.g., clarification). Second, membrane processes offer decreased operating complexity (Yoo et al., 1995). For example, problems and costs associated with sludge dewatering, handling, and disposal are eliminated.

The major obstacle to further incorporation of membrane processes into water treatment plants is membrane fouling (Potts et al., 1981; American Water Works Association Membrane Technology Research Committee, 1992). Fouling causes a decrease in the water flux across the membrane, an increase in salt passage through the membrane, and affects both the performance and longevity-of membranes.

RO membrane foulants can be broadly classified into four categories (Potts et al., 1981): (1) sparingly soluble salts, (2) biological growth, (3) dissolved organic compounds, and (4) colloidal or particulate matter. Colloids are small suspended particles ranging in size from a few nanometers to a few micrometers. They are ubiquitous in natural waters, and examples of them include clays, metal oxides, and organic particulates (Stumm, 1992; O'Melia, 1980).

Techniques for dealing with the precipitation of salts have been developed and used for many years. Measures for the prevention of biological attack or growth are also being taken. However, dissolved organics, together with colloidal matter, are the most difficult to remove during pretreatment and are considered the most serious foulants (Potts et al., 1981). Zhu and Elimelech (in press) investigated fouling of RO membranes by aluminum oxide colloids in an effort to gain a better understanding of the mechanisms of colloidal fouling. From this work, it was concluded that particle-membrane and particle-retained particle interactions must be considered for a more complete understanding of colloidal fouling.

The first step in evaluating the interaction of colloids and dissolved organics with membranes is to investigate membrane surface charge characteristics. This evaluation can be done by calculating the membrane zeta potential (charge) from streaming potential measurements. The zeta potential is the potential at the *plane of shear* between the surface and solution where relative motion occurs between them. Because the interaction of colloidal particles with membrane surfaces in aqueous media depends on the charge of the membrane surface, determination of the membrane surface zeta potential is critical to membrane fouling research.

The objectives of this research were (1) to develop a methodology to measure zeta potentials of RO and NF membranes by a streaming potential analyzer, (2) to investigate the zeta potential of leading commercial RO and NF membranes at various solution chemistries, (3) to delineate the mechanisms of surface charge acquisition by RO and NF membranes in aqueous solutions, and (4) to evaluate the implications of the results for minimizing colloidal fouling and for optimizing pretreatment of feed waters.

2. CONCLUSIONS AND RECOMMENDATIONS

2.1 NaCl Experiments

1. All the membranes have an i.e.p (iso-electric point); the membrane is positively charged below the i.e.p. and negatively charged above the i.e.p.
2. All the membranes are negatively charged at the typical pH of natural waters.
3. The NaCl concentration does not influence the i.e.p.
4. For some membranes, the zeta potential is more negative at higher NaCl concentration because of the close approach of co-ions.

2.2 $CaCl_2$ and Na_2SO_4 Experiments

1. Divalent cations specifically interact with the membrane and cause the surface charge to be less negative.
2. Divalent anions do not interact substantially with the membrane and thus, essentially, have no effect on surface charge.
3. Adsorption of divalent cations sometimes causes a shift in the i.e.p.

2.3 Humic Acid and Surfactant Experiments

1. Humic acid and surfactant readily adsorb to the surface of polymeric membranes.
2. Low concentrations of humic acid or surfactant can cause the charge of the membranes to become substantially more negative.
3. The membranes are negatively (or non-positively) charged at all pH values in the presence of humic acid or surfactant.

2.4 Surface Charge Acquisition Mechanisms by Membranes in Aqueous Solutions

Thin-Film Composite Membranes

- Negative charge develops because of the carboxyl functional groups of the aromatic ring.
- Positive charge develops most likely because of pendant amino groups.

Cellulose Acetate Membranes

- Negative charge develops because of one or more of the following: (1) remains of hydrolyzed acetic anhydride, (2) dissociation of di-carboxylic organic acid used in post treatment, or (3) adsorption of anions (hydroxyl, chloride)
- Positive charge develops because of impurities or divalent metals used in post treatment.

Further research in zeta potential characterization is necessary to determine a correlation between a membrane's surface charge and its performance. To do this research, the performance of the membrane (flux and rejection) should be analyzed immediately after the streaming potential is measured. Additionally, the zeta potential of fouled membranes needs to be investigated because in real applications, colloids, dissolved organic matter, and other solutes interact with the membrane and alter its surface properties

Results from further research in the area of zeta potential characterization of RO and NF membranes would be useful in efforts to understand and model the interaction of colloidal particles with membrane surfaces in aqueous media. By modeling membrane-colloid interaction, advances can be made in understanding the physico-chemical mechanisms of colloidal fouling. This understanding would eventually lead to a minimization in colloidal fouling of RO and NF membranes.

3. BACKGROUND AND RELATED RESEARCH

3.1 Polymeric Membranes

Two membrane structures are commercially available today: asymmetric and thin-film composite. Asymmetric membranes are made by casting a polymer-containing dope into a homogeneous film by a single-step phase inversion method. The result is a dense surface skin on a porous sublayer. The skin and the sublayer have the same chemical composition. Thin-film composite membranes, on the other hand, are made from a two-step procedure. First, a thick, porous support layer is created, and second, an ultrathin barrier layer is coated on top of the support layer. Unlike asymmetric membranes, the skin and the sublayer usually have different chemical compositions (Petersen, 1993).

The development of asymmetric membranes dates back to the early 1960s when Loeb and Sourirajan, working with a cellulose acetate membrane at U.C.L.A. (University of California at Los Angel&),-noticed that the membrane had a rough side and a smooth side. They found that when the rough side faced the feed, the rejection was low, but when the smooth side faced the feed, the rejection was high. This anisotropic property of the membrane led to the term "asymmetric" membrane (Loeb, 1980).

The concept of composite reverse osmosis membranes is attributed to Francis, who was working under a grant from the Office of Saline Water (U.S. Department of Interior) in 1964. To create the composite membrane, an ultrathin fihn of a polymer was float-casted on a water surface and then laminated to a microporous support. Initially, the asymmetric cellulose acetate membrane of Loeb and Sourirajan was used as the microporous support layer (Petersen, 1993).

The major advantage of thin-film composite membranes is that each layer can be optimized independently. The support layer can be optimized for maximum strength and compression resistance, and the ultrathin barrier layer can be optimized for the desired solvent flux and solute rejection. Thus, thin-film composite membranes generally have higher salt rejection than asymmetric membranes. Other advantages include a much wider feed pH range, less susceptibility to microbiological attack, and better hydraulic stability than asymmetric membranes. Additionally, the skin layer can be formed by numerous chemical compositions (including both linear and cross-linked polymers), whereas for asymmetric membranes, only a few linear polymers can be used. Linear polymers are less desirable than cross-linked polymeric compositions because they exhibit less hydrophilicity and chemical resistance (Petersen, 1993).

These advantages explain why numerous thin-film composite membranes are commercially available today. However, asymmetric membranes also have several advantages which keep them competitive in the commercial market.

The major-advantage of asymmetric membranes is their cost; manufacturing a homogeneous, asymmetric membrane is less expensive than manufacturing a composite membrane. For reverse osmosis applications that do not require the improved performance characteristics of composite membranes, asymmetric membranes are more desirable because they are less expensive (Petersen, 1993). Another advantage of asymmetric cellulose acetate membranes is pointed out by Glater et al. (1981a), Glater et al. (1981b), Glater et al. (1983), and Glater et al. (1994). Whereas cellulose acetate polymers can tolerate fairly high levels of feed water chlorine (and other chemical disinfectants), composite membranes are often very sensitive to chlorine exposure. Even with low levels of chlorine exposure, the performance of most thin-film composite membranes will rapidly deteriorate.

3.2 Electrokinetic Effects

Polymeric membranes acquire a surface charge when brought into contact with an aqueous solution. The surface charge is compensated by counterions in the solution close to the surface, forming the so-called electrical double layer. The distribution of ions at the solid-liquid interface can be described by several models, which are discussed elsewhere (e.g., Shaw, 1969; Westall and Hohl, 1980; Hunter, 1981; Elimelech et al., 1995).

The vital feature of the electric double layer is that the surface charge is balanced by counterions, some of which are located very close to the surface, in the so-called *Stern layer;* the remainder are distributed away from the surface in the *diffuse* layer (fig. 1). An important parameter of the electric double layer is the Stern potential, that is, the potential at the boundary between the Stern and diffuse layers. The Stern potential cannot, however, be measured directly; the electrokinetic (zeta) potential is often considered an adequate substitute. *The zeta* potential *is the* potential at *the plane of shear* between the surface and solution where relative motion occurs between them. Several techniques can be used to determine the zeta potential of surfaces. Among these techniques, the streaming potential technique is most suitable for membrane surfaces.

The relative motion between an electrolyte solution and a charged solid surface can result in one of four electrokinetic effects: (1) electrophoresis, (2) electroosmosis, (3) sedimentation potential, or (4) streaming potential (Shaw, 1969; Hunter, 1981). The induced electrokinetic effect depends on the driving force and the nature of the solid and liquid phases as schematically described on figure 2. Measurements made using techniques based upon each effect should, in principle, result in the same calculated value for the zeta potential. In practical situations, however, several factors conspire to produce dissimilar results. These factors include assumptions in the model for the electric double layer, inadequacies in the theory, and experimental errors related to the design and construction of the apparatus and sample preparation (Shaw, 1969).

The zeta potentials of flat surfaces, such as RO or NF (nanofiltration) membranes, can be measured by either the streaming potential or electroosmosis method. The streaming potential method is preferred over electroosmosis when measuring the zeta potential of flat surfaces because measuring small electrical potentials is more convenient than measuring small rates of liquid flow (Shaw, 1969).

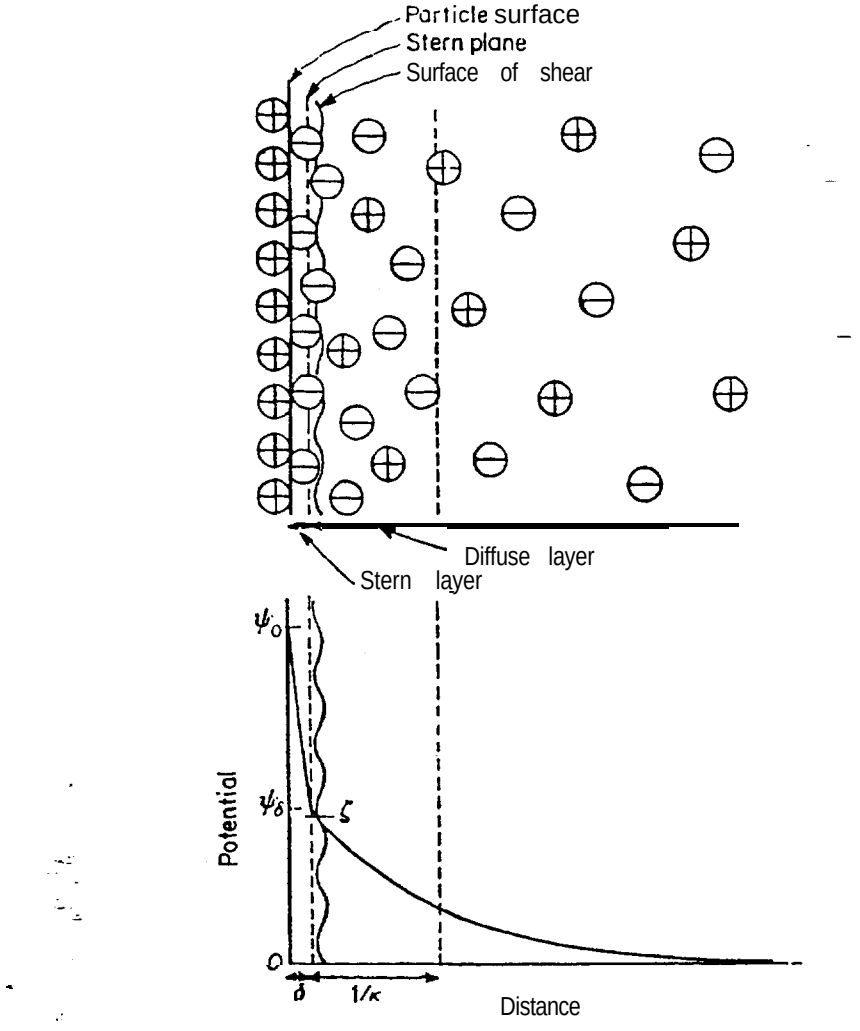

Figure 1. - Electric double layer according to Stern's model (after Shaw, 1969).

3.3 Streaming Potential

Streaming potential is the potential induced when an electrolyte solution flows across a stationary, charged surface. Streaming potential quantifies an electrokinetic effect which reflects the properties of the surface, the flow characteristics, and the chemistry and thermodynamics of the electrolyte solution in the experiment (Shaw, 1969).

A streaming potential is generated when an electrolyte solution is forced, by means of hydraulic pressure, to flow through a porous plug of material, across a channel formed by two plates, or down a capillary. The liquid in the channel carries a net charge. Its flow, caused by hydraulic pressure, gives rise to a streaming current, thereby generating a potential difference (fig. 3). This potential opposes the mechanical transfer of charge, causing back conduction by ion diffusion and electro-osmotic flow (caused by the potential difference). The transfer of charges caused by these two processes is called the leak current (fig. 3). When equilibrium is attained, the streaming current cancels the leak current, and the measured potential difference is the streaming potential (Shaw, 1969; Hunter, 198 1).

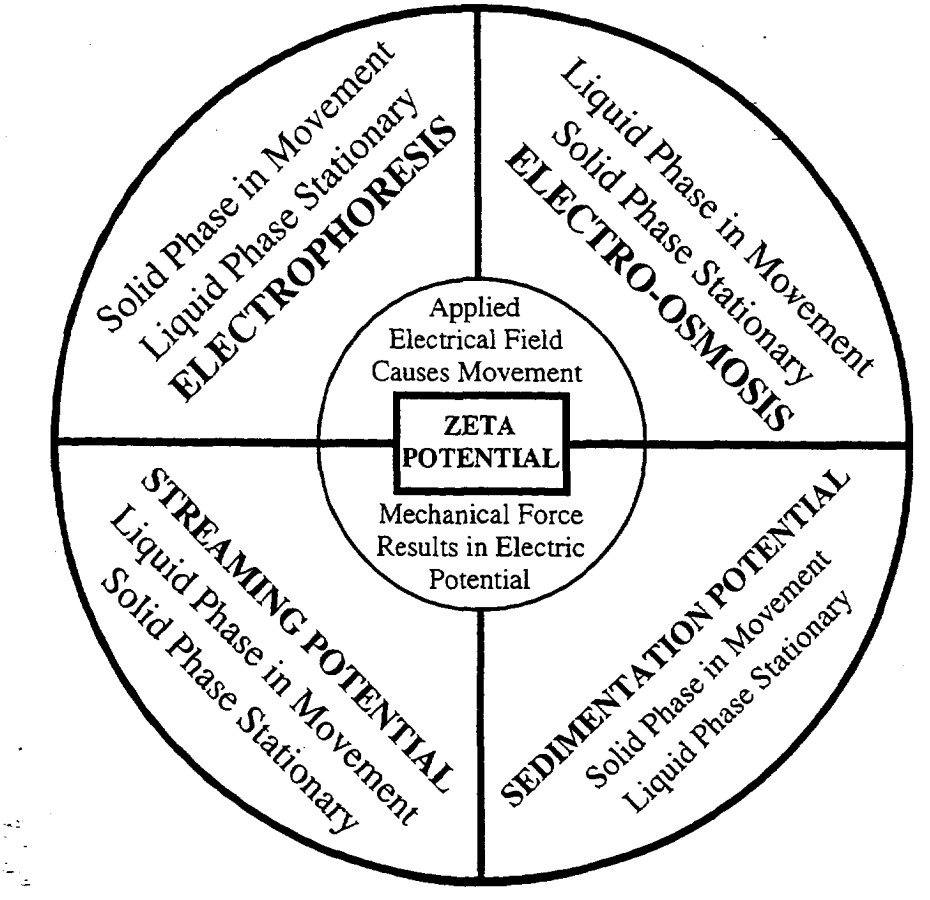

Figure 2. - Illustration of the four electrokinetii effects (after Elimelech et al., 1994).

3.4 Previous Works on Streaming Potential

Several works have been published on measuring the streaming potential of UF (ultrafiltration) membranes (Nyström et al., 1989; 1994; Causerrand et al., 1994). However, for UF membranes, the streaming potential of the pores, not the membrane surface, is being measured. The pore streaming potential is the potential induced when electrolyte flow is through the membrane; surface streaming potential is the induced potential when electrolyte flow is tangential to the membrane. Fewer works have been published on measuring the streaming potential of RO membranes, and of those works, only one (Elimelech et al., 1994) has been published in the last decade. Additionally, this is the only work to perform streaming potential measurements over a range of pH. Investigating the charge as a function of pH is crucial for understanding the acid-base properties of the functional groups on the membrane surface.

Tanny et al. (1971) performed theoretical and experimental studies on streaming potentials of RO membranes. Positive membranes were made of polylysine cross-linked in a collodion matrix, and negative membranes were obtained by succinylation of the positive membrane. A hyperfiltration cell with Ag/AgCl (silver/silver chloride) electrodes was used to measure salt rejection and streaming potential simultaneously at different pressures. Zeta potential was not calculated from the streaming potential measurements.

a. Electric Double Layer at Rest

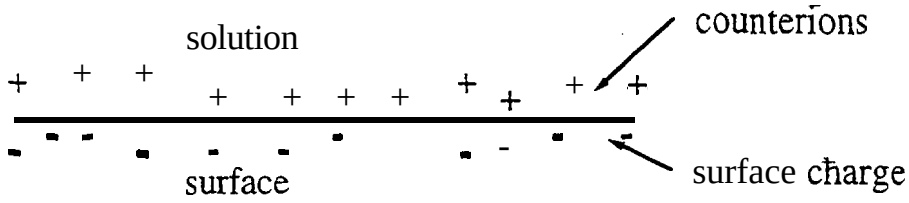

b. Movement of Ions Due to Liquid Flow

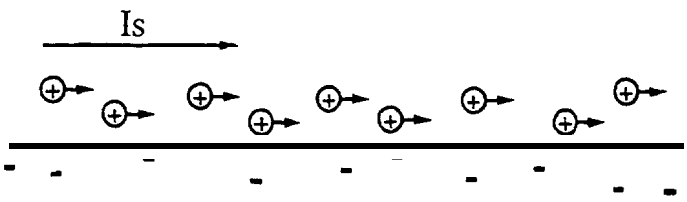

Movement of ions produces a streaming current, Is

c. Accumulation of Ions Downstream

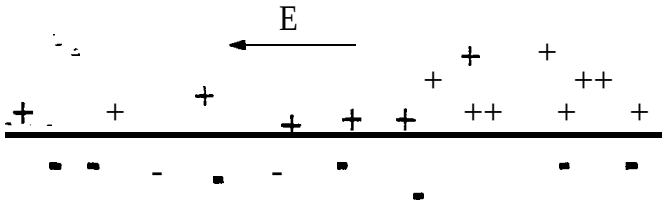

Accumulation causes formation of potential difference, E

d. Leak Current Through Liquid

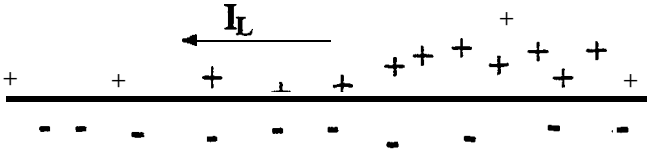

Potential difference, E, causes leak current, I_L

Figure 3. - Schematic of the processes at the solid-liquid interface (after Elimelech et al., 1994).

Kaneko and Yamamoto (1976) studied the streaming potential of regenerated cellulose and Loeb-type cellulose acetate membranes. Gold electrodes were used in the streaming potential cell. The streaming potential was measured as a function of time and feed concentration, but not as a function of pH. The zeta potential was calculated by a variation of the Helmholtz-Smoluchowski equation.

Khedr et al. (1985) measured streaming potentials of cellulose acetate membranes by the fast pulse method, in which several pressure pulses generated by nitrogen gas are applied to the measurement cell. The potential difference across the membrane was measured with Ag/AgCl electrodes. Again, the potential was measured as a function of time and feed concentration, but not of pH. Also, the zeta potential was not calculated. The intention of the authors was to show consistency between these results and results of electroosmosis experiments.

Elimelech et al. (1994) performed preliminary experiments on the feasibility of using the BI-EKA to determine zeta potential of cellulose acetate and thin-film composite membranes. This work was intended not only to demonstrate the use of a novel streaming potential analyzer but also to present a discussion on the origin of surface charge of polymeric surfaces in aqueous solutions as well as basic principles and theory of streaming potential measurements.

3.5 Helmholtz-Smoluchowski Equation

Zeta potential can be derived from the experimentally measured streaming potential. Zeta potential is the potential at the electrokinetic slipping plane between the surface and solution when relative motion occurs between them. The relationship between the measurable streaming potential and the zeta potential is given by the well-known Helmholtz-Smoluchowski equation (Abramson, 1934):

$$\zeta = \frac{U_s}{\Delta P} \frac{\mu}{\epsilon \epsilon_0} \frac{L}{A} \frac{1}{R}$$

where ζ is the zeta potential, U_s is the streaming potential, AP is the pressure difference across the channel, μ is the viscosity of the solution, ϵ is the permittivity of the solution, ϵ_0 is the permittivity of free space, and L, A, and R are the length, cross-sectional area, and electrical resistance of the channel, respectively. Several assumptions are inherent in this equation (Oldham et al., 1963; Christoforou et al., 1985; Cohen and Radke, 1991):

1. Flow is laminar.
2. Surface conductivity has no effect.
3. Width of the flow channel is much larger than the thickness of the electric double layer.
4. Capillary geometry or parallel plates geometry exists.
5. No axial concentration gradient occurs in the flow channel.
6. The surface has homogeneous properties.

3.6 Surface Conductivity

The second assumption above refers to the concept of surface conductivity. The Helmholtz-Smoluchowski equation is valid only if all or almost all of the current is transported by the bulk liquid. However, a significant proportion of current is often transported by layers near the surface or through the solid. This transport leads to an accumulation of charge in the double layer, which may in turn lead to unusually high conductivity, especially at low salt concentrations (Hunter, 1981). Surface

conductance depends on, among other variables, electrolyte concentration (Jacobasch et al., 1985). Hunter (198 1) asserts that surface conductivity causes a maximum in the absolute value of the apparent zeta potential at a concentration of about 10" M, because below this concentration, surface conductivity becomes increasingly important. Surface conductance adds greatly to the back flow of current and so reduces the'magnitude of the streaming potential which can accumulate.

3.7 Maximum in Electrokinetic Potential Curves

Electrokinetic potential curves of certain surfaces are found to pass through a maximum as a function of increasing ionic strength. This behavior is not explained by current double layer models, which predict a continuous decrease in potential with increasing ionic strength. Several explanations have been proposed to account for this anomalous behavior. These explanations include the close approach of co-ions, hairy layer effects, artifacts in measuring streaming currents and electrical conductance, and not accounting for surface conductance.

Close Approach of Co-Ions

Dunstan and Saville (1992) differentiate between specific adsorption and preferential solubility of ions in the interfacial region. Because specific adsorption is thermodynamically unfavorable, the effective surface charge and observed electrophoretic mobilities are postulated to arise from preferential solubility of ions in the interfacial region. Dunstan (1992) suggests that the mobility maximum occurs because of the interplay between preferential solubility and retardation effects. First, an increase in the concentration of KCl (potassium chloride) leads to an increase in the number of Cl^- ions preferentially solubilized in the interfacial region. This increase results in an increase in (negative) electrophoretic mobility with an increase in KC1 concentration. At the same time, the preferential solubility of the Cl- ions also gives-rise to strong electrophoretic retardation effects. At higher electrolyte concentrations, the range of the solubility region is decreased such that the retardation effects dominate and the mobility goes through a maxima (Dunstan, 1992).

Elimelech and O'Melia (1990) investigated the effect of various types and concentrations of counterions and co-ions on the electrophoretic mobility of negatively charged polystyrene latex particles, The investigation suggests that three competing processes are involved in determining the shape of the electrophoretic mobility curve in the presence of inorganic salts:

1. Neutralization of negative charge on the surface by adsorption of counterions causing a marked decrease in the electrokinetic potential (less negative).
2. Approach of co-ions close to the hydrophobic surface of the particles, causing a marked increase in the electrokinetic potential (more negative).
3 Compression of the diffuse double layer attributable to high bulk concentration of electrolyte, causing a decrease in electrokinetic potential (less negative).

The extent to which each process occurs at the interface determines the shape of the electrokinetic potential curve as a function of electrolyte solution.

Jacobasch and Schurz (1988) studied the relationship between maximum zeta potential and contact angle for several polymers in KC1 solution. They found that a linear relationship exists between maximum zeta potential and contact angle. The most hydrophobic polymer had the greatest maximum zeta potential, and vice versa. Thus, the close approach of co-ions theory holds best for hydrophobic surfaces.

Hairy Layer Effects

Another explanation for the maximum in electrokinetic potential curves is referred to as hairy layer effects. This explanation assumes that the surface of polymer lattices is comprised of polyelectrolyte chains carrying the surface charge. This layer expands as ionic strength decreases (because of repulsion between functional groups) and contracts as ionic strength increases (Goosens and Zembrod, 1979; van der Put and Bijsterbosch, 1983; van den Hoven and Bijsterbosch, 1987; Bonekamp et al., 1987). Expansion and contraction move the shear plane and affect electrokinetic potential. Although hairy layer model qualitatively explains the mobility behavior of 1: 1 electrolytes, it fails to explain both the mobility behavior of polyvalent counterions and co-ions and the normal decrease in mobility with salt concentration in hydrophilic lattices with high surface charge. These lattices have a significant hairy layer (Elimelech and O'Melia, 1990). Dunstan and Saville (1992) assert that because a mobility maximum is observed for particles that do not have polymeric hairs distending from the surface, surface hairiness may not cause the maximum in mobility observed for polystyrene lattices.

Artifacts in Measuring Streaming Current and Electrical Conductance

Streaming potential values obtained with non-reversible electrodes, or by applying d-c (direct- current) rather than a-c (alternating current) conductance, show a maximum in dependence on ionic strength (van der Linde and Bijsterbosch, 1990). Therefore, by using reversible electrodes and applying a.c. conductance, these experimental artifacts can be avoided and no maximum in electrokinetic potential curves will occur. However, Börner et al. (1994), using reversible electrodes and applying a.c. conductance still found a maximum in the potential curves. Börner et al. (1994) suggest that the pH of the electrolyte solution (which is often not quoted in the literature) plays an important role in the shape of the electrokinetic potential curves. At pH 5.0, for example, competition between electrolyte anions and hydroxyl ions would cause enough extra adsorption of the electrolyte ions to produce a maximum in the electrokinetic plot. At pH 6.5 or 7.0, though, less competition would occur, no extra adsorption of anions would occur, and hence, no maximum in the zeta potential plot would occur. Therefore, the authors who report a maximum in electrokinetic potential may have performed their experiments around a pH of 5.0, and those who report no maximum may have carried out measurements around a pH of 6.5.

Not Accounting for Surface Conductance

As mentioned-earlier, not accounting for surface conductance has been suggested as a possible partial cause for the maximum in electrokinetic potential curves. When surface conductance is considered, the electrokinetic potential appears to be a smooth function of ionic strength (van der Linde and Bijsterbosch, 1990). Midmore and Hunter (1988) also show that if surface conductivity is properly accounted for, the maximum in mobility does not imply a maximum in zeta potential. Dunstan (1993) suggests that although surface conductance may explain certain aspects of the anomalous behavior, it is not a comprehensive description.

4. EXPERIMENTAL METHODS

4.1 Streaming Potential Analyzer

A novel streaming potential analyzer (BI-EKA, Brookhaven Instruments Corp., Holtsville, New York) has been acquired for use in this research (fig. 4). This instrument includes an analyzer, a data control system, and a measuring cell. The analyzer consists of a mechanical drive unit to produce and measure the pressure that drives the electrolyte solution from a reservoir into and through the measuring cell. Operation can be controlled manually or by computer. The streaming potential and the streaming current are measured simultaneously by the instrument. Sensors for measuring the temperature and conductivity are located internally, and pH is measured externally. The test solution circulation path is shown on figure 5.

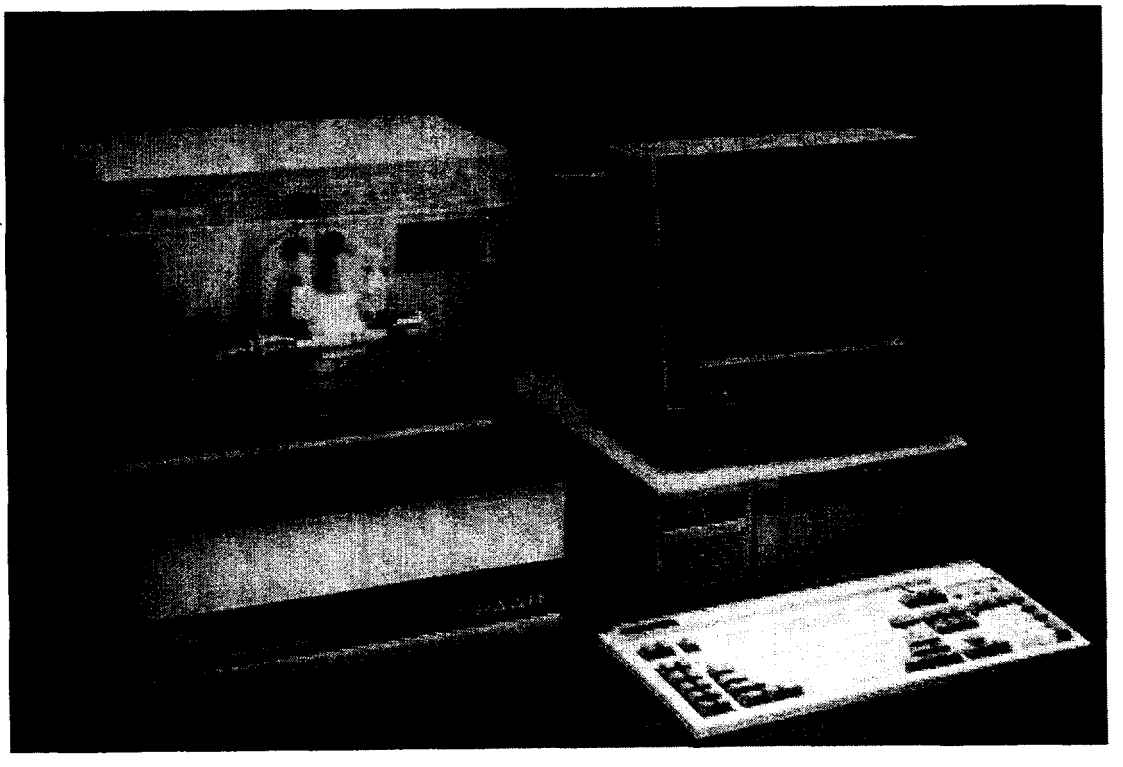

Figure 4. - Electra-kinetic analyzer.

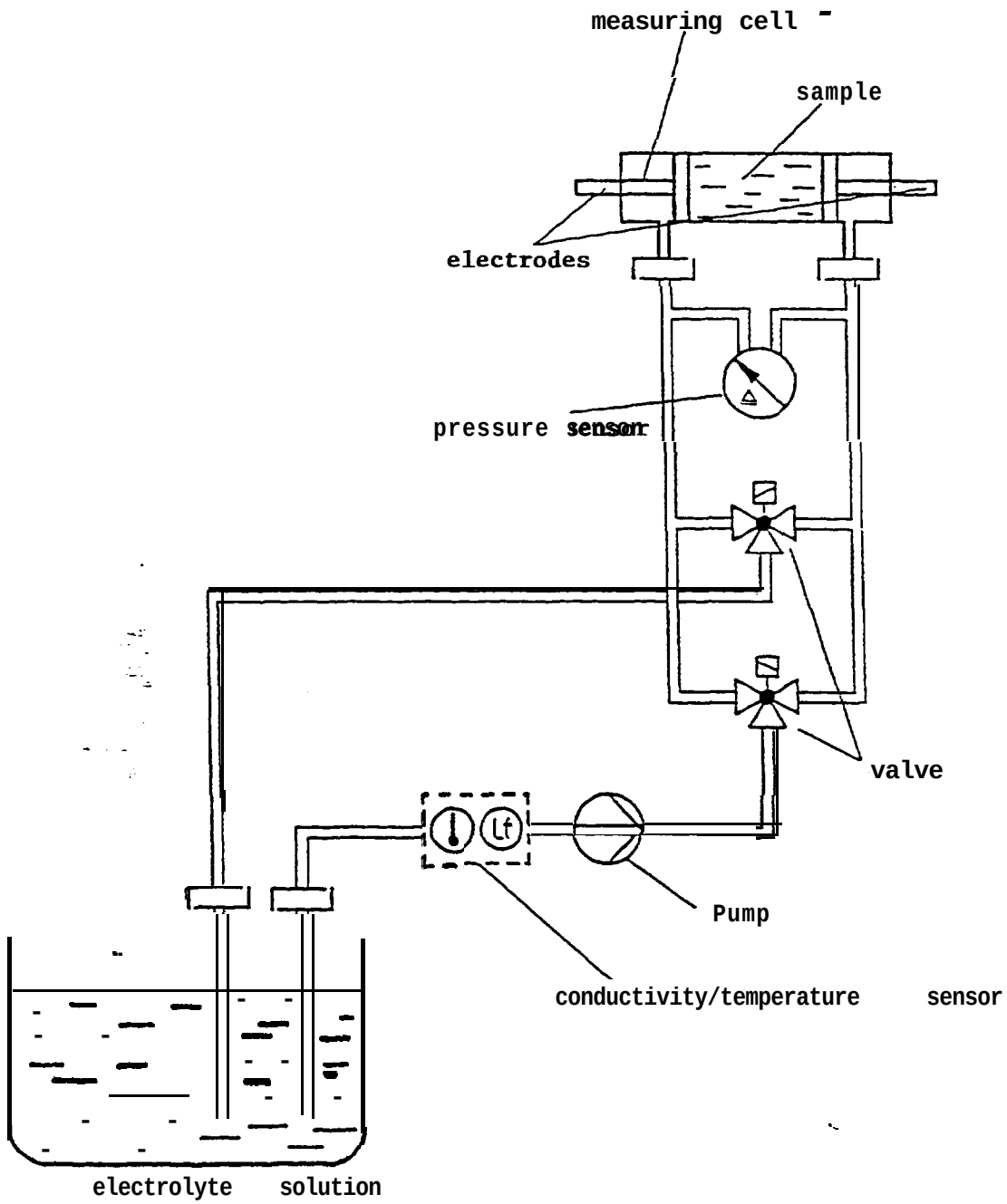

Figure 5. - Test solution circulation path.

The measuring cell that is used in this research is made of PMMA (polymethylmethacrylyte) and has dimensions of 125 by 50 mm (fig. 6). Two pieces of membrane are used for each measurement. One piece, with its active layer facing down, is attached to the upper part of the cell, and the other piece, with its active layer facing up, is attached to the lower part of the cell. A channel with dimensions of 85 by 10 mm is created by the use of PTFE (polytetrafluoroethylene) spacers. The number of spacers used depends on the amount of membrane swelling. As few spacers as possible should be used because-closer plates result in higher sensitivity. Also, too many spacers result in hydrodynamic limitations; in other words, the pump is not able to create the desired pressure drop. However, if too few spacers are used and the channel is not wide enough, laminar flow may not be maintained. Also, if the membrane samples are too close, surface effects may become dominant.

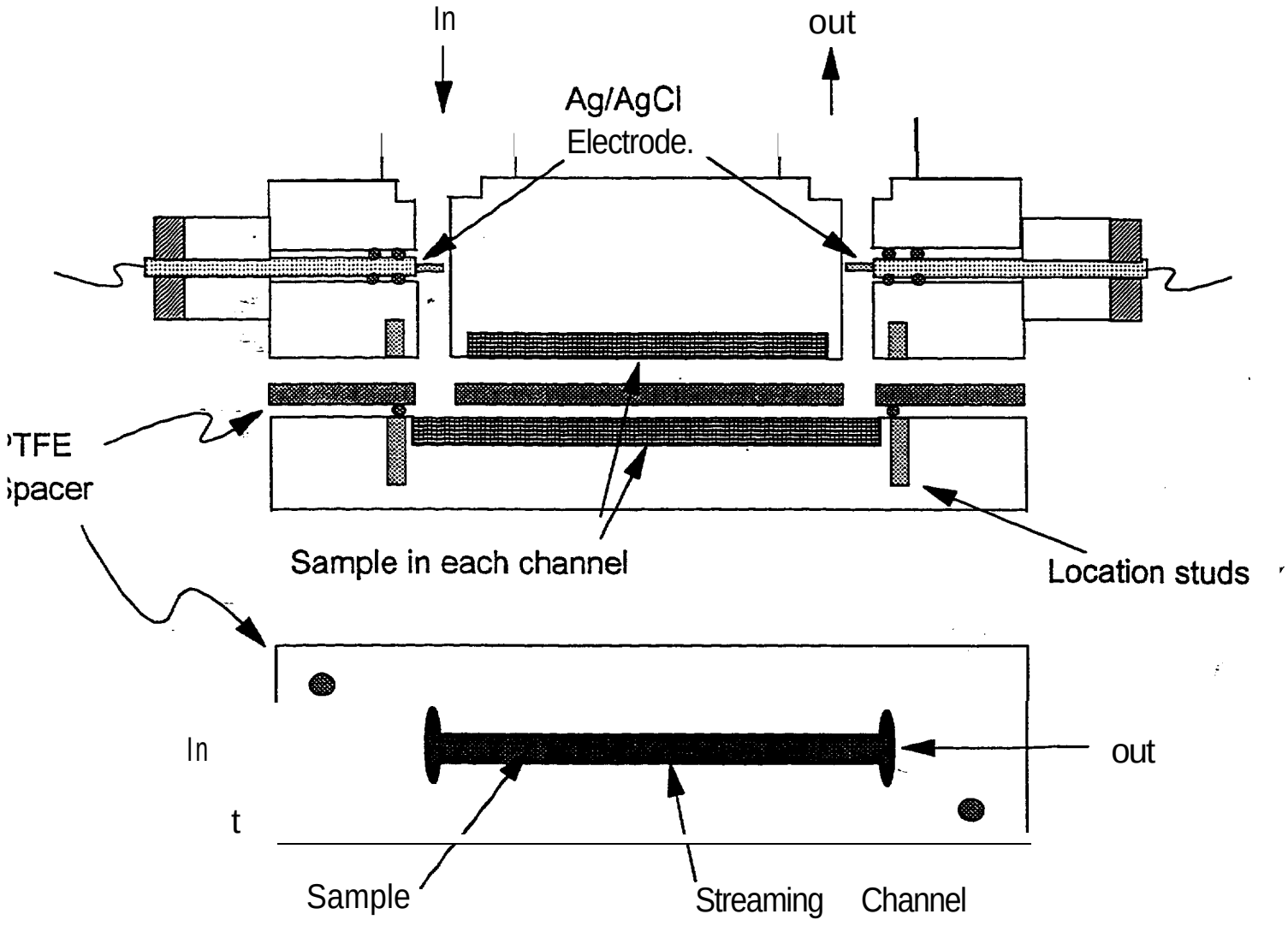

Figure 6. - Schematic of measuring ceil.

The Ag/AgCl electrodes that measure induced streaming potential are mounted at each end of the channel. These electrodes are not non-reactive and therefore may become polarized during the experiments. To prevent polarization, the direction of flow through the cell alternates for each run. Additionally, Brookhaven Instruments Corp. recommends storing the electrodes in 0.1-M HCl (hydrochloric acid) solution overnight to prevent excess charge build up on them.

The maximum pumping pressure depends on the type of membrane and the number of spacers used. In general, pumping as high a pressure as possible is desirable to give maximum points on the slope of potential versus pressure. The zeta potentials are calculated from the potential versus pressure curve using the Helmholtz-Smoluchowski equation.

Calculating Zeta Potential

Recalling the Helmholtz-Smoluchowski equation:

$$\zeta = \frac{U_s}{\mathbf{AP}} \frac{\mu}{\epsilon\epsilon_0} \frac{L}{A} \frac{1}{R} \qquad (1)$$

where: ζ is zeta potential
U_s is streaming potential
AP is pressure difference across channel
μ is viscosity of solution
ϵ ispermittivity of test solution
ϵ_0 is permittivity of free space
L is length of channel
A is-cross-sectional area of channel
R is resistance of channel

The ratio $U_s/\Delta P$, as mentioned above, is the slope of the potential versus pressure plot (fig. 7). The ratio L/A is determined using the Fairbrother and Mastin approach (described below). The resistance of the channel, R, can be calculated directly from the ratio of streaming potential to streaming current.

Using the Fairbrother and Mastin approach (Fairbrother and Mastin, 1924) for solutions with low surface conductivity (i.e., electrolyte concentration > about 10^{-3} M):

$$\frac{L}{A} = \kappa R \qquad (2)$$

Equation (1) becomes:

$$\zeta = \frac{U_s}{\Delta P} \frac{\mu}{\epsilon\epsilon_0} \kappa \qquad (3)$$

where κ is solution conductivity.

For solutions with high surface conductivity (i.e., electrolyte concentration < 1 0^{-3} M), the influence of surface conductivity has to be suppressed to determine L/A. This suppression is accomplished by replacing the electrolyte solution (after its streaming potential has been measured) with 0.1 -M KCl solution and performing a second measurement of streaming potential. Using the Fairbrother and Mastin approach:

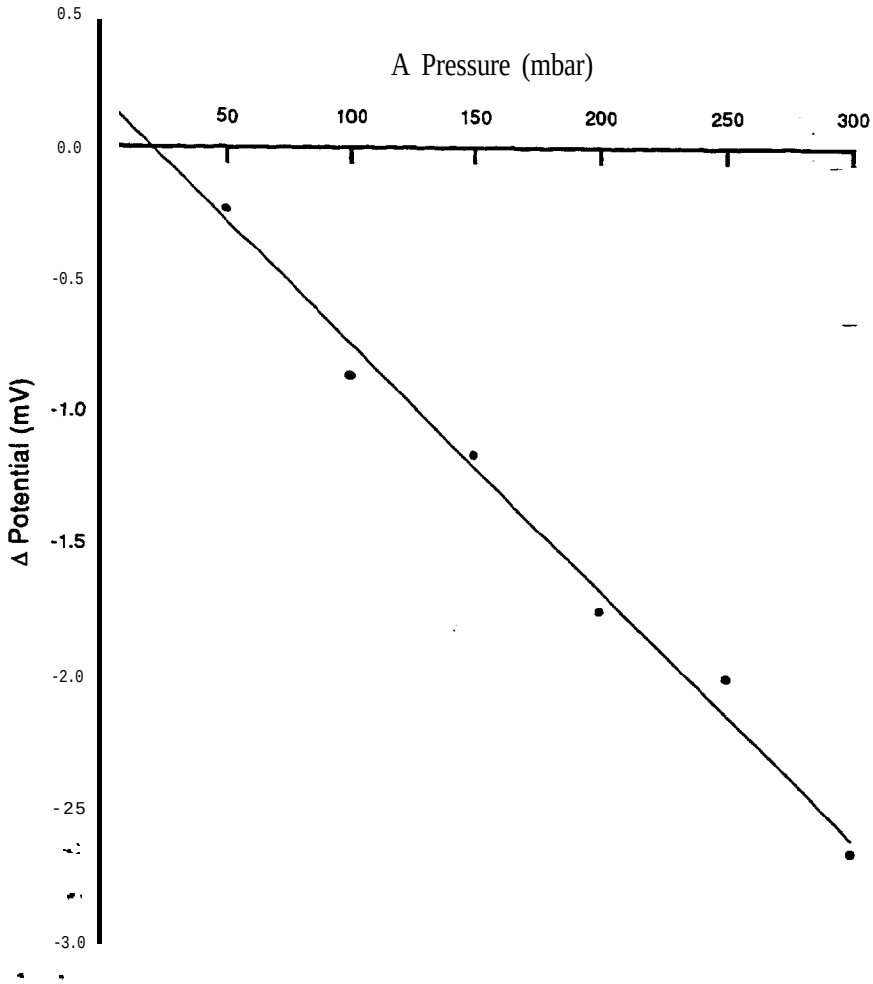

Figure 7. - Example of potential versus pressure plot.

$$\frac{L}{A} = \kappa_{KCl} R_{KCl} \tag{4}$$

equation (1) becomes:

$$\zeta = \frac{U_s}{\Delta P} \frac{\mu}{\epsilon \epsilon_0} \kappa_{KCl} R_{KCl} \frac{1}{R} \tag{5}$$

where: κ_{KCl} is conductivity of 0.1 -M KCl solution
R_{KCl} is resistance of channel when filled with KCl solution

Following the same reasoning, the equations for streaming current are:

$$\zeta = \frac{I_s}{\Delta P} \frac{\mu}{\epsilon \epsilon_0} \kappa R \tag{6}$$

and:

$$\zeta = \frac{I_s}{\Delta P}\frac{\mu}{\epsilon\epsilon_0}\kappa_{KCl}R_{KCl} \qquad (7)$$

for low and high surface conductivity, respectively.

4.2 Representative Membranes

Three different RO membranes and one NF membrane have been acquired for the investigation. A fully aromatic polyamide thin-film composite membrane and a thin-film composite membrane with enhanced rejection have been obtained from Fluid Systems Corporation (San Diego, CA), an asymmetric cellulose acetate membrane was obtained from Desalination Systems (San Diego, CA), and a thin-film composite nanofiltration membrane was obtained from FilmTec (Minneapolis, MN). Pertinent information on these membranes is summarized below.

Thin-Film Composite RO Membrane

The TFCL-LP is a low pressure reverse osmosis membrane. According to the manufacturer, the allowable operating pH range is between 4 and 11, and the allowable feedwater temperature range is between 1 and 45 °C (34 and 113 "F). The maximum operating pressure is 350 lb/in*. The manufacturer also claims that this membrane can tolerate 1000 p/m-hr exposure to free chlorine. The nominal water flux is reported to be between 28 and 34 GFD (gallons per square foot per day) and the minimum salt rejection is 98.5 percent. These performance data are determined with 2000-p/m NaCl (sodium chloride) solution at 220 lb/in*, 25 °C (77 "F), and pH 7.5.

The TFCL-LP membrane is produced by the inter-facial polymerization reaction of aromatic diamines in the aqueous phase with triacyl chlorides in the solvent phase (Cadotte, 1985). Data comparing this membrane to the FilmTec FT-30 have led to speculation that these membranes consist of essentially the same chemistry", both are essentially the reaction product of 1,3-benzenediamine with trimesoyl chloride (Petersen, 1993). The likely structure of this membrane is shown on figure 8. In addition to the linear chain formation, reactions of diamines with triacyl chlorides can also lead to two types of side reactions. These reactions are either hydrolysis of one of the chloride groups of trimesoyl chloride to carboxylic acid or reaction of the chloride groups with another diamine molecule to produce cross-linking.

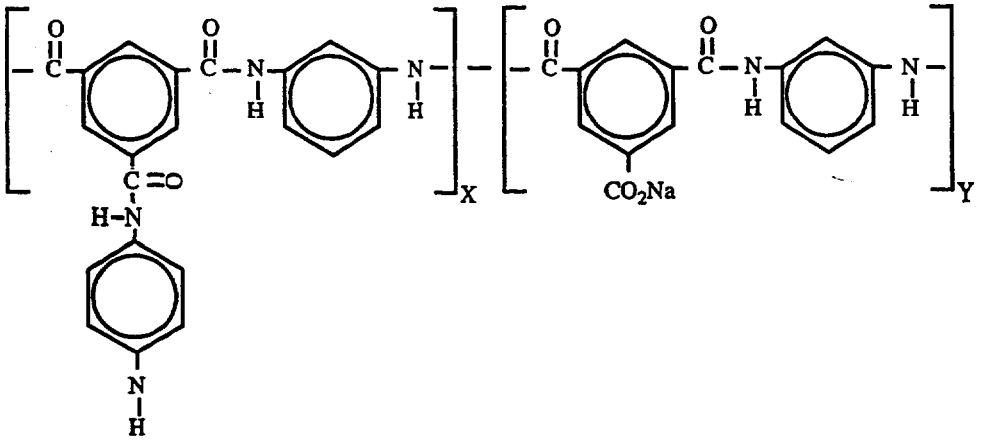

Figure 8. ▪ Cross-linked aromatic polyamide membrane.

During interfacial polymerization of fully aromatic polyamide membranes, "impurities" may be added to the aqueous solution above the microporous support in order to improve the membrane performance. For example, a monomeric amine salt (Tomaschke, 1990) or anionic surfactant (e.g., sodium dodecyl benzyl sulfate or sodium lauryl sulfate) may be added to the aqueous solution (Elimelech et al., 1994). Also, an organic acid with carboxyl functional groups (e.g., acetic acid) may be added to the aqueous solution to adjust the pH (Elimelech et al., 1994). Such additives, however, are proprietary, and no information regarding the membranes used in this research have been disclosed.

Thin-Film Composite RO Membrane with Enhanced Rejection

This thin-film composite membrane is believed to have basically the same chemical composition as the TFCL-LP except for the addition of proprietary additives in its active layer, which results in higher rejection of solutes. The allowable operating ranges are similar to the above thin-film composite membrane. The nominal water flux is between 20 and 26 GFD, and the nominal salt rejection is 99.5 percent for 2000-p/m NaCl at 200 lb/in², 25 °C (77 "F), and pH 7.5.

Cellulose Acetate RO Membrane

This membrane (denoted CE by the manufacturer) is an asymmetric cellulose acetate membrane acquired from Desalination Systems (San Diego, CA). The manufacturer reports that the allowable operating pH range is between 5 and 6.5, and the maximum temperature is 35°C (95 "F). The typical operating pressure range is 140 to 400 lb/in², and the maximum operating pressure is 450 lb/in². The nominal water flux is about 26 to 27 GFD and the nominal salt rejection is 97 to 98.5 percent for 2000-p/m NaCl at 400 lb/in² and 25°C (77 "F).

The structure of this membrane is shown on figure 9. The cellulose acetate polymer backbone consists of gluco-pyranose rings connected by β-glycoside (ether linkages) (Kesting, 1985). The cellulose acetate acquired from Eastman Kodak is very pure. The cellulose powder is first completely acetylated to form tri-acetate. Then the hydroxyl groups of the cellulose acetate are partially hydrolized with sodium hydroxide to achieve various levels of acetylation (Kesting, 1985).

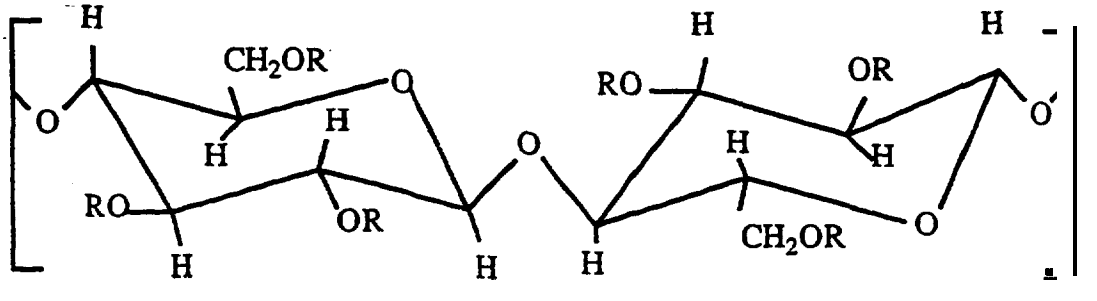

Figure 9 • Cellulose acetate blended membrane.

As with the TFCL-LP membrane, various chemicals are often used in the production of a cellulose acetate membrane to improve performance. According to the manufacturer, various glycols or alcohols may be used in producing the membrane, and formamide may serve as a swelling agent. Though these chemicals are not part of the actual cellulose polymer structure, as "impurities" they may be attached to the membrane and therefore affect the surface properties of the membrane (Elimelech et al., 1994).

Nanofiltration Membrane

The nanofiltration membrane (NF-70) acquired from FilmTec (San Diego, CA) is a thin-film composite membrane with a flux rate of 25 GFD at 70 lb/in^2 net driving pressure. It has a maximum operating pressure of 250 lb/in^2 and a maximum operating temperature of 35 °C (95 "F). The allowable pH operating range is from 3 to 9. The nominal salt rejection is 60 percent for 2000-p/m NaCl at 70 lb/in^2, 25 °C (77 "F), and pH 7.0.

The actual composition of this membrane (other than that it is an aromatic polyamide) has not been disclosed. Petersen (1993) mentions that examination of FilmTec patent literature shows a patent in which a membrane having an interfacially formed, cross-linked, aromatic polyamide barrier layer was treated with a combination of hot phosphoric acid and tannic acid. The result was a modified membrane with a greatly increased water flux and reduced salt rejection. The NF-70 membrane may have been created by this patented membrane preparation procedure.

4.3 Membrane Storage

The above thin-film composite membranes (TFCL-LP, TFCL-I-R, and NF-70) are stored in 0.75-percent $Na_2S_2O_5$ (sodium meta-bisulfite) and are kept in a refrigerator at about 5 °C (41 "F). This storage procedure follows the recommendations in *The Desalting and Water Treatment Membrane Manual: A Guide to Membranesfor Municipal Water Treatment* (Chapman-Wilbert, 1993) and was also agreed on by the manufacturer. The cellulose acetate membrane is unique from the other membranes because of the manner in which it is stored. Unlike the other membranes which are stored wet, this membrane (which is supplied as a dry, rolled sheet) is stored as received at room temperature. The manufacturer suggests that the CE membrane be dipped in alcohol for a few seconds prior to use to remove preservatives. Therefore, after the membrane samples are cut from the sheet, they are dipped in 65-percent methanol. Following that step, the membranes are rinsed in DI (deionized) water and left overnight (about 16 hours) in a covered beaker containing DI water.

4.4 Fabrication of Templates, Formers, and Spacers

The measuring cell is composed of seven layers (fig. 10). The outermost layers are called formers. The formers are recommended to be made of PTFE, but the original ones sent by Brookhaven Instruments Corp. were made of an unknown plastic material. Next to the formers is Parafilm, which serves to minimize leakage from the cell. Next to the Parafilm are the membrane samples which are separated by spacers (generally, three are used). The original spacers sent by Brookhaven Instruments Corp. were not cut uniformly and were of different thicknesses. New formers and spacers were made to avoid any problems associated with using the original formers and spacers. Also, a template was made because accurate cutting of the membranes and Parafilm by freehand was difficult. The metal template was made out of 304 stainless steel. A second template was made to cut three spacers out of 0.001-inch-thick PTFE. Additionally, two formers were made out of 0.062-inch-thick PTFE.

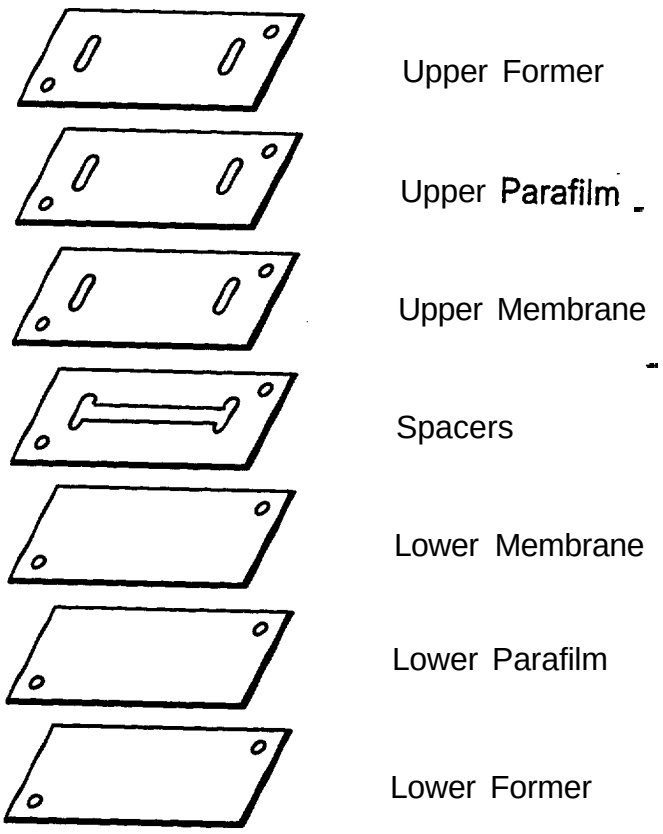

Figure 10. - Seven layers of measuring cell.

4.5 Reproducibility and Equilibration Experiments

A set of experiments was run to determine the variability in streaming potential results when two different samples of the same membrane are used: Eight of the nine measurements for the two different samples varied by less than 1 mV (about 10 percent) and the other measurement varied by less than 2 mV (about 20 percent). Additionally, the experiments revealed that only new membrane samples should be used each day. In other words, results varied by more than 2 mV when a membrane sample was used (with a 0.01-M NaCl solution), stored overnight in the measuring cell, and then used again the next day (with 0.01-M NaCl solution).

Salt Experiments

A set of experiments was run to determine the time needed for equilibration with the salt solution. The experiment revealed that a 30-minute equilibration period was necessary. At 30 minutes and beyond, the streaming potential value fluctuated minimally. Another set of experiments to determine the amount of equilibration time for pH adjustments determined that 10 minutes of equilibration time was necessary after pH adjustments are made.

Humic Acid Experiments

A set of experiments was performed to determine the time needed for the membrane to equilibrate with the humic acid solution. The humic acid appeared to adsorb instantaneously to the membrane surface. However, to ensure that complete equilibration occurred, the

membrane was flushed for 20 minutes with the humic acid solution before any measurements were taken. As with the inorganic salt experiments, only 10 minutes of equilibration time are necessary between pH changes.

Surfactant Experiments

The same equilibration times used in the humic acid experiments were found to be adequate for the surfactant experiments.

4.6 Measurement Procedure

Before any runs were performed, the inlet and outlet Tygon tubing was replaced and the internal conductivity meter was calibrated. Subsequently, the tubing was replaced and the conductivity was calibrated between sets of experiments (e.g., between salts and humics, between humics and surfactants).

Electrode Plating

Prior to any measurements being taken and intermittently throughout the experiments, the Ag/AgCl electrodes were replated. Replating was necessary if "spots" of Ag were visible on the electrode surface. These spots indicated that AgCl had worn away and that an even AgCl coating no longer existed over the entire electrode surface. Additionally, replating was performed when the asymmetry potentials were high or the standard deviation in the measured streaming potential was consistently high.

Before the electrodes could be replated, the old AgCl coating had to be removed. The basic procedure for removing the old coating was given by Brookhaven Instruments Corp., but was implemented with additional steps as necessary. First, the electrodes were dipped in a vial of concentrated ammonium hydroxide in an ultrasonic bath. Second, extra fine sand paper was used to rub the surface of the electrodes. Third, the electrodes were dipped again in the ammonium hydroxide. And finally, the electrodes were rinsed with DI water. Also, the electrodes were dipped in concentrated nitric acid to see if any organics were on the electrode surface.

The electrodes were replated by an electrolytic deposition process given by the following equation:

$$Ag^{+}(s)+Cl^{-}(aq) \rightarrow AgCl(s)+e^{-} \qquad (8)$$

The Ag electrode was used as the anode and an Au (gold) electrode was used as the cathode. Both electrodes were attached to connectors in the side of the ERA and were placed in a beaker of 0.1-M HCl. The HCl solution was stirred throughout the entire deposition process, which lasts about 3 to 5 minutes. After the first Ag electrode was replated, the second Ag electrode was replated for exactly the same length of time. After both electrodes were replated, they were rinsed with DI water and placed in 0.1-M HCl for 24 hours before being used. This process minimized any asymmetry potential resulting from the plating process. Again, the basic procedure for replating the electrodes was given by Brookhaven Instruments Corp. and was augmented as necessary.

Preparation of Membranes

Two 2 by 5 membrane samples were cut from the membrane sheet (which was stored as previously mentioned). Using the template, the necessary holes and channels were cut into the samples. The membranes were then rinsed with DI water and put into a beaker containing the first electrolyte solution to be tested. Next, the Parafilm was cut in the same manner as the membranes. After the membranes soaked in the solution for about 20 minutes, the membranes, Parafilm, formers, and spacers were assembled in the measuring cell.

Rinsing the Cell

The cell was then flushed for about 3 minutes with DI water, after which it was flushed with the test solution for long enough to displace all the DI water in the system. The test solution was then recirculated through the cell for 30 minutes (20 minutes for humic acid and surfactant runs). The pH meter was calibrated with pH 4 and pH 10 buffers and checked with pH 7 buffer. The pH was then adjusted with HCl and the solution was recirculated for 10 minutes before the first measurement (at pH 2 or 3) was made. Subsequently, the pH was adjusted with NaOH (sodium hydroxide), and the same procedure was followed until the last measurement was made (at pH 9 or 10). At the end of the run, the system was flushed again for about 3 minutes with DI water.

Measuremen ts

Eight runs were performed (four in each direction) for each pH. The first two runs were automatically dropped, and the remaining six (three in each direction) were averaged to calculate the zeta potential at each pH. Also, if one stray value occurred within the six runs, that value was dropped and the zeta potential was calculated from the average of the remaining runs.

4.7 Solution -Chemistry

pH

Keeping the ionic strength constant, the pH was varied from 3 to 9 or from 4 to 10 depending on the i.e.p. of the membrane. In all cases, the pH did not exceed 10 because above pH 10, the danger of stripping the Ag/AgCl electrodes exists. The pH was adjusted using HCl and NaOH (certified grade).

Inorganic Electrolytes

Sodium chloride, $CaCl_2$ (calcium chloride), and Na_2SO_4 (sodium sulfate) salts (certified A.C.S. grade) were used. The effects of $CaCl_2$ and Na_2SO_4 were both evaluated in the presence of NaCl. The concentrations of $CaCl_2$ and Na_2SO_4 were selected because they were typical‘of concentrations found in natural waters. The world average river concentrations of Na, Ca, Cl, and SO, are shown in table 1.

Table 1. - Model freshwater composition (from Bemer and Bemer [19871).

Constituent	World Average River (Mg/L)	World Average River (mol/L)
SiO_2 (silica)	10.4	1.7×10^{-4}
Ca (calcium)	14.7	3.7×10^{-4}
Mg (magnesium)	3.7	1.5×10^{-4}
Na (sodium)	6.2	2.7×10^{-4}
K (potassium)	1.4	3.6×10^{-4}
CO, (carbonate)		
HCO, (bicarbonate)	53.0	8.7×10^{-4}
SO, (sulfate)	11.5	1.2×10^{-4}
Cl (chloride)	8.3	2.3×10^{-4}
NO, (nitrate)		
F (fluoride)		
B (boron)		
Br (bromide)		
PO, (phosphate)	0.077	8.0×10^{-7}

Humic Substances

About 100 mg of Suwannee River Humic Acid Reference (Code: 1R101H) was received in solid (powder) form (IHSS [International Humic Substances Society], Golden, CO). The humic acid powder was dissolved in DI water; pH was measured to be 3.3. Sodium hydroxide was then added to the humic acid solution to make the pH more basic (about 7.5). (At an acidic pH, humic acid will precipitate out of solution; whereas at a basic pH, humic acid will dissolve more completely.) The resulting humic acid stock solution had a concentration of 0.47 g/L. The solution was stored in an HDPE (high density polyethylene) plastic bottle, which was wrapped in foil and kept at about 5°C (41 "F).

Two concentrations of Suwannee River Humic Acid were tested for each membrane. For the TFCL-LP membrane, 1-mg/L and 10-mg/L test solutions were evaluated. These concentrations were selected because the typical concentration of dissolved organic matter in groundwater and rainwater is 1 mg of C (carbon) per liter of DOC (dissolved organic carbon); in lakes, 2 to 10 mg of C per liter; in rivers, 10 to 50 mg of C per liter; and in oceans, anywhere from 1 mg of C per liter (in deep waters) to 10 mg of C per liter (in surface waters). Humic acids are the fraction of DOC that precipitates at very low pH and usually make up about 10 percent of the organic compounds in seawater (Morel and Hering, 1993). It should be noted that the above concentrations of DOC are given in milligrams of C per liter. Assuming that 10 percent of the DOC is humic material and that the amount of carbon in humic acid is around 50 percent (Thorn et al., 1989), 5 mg of C per liter would convert to about 1 mg humics per liter, and 50 mg of C per liter would be about 10 mg of humics per liter.

After evaluating the results with the TFCL-LP membrane, even smaller concentrations of humic acid appeared to be enough to alter the membrane surface charge. Therefore, for the other three membranes, concentrations of 0.2 mg/L and 2 mg/L were evaluated. Using the above conversion, 0.2 mg of humics per liter converted to 1 mg of C per liter, and 2 mg of humics per liter converted to 10 mg of C per liter. Both values of DOC were still well within the range of concentrations found in natural water.

Surfactants

Rosen (1989) defines a surfactant as a substance that, when present at low concentration, will adsorb onto the surface of the system and markedly alter the surface free energy. Surfactants have an amphipathic structure; that is, they have a hydrophobic group at one end and a hydrophilic group at the other. The hydrophobic group is usually a long-chain hydrocarbon residue, and the hydrophilic group is an ionic or highly polar group. For anionic surfactants, the surface-active portion of the molecule (hydrophilic group) bears a negative charge (Rosen, 1989). Common anionic surfactants are sulfates and sulfonates (Sawyer et al., 1994).

Sodium dodecyl sulfate (SDS) (certified grade) was used in streaming potential measurements. SDS was selected for the surfactant test solution because it is used in detergents, toothpastes, and food and cosmetic emulsions (Rosen, 1989) and is therefore commonly found in waste waters. The two concentrations of SDS used were 10^{-5} M and 10^{-4} M. These concentrations were below the CMC (critical micelle concentration), which is about $10^{-3.2}$ M (in the presence of 0.01-M NaCl) as reported by the National Bureau of Standards (Mukerjee and Mysels, 1971). The CMC is a sharply defined concentration above which micelles (surfactant aggregates) are formed (Mysels and Mysels, 1965).

5. RESULTS AND DISCUSSION

Tables listing values used to construct the figures referenced below are located in the appendix.

5.1 Inorganic Salt Experiments

Sodium Chloride (NaCl)

Figure 11 shows zeta potential versus pH for the TFCL-LP membrane with NaCl solutions. The i.e.p. is about 4.3 for the 0.001-M NaCl solution and about 4.4 for the 0.01-M NaCl solution. Figure 12 shows zeta potential for the TFCL-HR membrane. For this membrane, the i.e.p. is about 2.8 for the 0.00 1 -M NaCl solution and about 3.0 for the 0.01-M solution. Essentially, both membranes are positively charged at low pH values and negatively charged at high pH values. In both cases, the zeta potential becomes more negative as the pH increases.

As mentioned earlier, in the formation of the TFCL-LP and TFCL-HR membranes, the third acyl group of the trimesoyl chloride hydrolizes to a carboxylic acid. Generally, at low pH, the carboxyl groups will be protonated and will have a neutral charge. At high pH, the carboxyl groups will deprotonate and have a negative charge. Edwards et al. (1995), in studying the acidity of NOM (natural organic matter), found the deprotonation of carboxyl groups to be more complex than it appears. Edwards et al. (1995) found that strongly acidic functional groups (those that are deprotonated to a significant extent at pH 3.0) were a significant portion of the total acidity in samples of organic matter. These groups are considered to be carboxylic groups whose acidity is enhanced by the presence of adjacent functional groups on the same molecule. This early deprotonation combined with associated conformational changes in the NOM were found to decrease the acidity of other carboxylic acids on the same molecule. These weaker acids would then remain protonated until above pH 8. This "staggered" deprotonation can also be applied to the carboxyl groups on the surface of TFCL-LP membranes. Although the pKa of simple carboxylic acids (such as benzoic) in solution is about 4 (McMurry, 1988), on the membrane surface, the carboxylic acids will start ionizing at lower pH and will continue to ionize at pH above 4 because of the effect of neighboring functional groups.

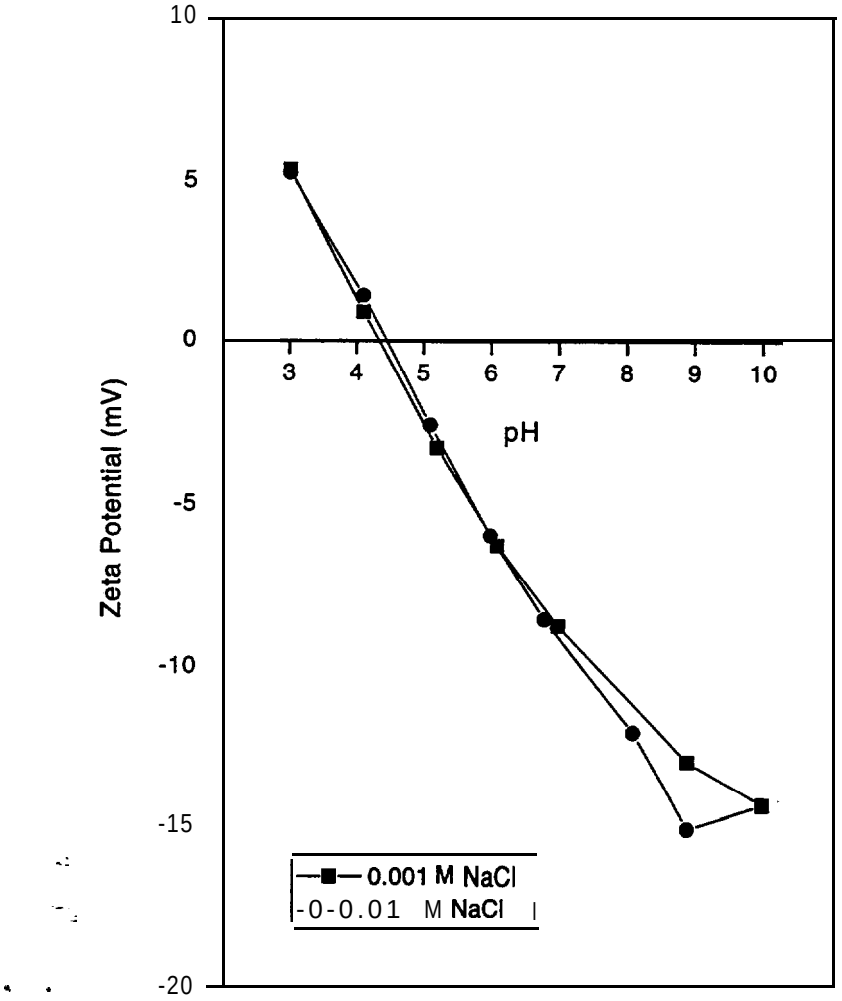

Figure 11. - Zeta potential versus pH for TFCL-LP membrane.

Other ionizable functionalities can also influence the surface charge of the membrane. According to the manufacturer, unreacted "pendant" amino groups will exist on the membrane surface and will be positively charged at low pH. These "pendant" groups include terminal groups on the edges of the polyamide structure as well as groups within the structure. Elimelech et al. (1994) suggest that the impurities mentioned earlier, although not part of the chemical structure of the aromatic polyamide, can markedly influence the surface charge. For example, at low pH, amine salts would be positively charged and anionic surfactants would be negatively charged.

On figure 11, at higher pH values, zeta potentials for the higher concentration of NaCl are slightly more negative than zeta potentials for the lower concentration of NaCl. On figure 12, the zeta potentials are substantially more negative for the higher concentration of NaCl. This characteristic of both curves may be attributed to the "close approach of co-ions" theory discussed earlier in Section 2.7. In aqueous solutions, because anions are less hydrated than cations, they can more closely approach the membrane surface. The surface will then acquire a more negative zeta potential because of the presence of anions beyond the plane of shear. The concentration of Cl- and OH- in solution increases with increasing NaCl concentration and increasing pH. As a result, the streaming potential of the 0.01-M NaCl solution is more negative than the streaming potential of the 0.001-M solution at higher pH values.

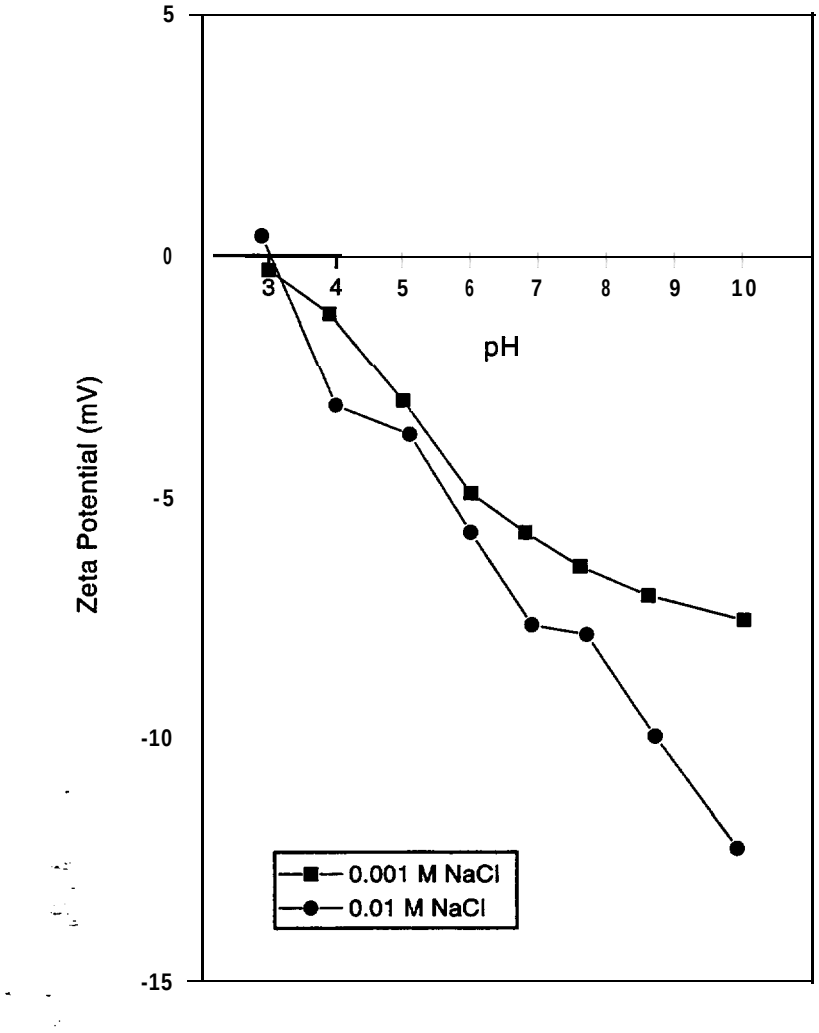

Figure 12. - Zeta potential versus pH for TFCL-HR membrane.

Figure 13 shows zeta potential versus pH for the NF membrane at two concentrations of NaCl. Except for the data points at pH 3, the plots for the two concentrations of NaCl are essentially the same. The i.e.p. appears to be around pH 4. The data points at pH 3 demonstrate the difficulty encountered with streaming potential measurements taken in the immediate vicinity of the i.e.p. This difficulty will be discussed in more detail later. Nonetheless, no specific interaction of the NaCl with the membrane surface appears to occur.

Figure 14 shows results for the CE membrane with NaCl solutions. As with the composite membranes, the zeta potential is positive at low pH values and negative at high pH values. Unlike the composite membranes, however, this behavior cannot be explained by dissociation of polymer functional groups. The acetyl and hydroxyl groups of the polymeric structure of the cellulose acetate membrane do not dissociate at the given chemical conditions. Instead, the positive charge of the membrane surface at low pH may be attributed to a divalent cation post-treatment which the manufacturer uses to increase the ionic character of the membrane surface. Because of the proprietary nature of the post-treatment, additional information has not been released.

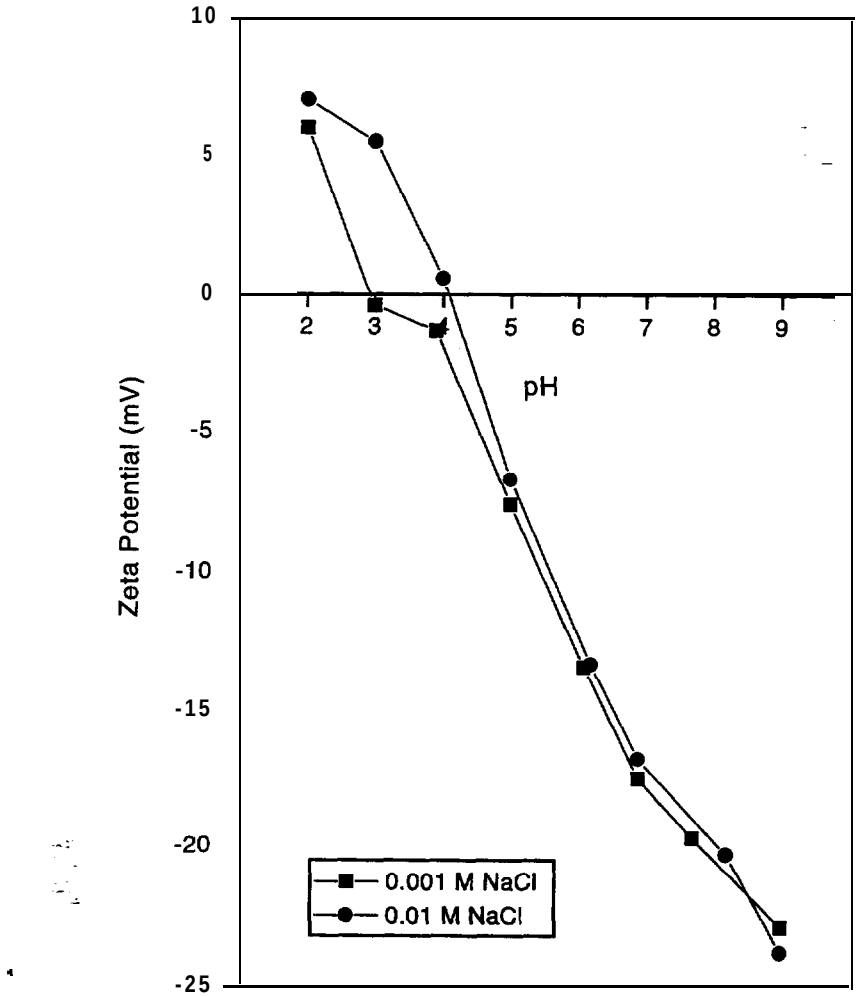

Figure 13. - Zeta potential versus pH for NF membrane.

At high **pH** values, several factors contribute to the negative charge of the membrane surface. The negative surface charge can result from adsorption of anions (Cl^- and OH^-) from solution. Preferential adsorption of anions has been used to explain surface charge behavior for several non-ionogenic surfaces (i.e., surfaces with no ionizable functional groups). For example, preferential adsorption has been suggested in the study of hydrocarbon droplets (Abramson, 1934; Jordan and Taylor; 1952, Stachurski and Michalek, 1985) and in the study of hydrophobic polystyrene latex colloids (Goff and Luner, 1984: Elimelech and **O'Melia,** 1990; Voeglti and Zukoski, 1991). However, as mentioned earlier, this theory is most **applicable** to hydrophobic surfaces, which the CE membrane is not.

Alternatively, the acid-base behavior of the membrane surface can be attributed to **post-**treatment with a dicarboxylic polymeric organic acid. This post-treatment occurs prior to the post-treatment with **divalent** cations, and information concerning it is also proprietary. The post-treatment explains why the zeta potential curve of the CE membrane has a shape **similar** to that of the TFCL-LP membrane, a shape which is characteristic of a surface containing weakly acidic functional groups.

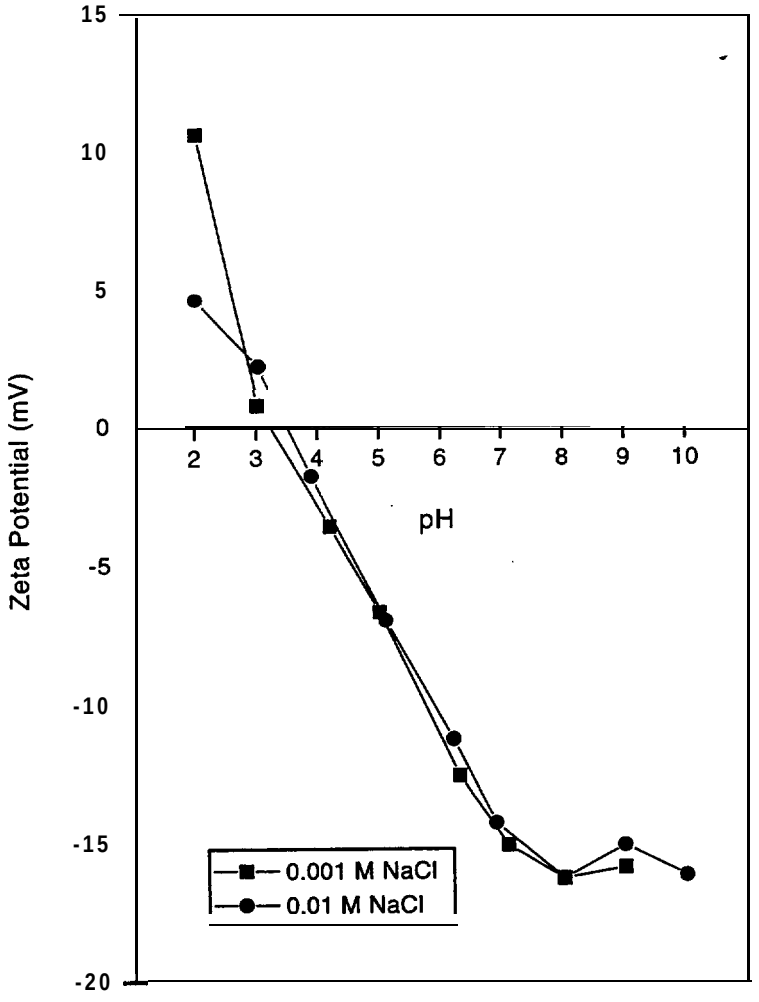

Figure 14. - Zeta potential versus pH for CE membrane.

Another explanation for the negative charge at high pH is hydrolysis of excess acetic anhydride. Acetic anhydride is the usual acetylating agent for cellulose. Excess compound is rinsed from the polymer with water and rapidly hydrolizes to acetic acid. Traces of this weak acid are probably adsorbed on polymer particles and may influence the surface charge of the membrane (Elimelech et al., 1994).

Impurities which are attached to the membrane surface (as mentioned earlier) may contribute to the negative zeta potential of CE membranes. Although no information is available on these various chemicals, they may contain acidic functional groups. These functional groups would deprotonate at higher pH values and cause the surface charge to be more negative.

As shown on figure 14, the i.e.p. of the CE membrane is about 3.3. As with the NF membrane (fig. 13), essentially no difference exists between the two concentrations of NaCl. This lack of specific interaction is probably attributable to the fact that the "close approach of co-ions" theory is not as significant for hydrophilic surfaces.

Calcium Chloride ($CaCl_2$)

Figure 15 shows the zeta potential of the TFCL-LP membrane for two $CaCl_2$ solutions. Comparing figures 11 (NaCl only) and 15 ($CaCl_2$ only), the i.e.p. shifts to a higher pH value for the $CaCl_2$ runs (from pH 4.4 to pH 5). Adsorption of the divalent cation to the membrane surface would best describe this shift. Beckett and Le (1990) found that the minor cations in seawater (Ca^{2+} and Mg^{2+}) were substantially more effective in reducing the magnitude of the surface charge of suspended particles than the major cation (Na^+).

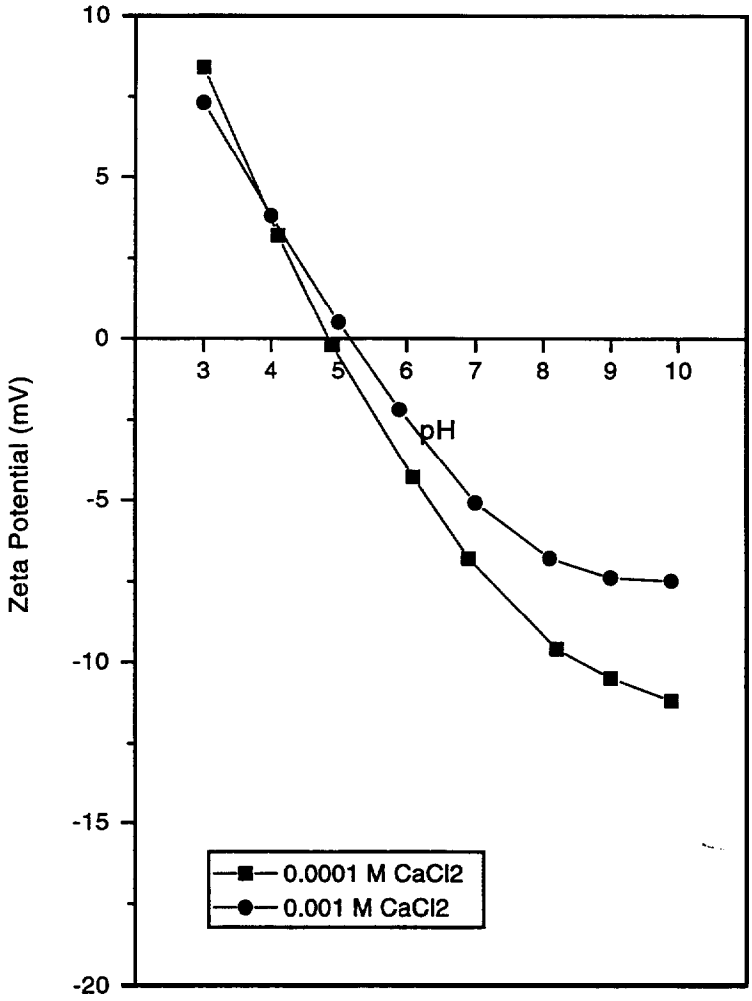

Figure 15. • Zeta potential versus pH for TFCL-LP membrane.

Because the membrane is negatively charged above the i.e.p., surface complex formation of the Ca^{2+} ion on the membrane surface would be favorable. In surface complex formation, the ion may form an inner-sphere complex ("chemical bond"), an outer-sphere complex (ion pair), or be in the diffuse swarm of the electric double layer (Stumm, 1992). If electrostatic attraction is the only bonding mechanism, the Ca^{2+} would bean outer-sphere complex. However, if covalent bonding or some combination of covalent and ionic bonding occurs, then inner-sphere complexes are formed. Either way, adsorption of Ca^{2+} to the membrane surface causes the i.e.p. to shift to a higher pH value. Adsorption of the divalent cation also explains why the zeta potential of the 0.001-M $CaCl_2$ solution is less negative than the zeta potential of the 0.0001 -M $CaCl_2$ solution at higher pH values.

For the graph of $CaCl_2$ in the presence of NaCl (fig. 16), the effect of the divalent cation is present, but is less noticeable than it is on figure 15. When both NaCl and $CaCl_2$ are present, the close approach of the co-ion (Cl) appears to counteract some of the effect of the adsorbed cation (Ca^{2+}). The i.e.p. shifts only slightly, and the zeta potentials at the two concentrations are essentially the same in the higher pH region.

On figures 17, 18, and 19 the difference between the two concentrations of $CaCl_2$ at high pH for the membranes is attributed to adsorption of the divalent cation. The i.e.p. of the TFCL-HR membrane (fig. 17) shifts from a pH of about 2.9 (in the presence of 0.01-M NaCl) to a pH of about 4.2 (in the presence of 0.01-M NaCl and 0.001-M $CaCl_2$). For the same conditions, the i.e.p. of the NF membrane (fig. 18) shifts only slightly (from 4.1 to 4.3); however, zeta potentials for the 0.001-M $CaCl_2$ solution are substantially less negative than zeta potentials for the 0.0001-M $CaCl_2$ solution. The i.e.p. of the CE membrane (fig. 19) did not shift substantially, but again, the effect of the adsorbed cation can be seen in zeta potential values at higher pH.

Sodium Sulfate (Na_2SO_4)

Comparing two concentrations of Na_2SO_4, figure 20 shows that below the i.e.p., adsorption of the divalent anion (SO_4^{2-}) may cause a very slight decrease in positive zeta potential. This effect is opposite to the effect of divalent cations and is most obvious below the i.e.p., where the membrane is positively charged. For the TFCL-HR membrane, comparison of the streaming potential measurement with $CaCl_2$ (fig. 17) to the measurement with Na_2SO_4 (fig. 2 1) shows that adsorption of the divalent anion causes a substantial shift in the i.e.p. from 3.0 to 2.0. For the NF-70 (fig. 22) and CE (fig. 23) membranes, adsorption of the divalent anion does not appear to be a key mechanism in the acquisition of surface charge.

The divalent anion (SO_4^{2-}) does not appear to be as readily adsorbed as the divalent cation (Ca^{2+}). This difference may be caused by the fact that the membrane has a positive charge over only a small portion of the pH range, whereas it is negatively charged over the majority of the pH range. Thus, the divalent cation would be expected to play a more dominant role in surface charge acquisition than the divalent anion in pH values found in natural waters.

5.2 Humic Acid Experiments

All humic acid experiments were performed with a background electrolyte concentration of 0.01-M NaCl. Results are not shown for the TFCL-HR membrane because this membrane's surface properties changed between the testing time for the inorganic salt solutions and the humic solutions. Apparently, the storage procedure for the TFCL-HR membrane did not keep the surface properties stable.

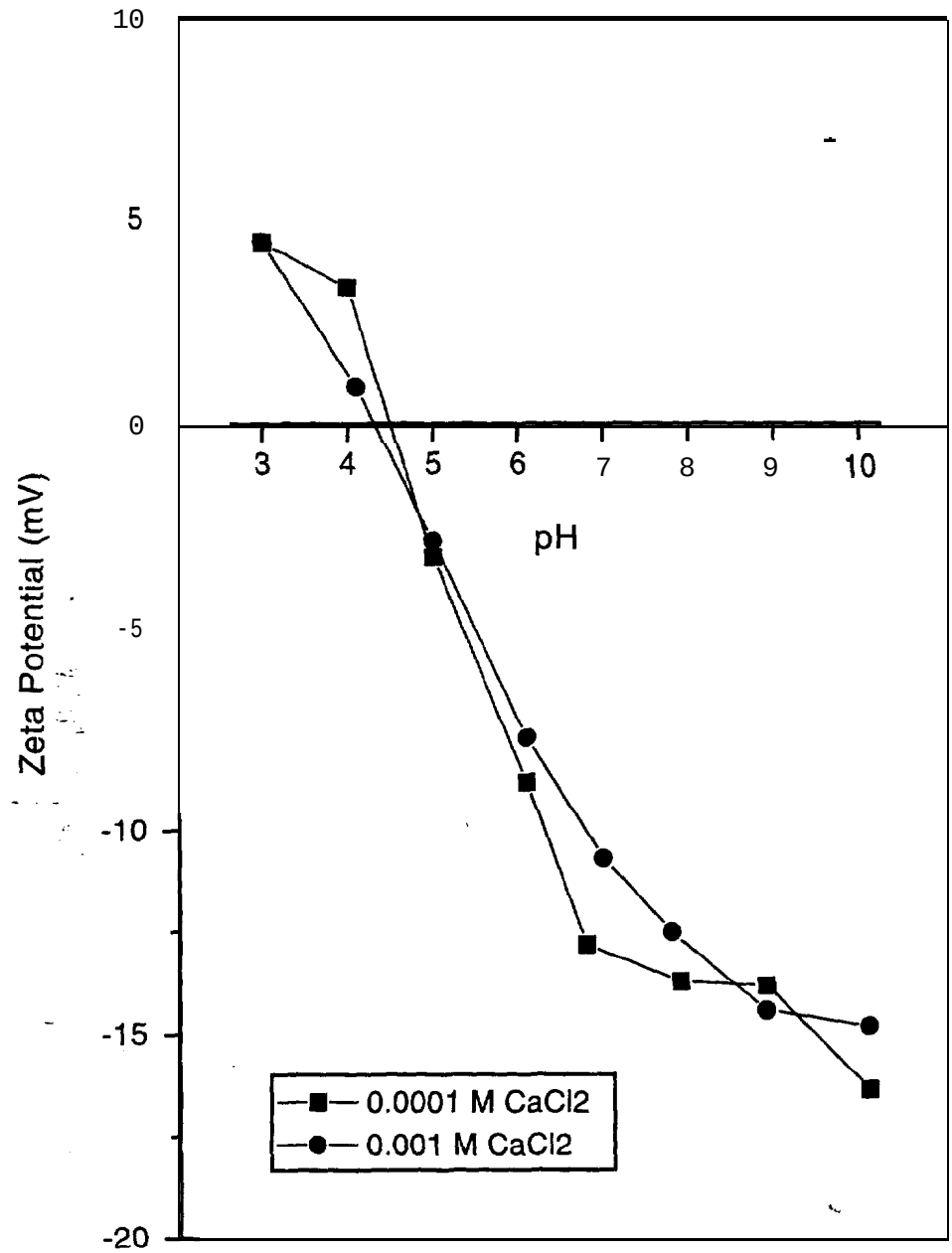

Figure 16. - Zeta potential versus pH for TFCL-LP membrane-O.01 -M NaCl as background electrolyte.

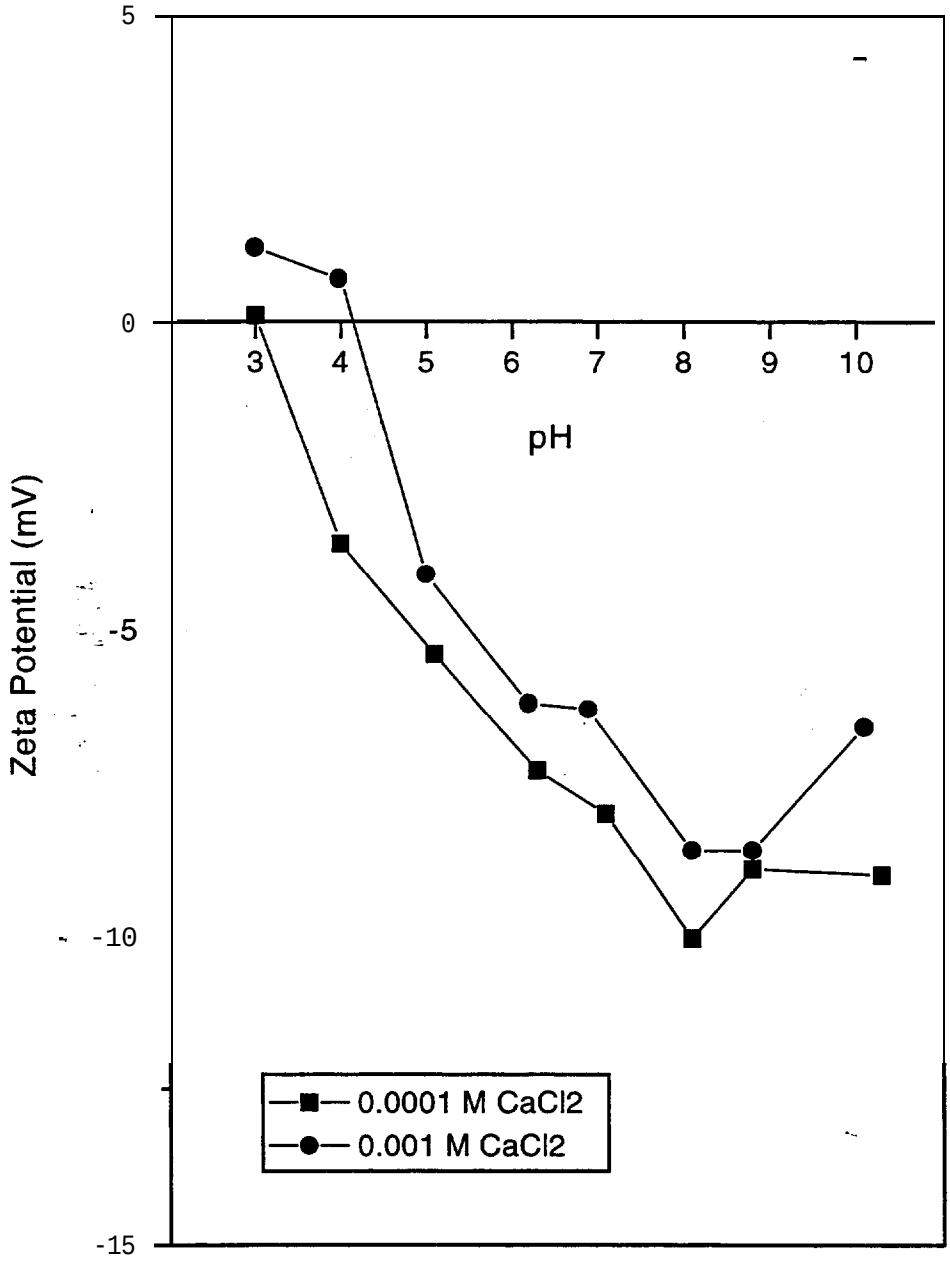

Figure 17. ▪ Zeta potential versus pH for TFCL-HR membrane-O.01 -M NaCl as background electrolyte.

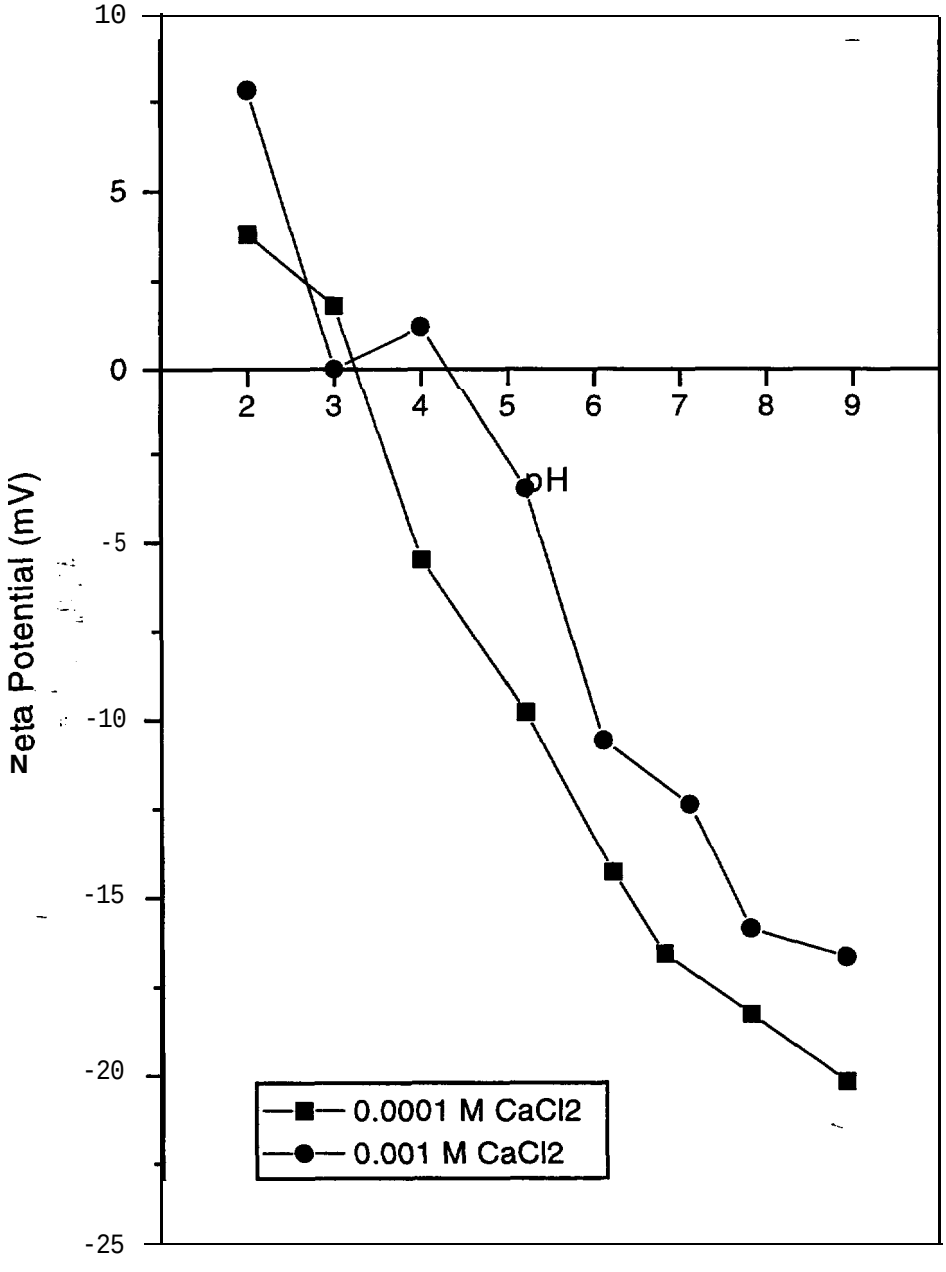

Figure 18. - Zeta potential versus pH for NF membrane—0.01-M NaCl as background electrolyte.

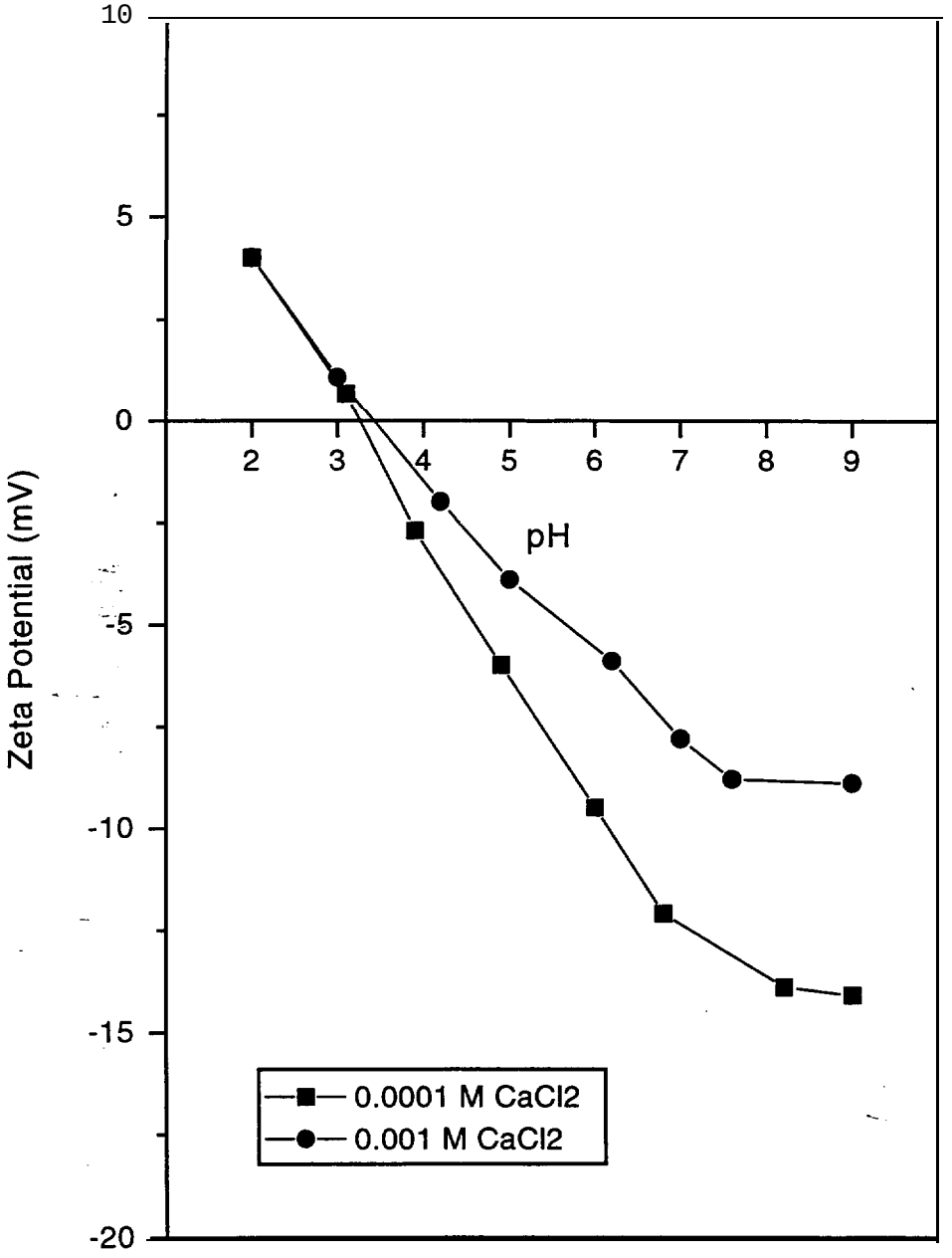

Figure 19. - Zeta potential versus pH for CE membrane-O.01 -M NaCl as background electrolyte.

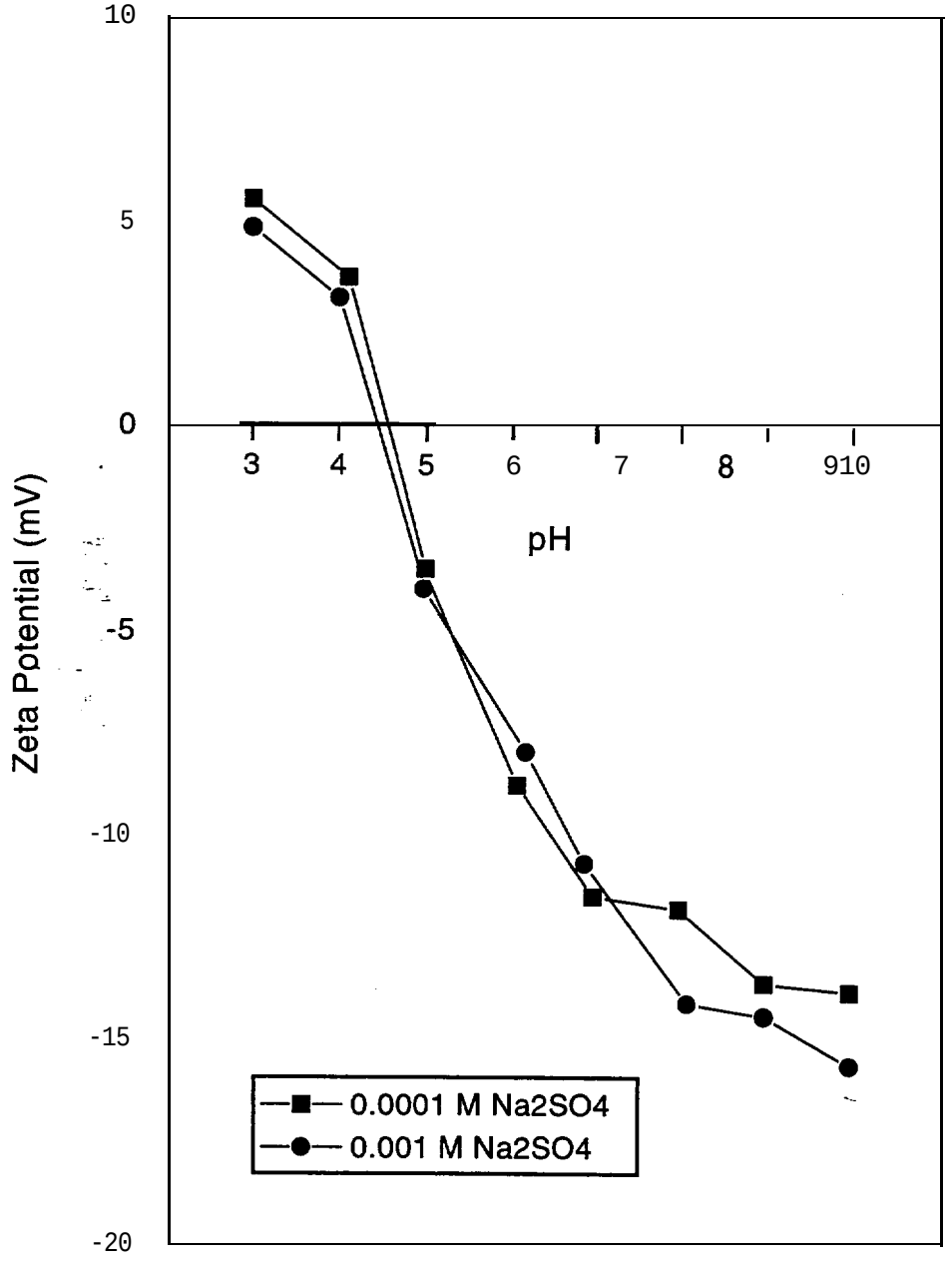

Figure 20. - Zeta potential versus pH for TFCL-LP membrane-O.01 -M NaCl as background electrolyte.

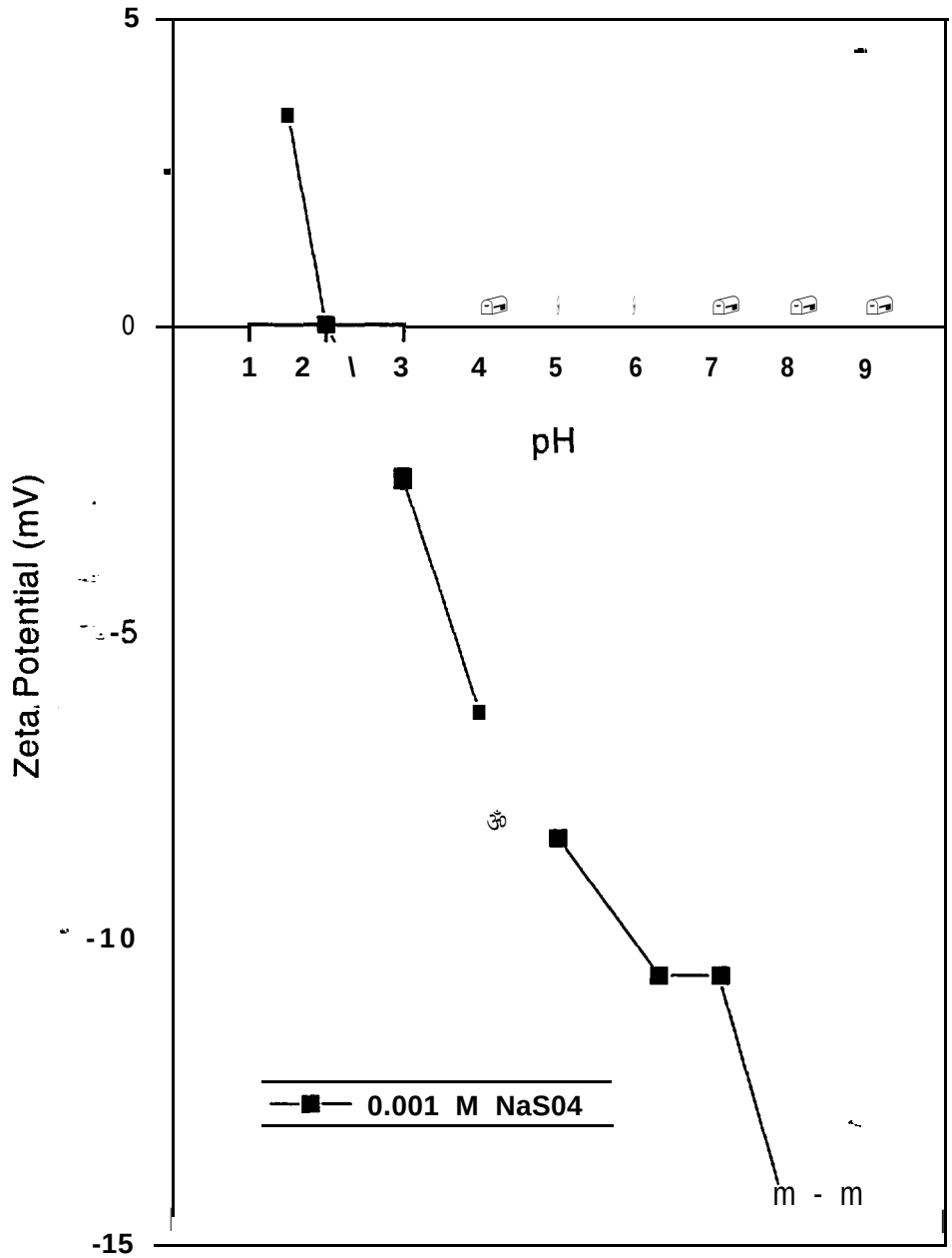

Figure 21. - Zeta potential versus pH for TFCL-HR membrane—0.01 -M NaCl as background electrolyte.

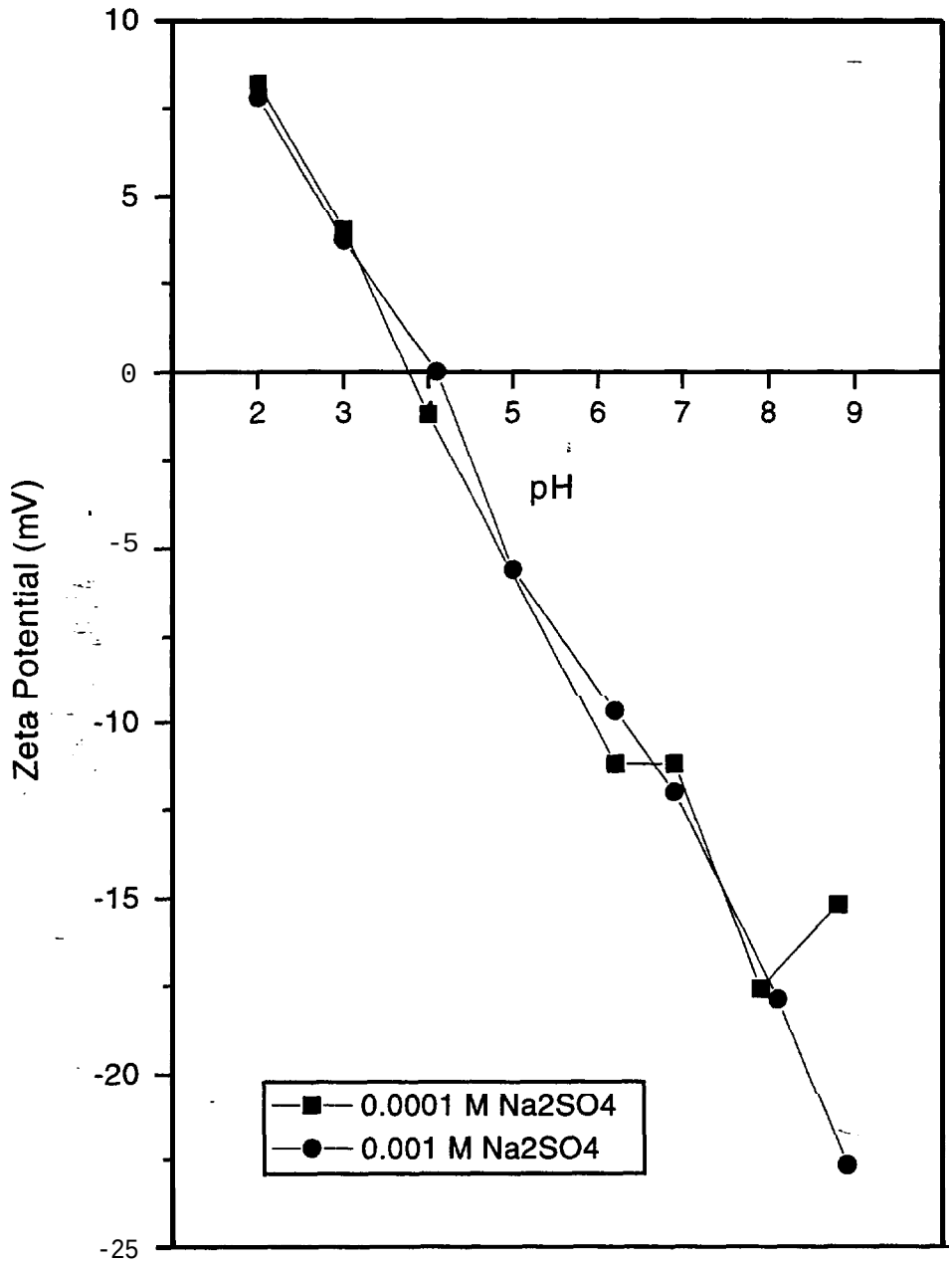

Figure 22. • Zeta potential versus pH for NF membrane—0.01-M NaCl as background electrolyte.

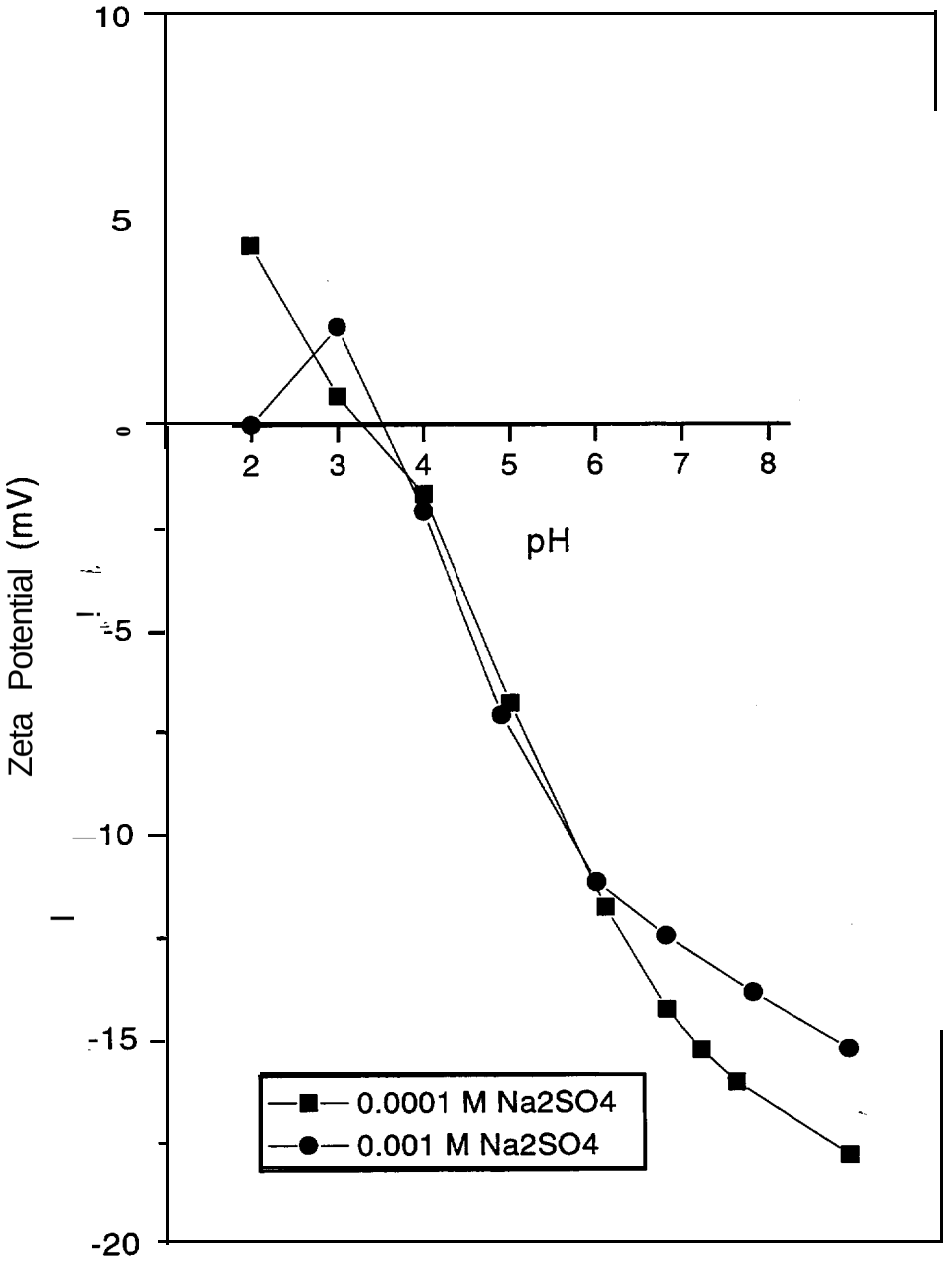

Figure 23. - Zeta potential versus pH for CE membrane—0.01-M NaCl as electrolyte.

Figure 24 shows zeta potential versus pH for the TFCL-LP membrane. The zeta potential of this membrane appears to be dramatically affected by 1-mg/L humics. Whereas when no humics are present, the membrane has a positive charge below a pH of about 4.5. When 1-mg/L humics are present, the membrane does not have a positive charge at any pH (3 to 10). In the case of 10-mg/L humics, the zeta potential is‘ only slightly more negative than the 1-mg/L case at lower pH values. For both concentrations,-the humics are readily adsorbed onto the membrane surface, and the negatively charged functional groups of the humics dominate the surface charge of the membrane.

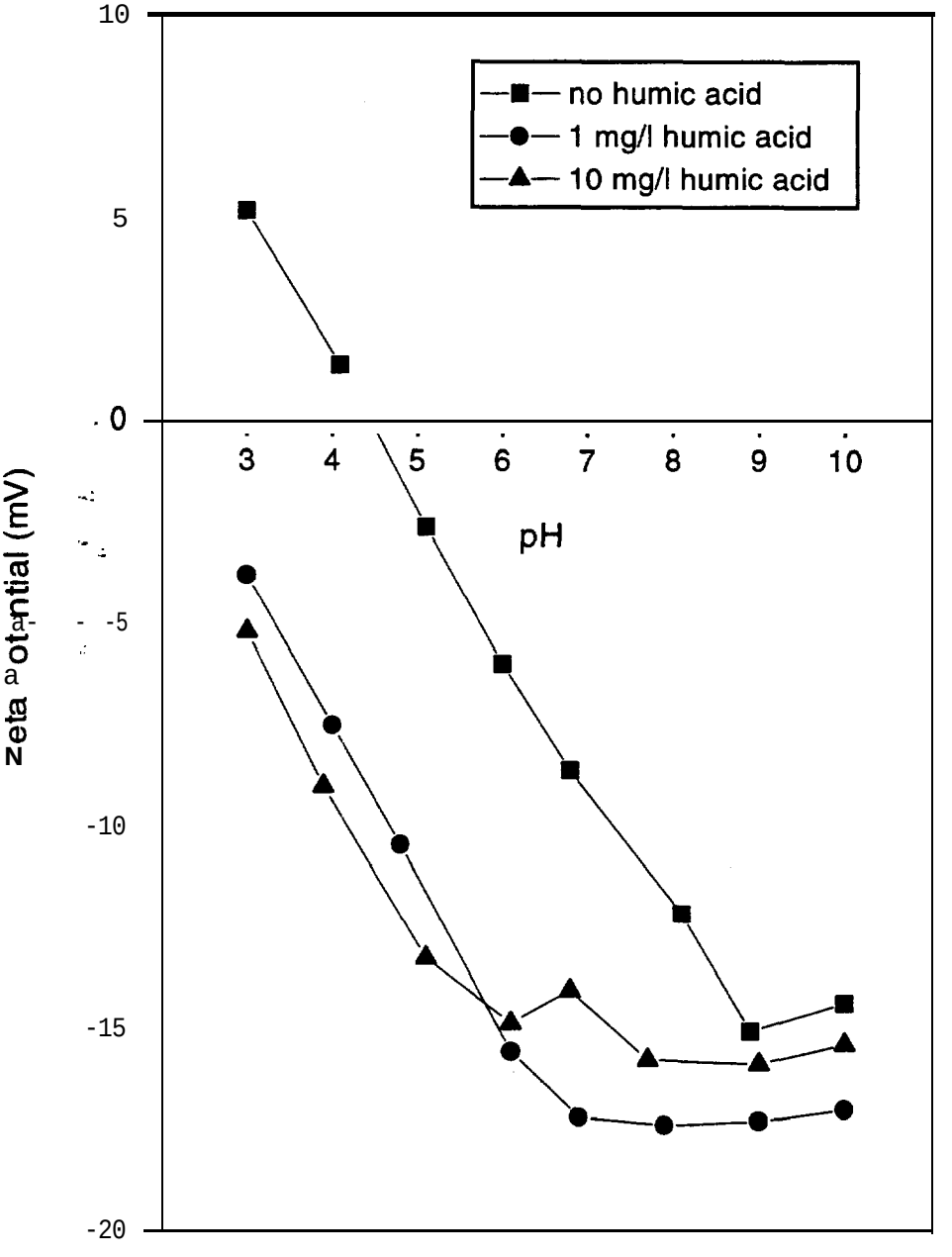

Figure 24. • Zeta potential versus pH for TFCL-LP membrane—0.01-M NaCl as background electrolyte.

Thorn et al. (1989) characterized the IHSS Suwannee River Humic Acid Reference by solution state carbon-13 and hydrogen-l NMR (nuclear magnetic resonance) spectrometry. The composition of the humic acid includes 4.1 meq/g of carboxyl (COOH) functional groups and 2.1 meq/g of OH (phenolic) functional groups, both of which are negatively-charged at neutral pH. Once the humic matter is adsorbed to the membrane, these ionizable functional groups determine the surface charge of the membrane. The surface and colloid properties of aquatic particles are strongly influenced by adsorbed organic compounds, particularly humic substances (Stumm and Morgan, 1981; Beckett and Le, 1990; Morel and Hering, 1993). The surface properties of membranes are also strongly influenced by adsorbed humics.

On figure 25, the zeta potential versus pH for the NF membrane is shown for two concentrations of humic acid. For a humic concentration as low as 0.2 mg/L, the membrane is negatively (or non-positively) charged at all pH values (2 to 9). At lower pH values, the zeta potential is only slightly more negative for the higher concentration (2 mg/L) of humics.

On figure 26, which shows the results for the CE membrane, the different concentrations of humics have a slightly different effect. As before, the 0.2-mg/L concentration of humics causes the membrane to become negatively (or non-positively) charged at all pH values (2 to 9). However, this time, the 2-mg/L concentration appears to have a more substantial effect on the zeta potential. For example, at pH 2, the zeta potential drops from 5 mV when no humics are present to about 0 mV for 0.2-mg/L humics and about -7.5 mV for 2 mg/L humics.

Below the i.e.p., the humic acid and the membrane surface are oppositely charged and adsorption is dominated by electrostatic attraction. Above the i.e.p., where the humic acid and the membrane surface are similarly charged, adsorption is dominated by hydrophobic interactions. However, above the i.e.p., electrostatic interactions still play a role. For example, above neutral- pH, adsorption caused by hydrophobic interactions decreases because of electrostatic repulsion. Also, adsorption of humics may have less effect on the negative charge of the membrane surface if the surface becomes "saturated" with negative charge.

5.3 Surfactant Experiments

These experiments were performed at a background electrolyte concentration of 0.01-M NaCl.

Figure 27 shows zeta potential versus pH for the TFCL-LP membrane in the presence of two concentrations of SDS. At 10^{-5}-M SDS, the i.e.p. drops from about 4.4 to about 3.7. At 10^{-4}-M SDS, the effect of the surfactants is more substantial in that an i.e.p. no longer exists (at pH 3, the zeta potential is about -14 mV). Once the SDS adsorbs to the membrane surface, the membrane will have a more negative charge because of the negatively charged (pKa about 2 [Morel and Hering, 1993]) sulfate functional groups on SDS.

Rosen (1989) lists six mechanisms by which surfactants may adsorb onto a solid surface from an aqueous solution. Ion exchange, ion pairing, acid-base interaction, and adsorption by polarization of π electrons involve adsorption of a surfactant onto an oppositely charged surface. However, mechanisms for adsorption of a surfactant onto a similarly charged membrane are of more interest because the membranes are negatively charged over most of the pH range. The mechanism most responsible for adsorption of the anionic surfactant onto the negatively charged. membrane surface is hydrophobic attraction. By this mechanism, the surfactant will adsorb not only to the membrane surface, but also to other surfactant molecules already adsorbed. London-van der Waals dispersion forces are also expected to contribute to the adsorption of surfactant.

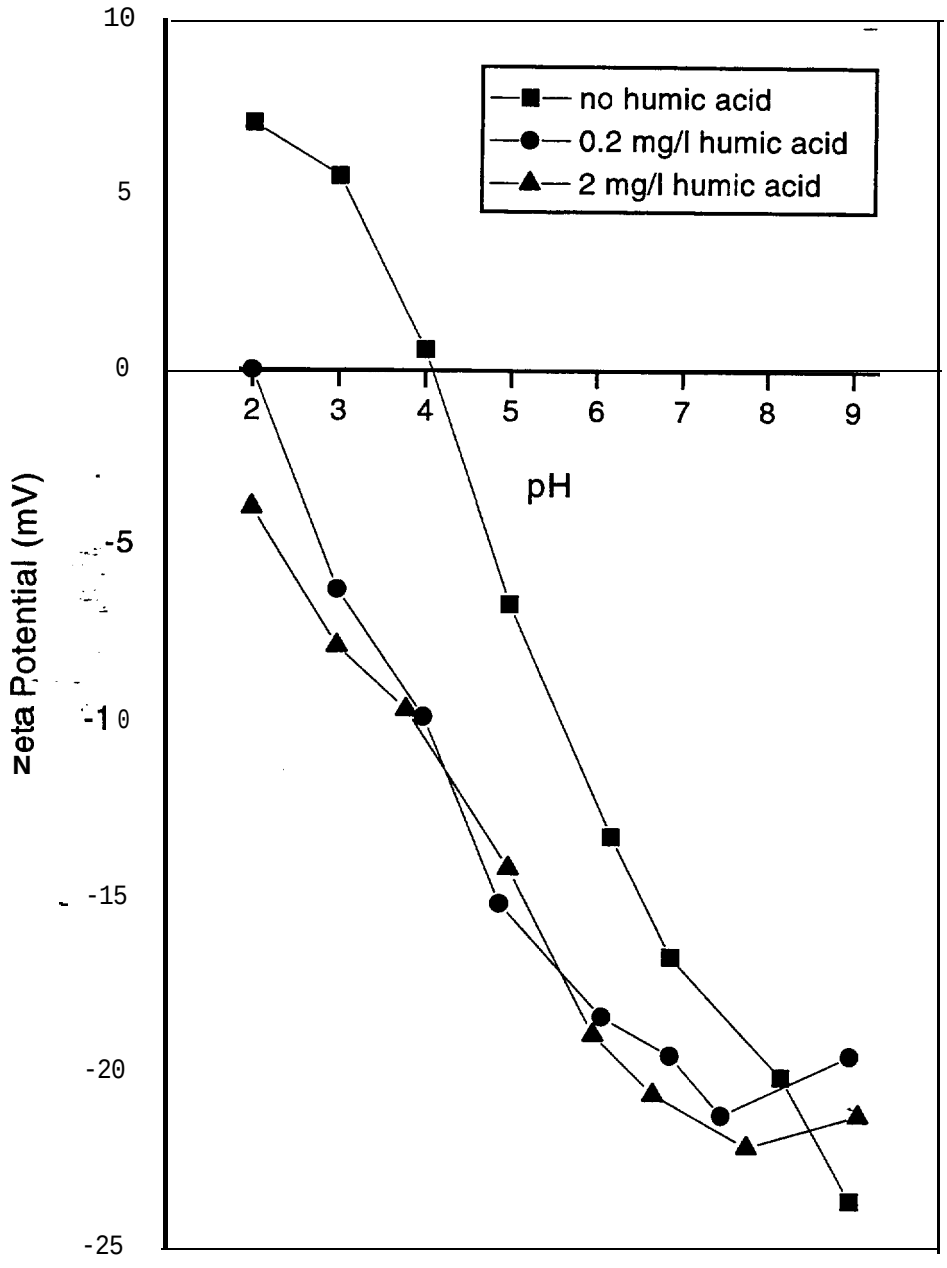

Figure 25. • Zeta potential versus pH for NF membrane—0.01-M NaCl as background electrolyte.

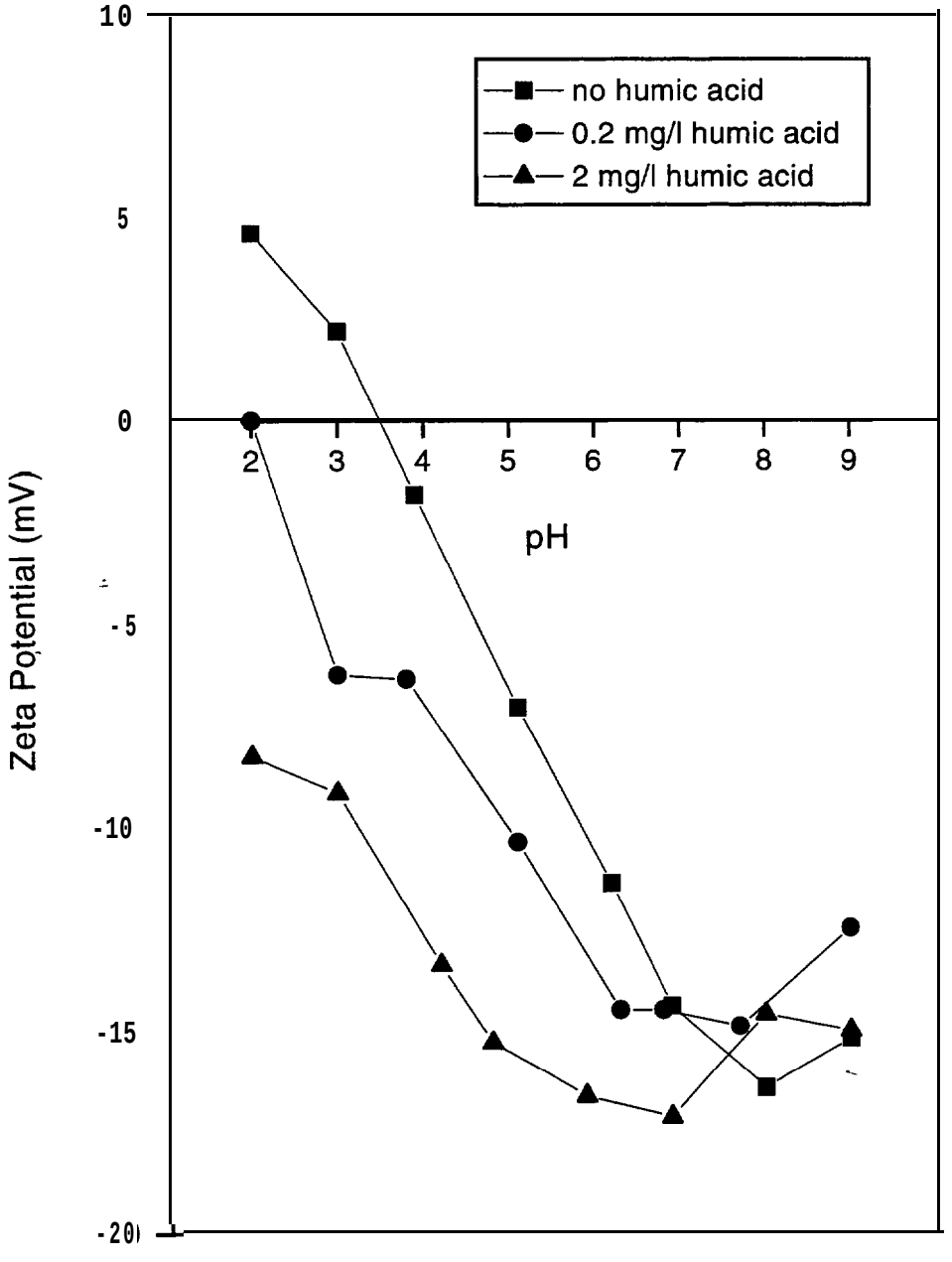

Figure 26. • Zeta potential versus pH for CE membrane-O.01 -M NaCl as background electrolyte.

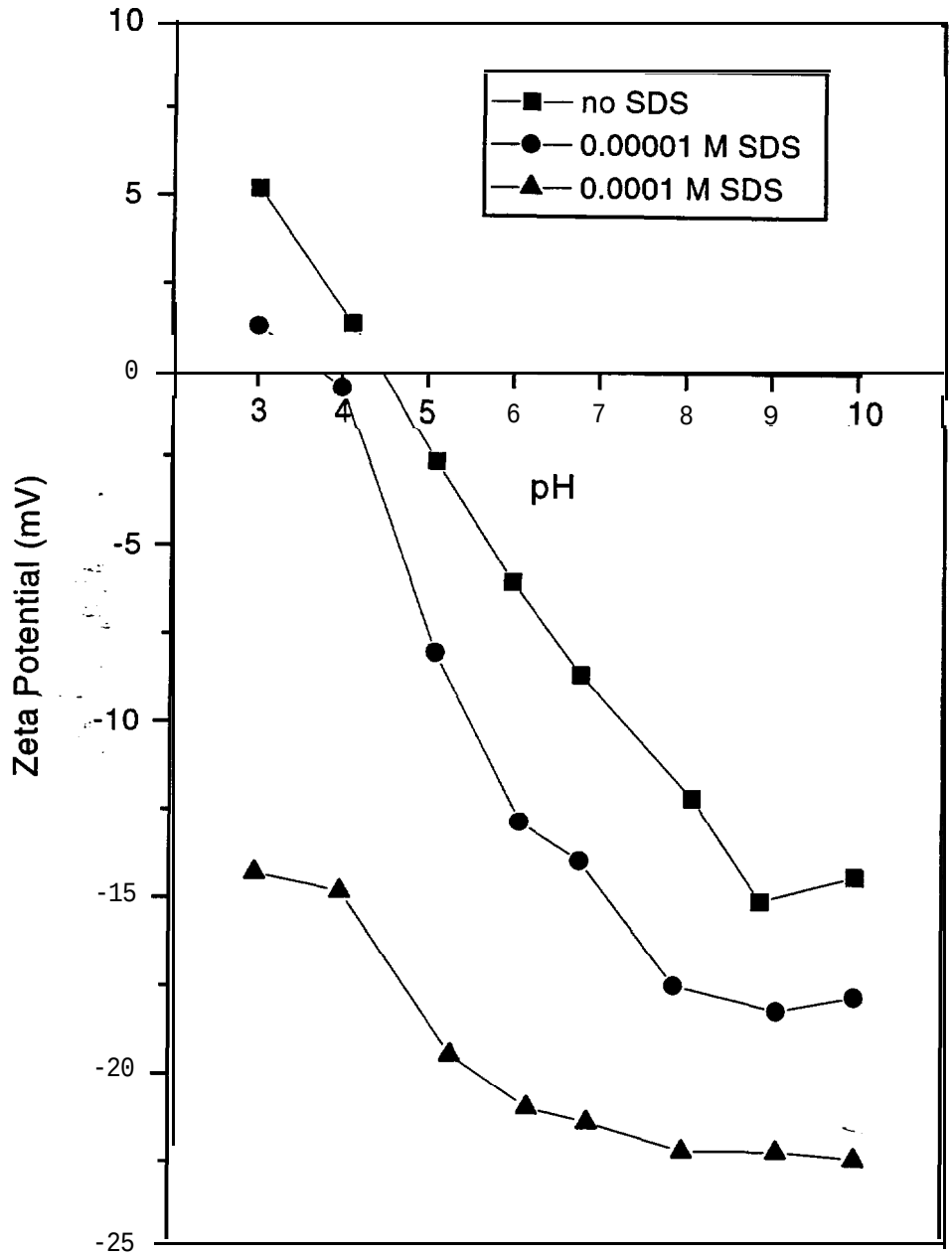

Figure 27. - Zeta potential versus pH for TFCL-LP membrane—0.01-M NaCl as background electrolyte.

This mechanism accounts for the ability of surfactant ions to displace equally charged simple inorganic ions from solid surfaces by an ion exchange mechanism.

Litton and Olson (1994) studied adsorption of SDS onto carboxyl latex surfaces and found that the SDS had a significant influence on the zeta potential of the surfaces. For example, in the presence of 10^{-3}-M SDS, the latex particles had a zeta potential that was about 20 mV more negative than when no SDS was present. The mechanism considered responsible for the adsorption is hydrophobic association of the surfactant alkyl chain with polystyrene oligimer exposed at the surface (Litton and Olson, 1994).

Figure 28 shows the effects of SDS on the zeta potential of the CE membrane. For both concentrations of SDS, no i.e.p. exists for the membrane. Below pH 7.5, the 10^{-4}-M SDS has a more substantial effect on the membrane than the 10^{-5}-M SDS. Above pH 7.5, the effect of the two concentrations of SDS is not as apparent, perhaps because the membrane surface functional groups have become saturated with negative charge.

5.4 Cleaning Experiments

As mentioned previously, the characteristics of the TFCL-HR membrane changed while in storage. Therefore, an attempt was made to "clean" the membrane back to its original characteristics. Figure 29 shows the results of various "cleaning processes". In the DI cleaning, the membranes were placed in a beaker of about 500-mL DI water, which was then placed in an ultrasonication bath for 20 minutes. In the acid cleaning, the membranes were placed in about 500 mL of a acid solution (pH adjusted to 2.5 with HCl) and sonicated for 20 minutes. In the base cleaning, the membranes were placed in about 500 mL of a base solution (pH adjusted to 10 with NaOH) and sonicated for 20 minutes. The pH values of 2.5 and 10 are the manufacturer's limits for cleaning the membrane.

As can be seen on figure 29, the cleaning appears to be effective in returning the surface charge of the membrane close to its original values. The runs that are cleaned with acid and base are very similar (especially between pH 4 and 7), but the run that was cleaned with DI is slightly more negative. This result is contrary to what is expected for an aromatic polyamide membrane. Sonicating in DI water would not be expected to alter the surface charge of the membrane more than sonicating in acidic or basic solutions. Sonicating is expected to physically remove any impurities on the membrane but not to change any of the chemical properties of the membrane.- Cleaning the membrane in base would be expected to result in a more negative charge. on the membrane surface and cleaning the membrane in acid would result in a more positive charge. This result would especially be expected at low pH, around the i.e.p. of the membrane. However, this result is not the case; the i.e.p. of the membrane cleaned in base is about ½ pH unit higher than the i.e.p. of the membrane cleaned in acid.

Because none of the three cleaning processes returned the membrane exactly to its original zeta potential, more research would be needed in this area before the membrane could be considered to be "cleaned" to its original state. Modifications in the cleaning procedure would need to be evaluated, and the reproducibility of the cleaning process would also need to be more thoroughly investigated. However, these preliminary tests found that a cleaning process is feasible for the TFCL-HR membrane if the surface charge of the membrane changes while in storage.

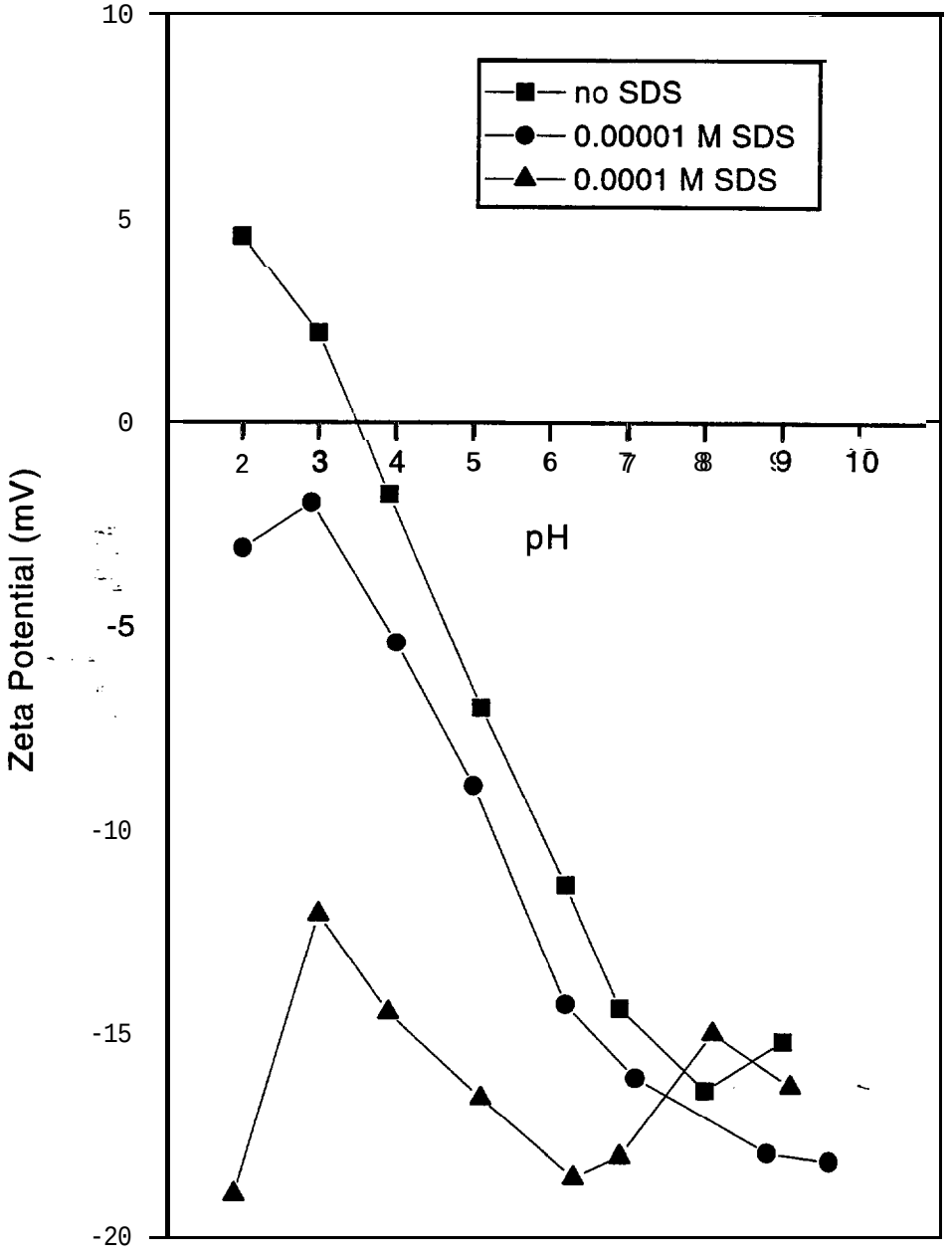

Figure 28. • Zeta potential versus pH for CE membrane—0.01-M NaCl as background electrolyte.

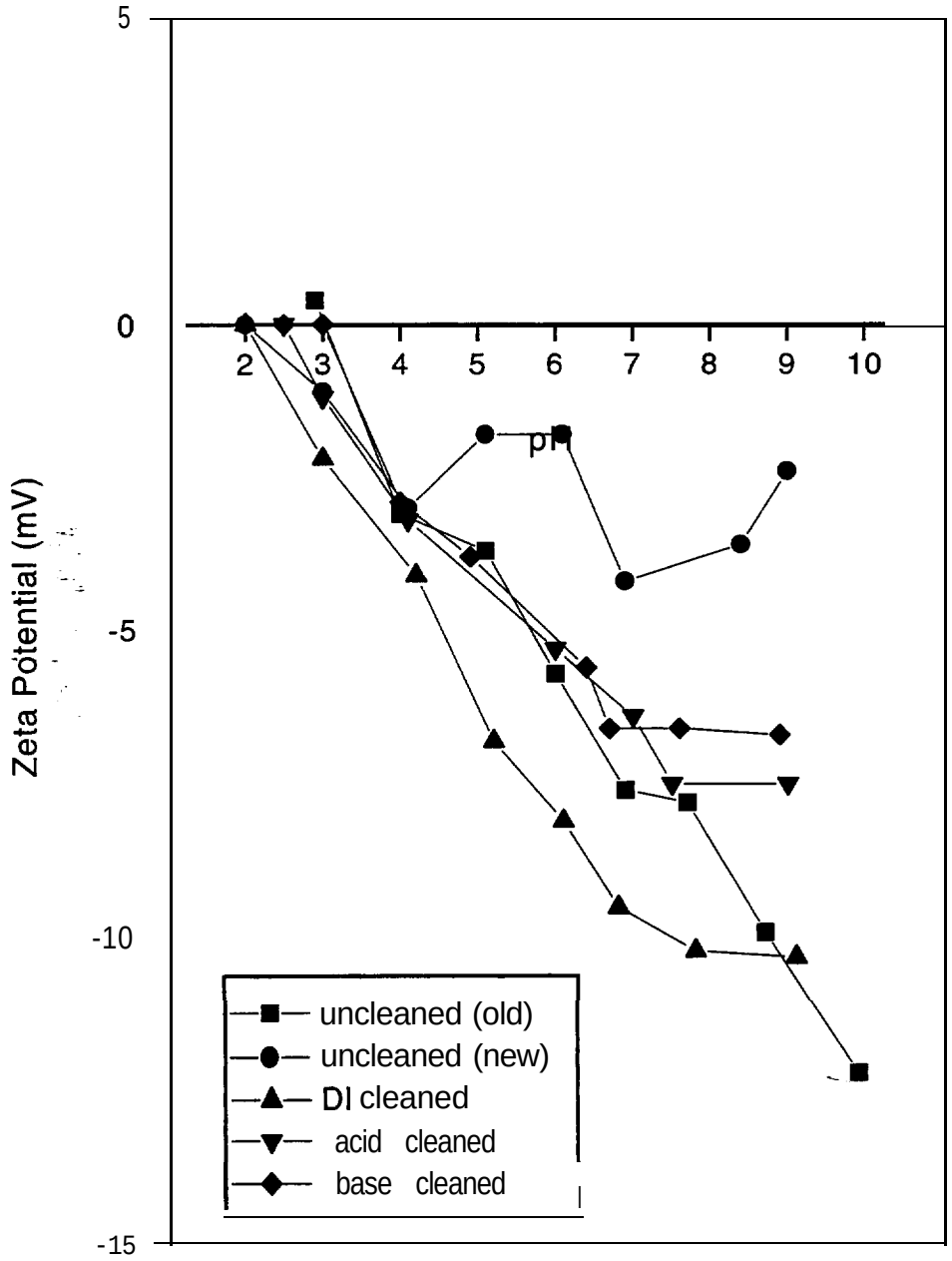

Figure 29. • Zeta potential versus pH for TFCL-HR membrane—0.01-M NaCl as background electrolyte.

Figure 30 shows results of the three cleaning processes for the CE membrane. In this case, the three cleaning processes were evaluated to determine their effect on the post-treatment of the membrane, not because the membrane's surface characteristics changed while it was in storage. Additionally, this graph shows results of two runs that were performed to determine the necessity of soaking the membrane overnight in DI water. The "DI cleaned" run is when the membrane was soaked overnight (about 16 hours) in DI water and then cleaned with DI water in the same manner as the TFCL-HR membrane. The "DI cleaned (6 hours)" is when the membrane was soaked in DI water for 6 hours prior to cleaning with DI water. The "DI cleaned (0 hours)" is when the membrane was not soaked in DI prior to cleaning with DI water.

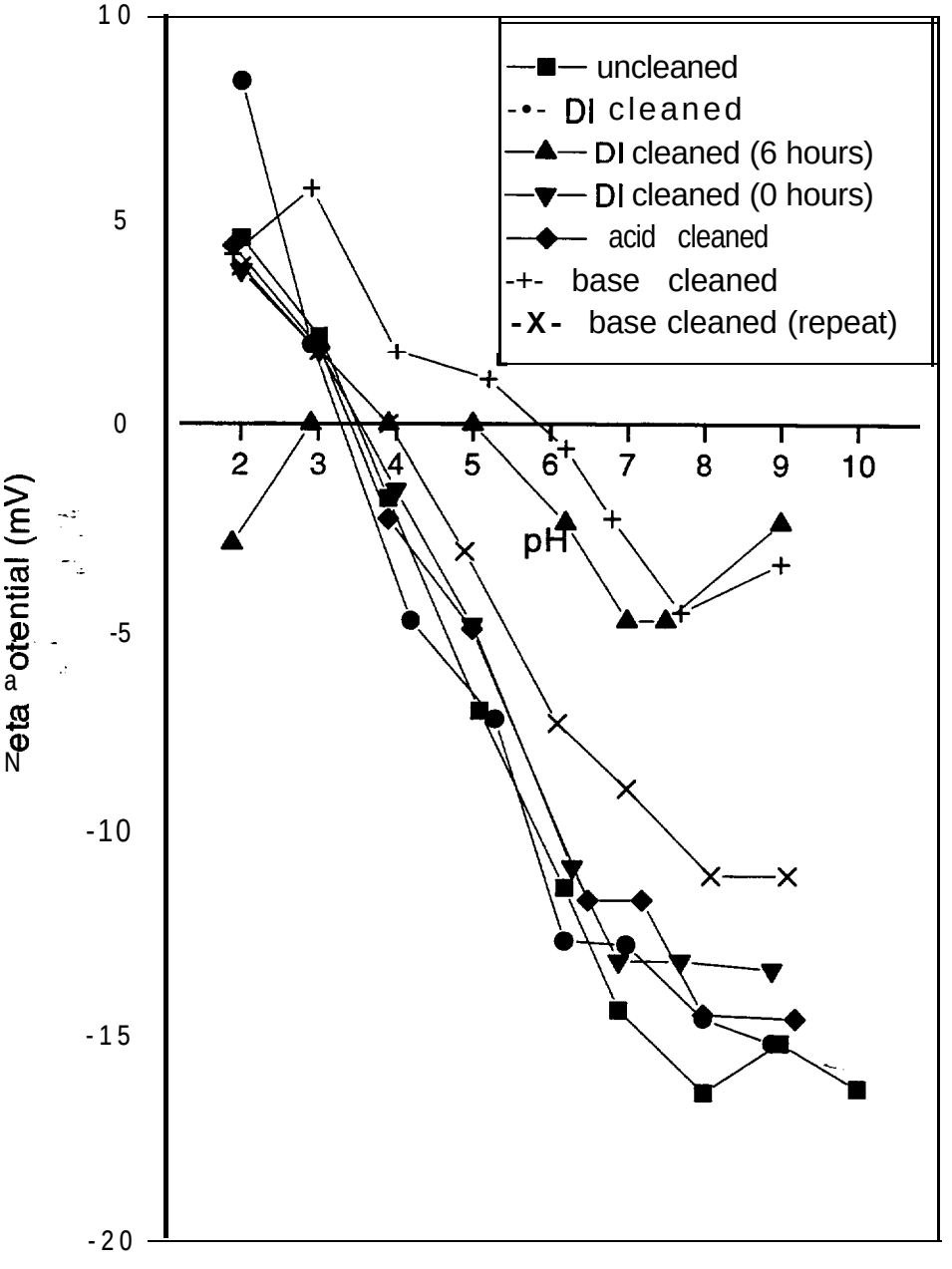

Figure 30. - Zeta potential versus pH for CE membrane—0.01-M NaCl as background electrolyte.

On figure 30, two of the above cleaning processes appear to cause the membrane surface to hydrolyze. Above pH 4, the 'base cleaned" and the "DI cleaned (6 hours)" runs had the same effect on the membrane in that they made the surface charge substantially less negative. Below pH 4, the 'base cleaned" run resulted in a more positively charged membrane, and the "DI cleaned (6 hours)" resulted in a more negatively charged membrane. However, the "base cleaned (repeat)" did not appear to have the same effect on the membrane as the original run. Additionally, the "DI cleaned (0 hours)" run did not have an effect similar to the "DI cleaned (6 hours)," as would be expected.

The inconsistencies in the runs make the mechanisms difficult to understand. Because the base appears to hydrolyze the membrane surface (the extent to which is variable), the acid would also be expected to hydrolyze the surface. As can be seen from the "acid cleaned" run,. this result did not occur. Some of the inconsistencies in the runs may have been caused by spots on the membrane that are slightly discolored. The surface properties may have been altered at these spots. These spots were on the membrane when the membrane was received from the manufacturer and have not appeared to change or become more numerous while the membrane was in storage.

It should be noted that the TFCL-HR and CE membrane are the only membranes of those that were tested to have undergone some sort of post-treatment. Without more understanding of the post-treatment processes, the effects of storage instability (in the case of the TFCL-HR membrane) and discoloration of the membrane (in the case of the CE membrane) are difficult to evaluate. In the meantime, the TFCL-HR membrane is no longer being evaluated, and care was taken with the CE membrane to ensure that the discolored sections of the membrane were not used in the investigation.

5.5 Error and Precision

Three parameters are available to evaluate the quality of the streaming potential measurements. Within each measurement, the asymmetry potential is calculated. The asymmetry potential reflects the amount of polarization at the electrodes. The asymmetry potentials of the above measurements are usually less than 1 mV, and they are almost always less than 2 mV, the exception being the TFCGLP run that was done with 0.0001-M $CaCl_2$ and no NaCl. The 'highest asymmetry potential is 2.3 mV in this exception. The asymmetric potential appears to increase when surface conductance becomes dominant (i.e., at ionic strengths less than 0.001 M). Also, within each measurement, the correlation of the line representing streaming potential versus pressure difference is determined. This value is almost always greater than 90 percent and is usually around 99 percent. As mentioned earlier, six measurements of streaming potential are averaged together to get the zeta potential for each pH point. The standard deviation of these measurements reflects the error involved in the calculation. The standard deviation is generally less than 10 percent. However, the standard deviation increases around the i.e.p. because the slope of the Iine representing streaming potential versus pressure difference is very small. Therefore, any difference in the slope is magnified and causes the standard deviation to exceed 10 percent of the zeta potential value.

6. IMPLICATIONS FOR MEMBRANE FOULING

Colloidal fouling of reverse osmosis membranes involves the deposition of suspended particles onto the surface of the membranes. The accumulation of particles at the membrane surface increases the resistance to water flow and thus reduces the water flux through the membrane. The initial rate of colloid deposition depends on the colloidal interaction forces between particles and membrane surfaces, among which double layer forces are most important. The double layer forces between particles and the membrane surface are determined by the zeta potentials of particles and membranes and by solution chemistry.

Analysis of transport and deposition mechanisms in crossflow membrane filtration (Song and Elimelech, 1995) and the vast literature on particle deposition onto non-permeable surfaces (e.g., Song and Elimelech, 1993; Elimelech et al., 1995) results in the following mechanistic explanation for colloidal fouling of RO membranes. The fouling behavior of RO membranes is related to solution chemistry, stability of the colloids, zeta potential of particles and membranes, and permeation drag. Four different fouling scenarios, based on the ionic strength and the electrokinetic charge (or zeta potential) of membranes and colloids, are discussed. These cases are for (1) moderate to high ionic strength when particles and membranes are similarly charged, (2) moderate to high ionic strength when particles and membranes are oppositely charged, (3) low ionic strength when particles and membranes are similarly charged, and (4) low ionic strength when particles and membranes are oppositely charged.

6.1 Moderate to High Ionic Strength When Particles and Membranes are Similarly Charged .

At high ionic strength, the repulsive double layer forces between the particles and the membrane surface are small because of double layer compression. As a result, particles which are transported to the membrane surface by the inherent permeation drag deposit favorably onto the membrane. At high ionic strength, no significant lateral repulsion occurs between deposited particles so their density on the membrane surface can be relatively high (Privman et al., 1991; Song and Elimelech, 1993; Adamczyk et al., 1994; Johnson and Elimelech, 1995). Because the particles are less stable at high ionic strength, the deposition of suspended particles onto previously retained particles is also favorable. This deposition behavior results in a thick fouling layer, the thickness of which depends highly on the hydrodynamic conditions. A schematic representation of this case is shown on figure 31. The total resistance to water flow, R_T, is the sum of the clean membrane resistance, R_m, and the fouling layer resistance, R_f. These conditions are hypothesized to cause significant membrane fouling.

This situation applies to most RO desalination units processing brackish or sea water because particles in aquatic environments are usually negatively charged (e.g., O'Melia, 1980; Tipping and Higgins, 1982; Stumm, 1992), and all available commercial RO membranes are negatively charged at the pH range of operation (as found in this research). It should also be noted that the fouling behavior described here may be suitable to RO systems operating at a moderate ionic strength because an elevated salt concentration at the membrane surface is formed by concentration polarization. In addition, large permeation drags can overcome small double layer repulsion which develops at moderate ionic strengths. Hence, pretreatment of feed waters to remove colloidal particles is necessary in this case to minimize colloidal fouling.

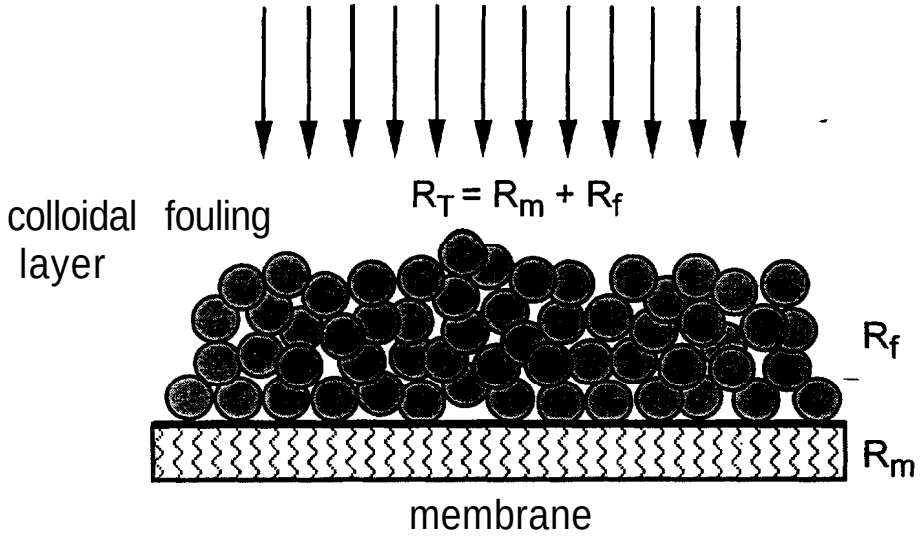

Figure 31. Schematic description of a colloid fouled membrane at high ionic strength.

6.2 Moderate to High Ionic Strength When Particles and Membranes are Oppositely Charged

In this case, the initial deposition of particles onto the oppositely charged membrane surface is favorable because of the attractive double layer forces. At high ionic strength, no significant lateral repulsion occurs between deposited particles, so their density on the membrane surface is relatively high as in the previous case. Because the particles are unstable at high ionic strength, the deposition of suspended particles onto previously retained particles is also favorable. This deposition behavior results in a thick fouling layer and extensive fouling as discussed for the previous case. The outcome of cases (1) and (2) is similar (i.e., significant fouling) despite the two quite different situations; this behavior is caused by the overwhelming effect of double layer compression.

6.3 Low Ionic Strength When Particles and Membranes are Similarly Charged

In this case, a strong double layer repulsion exists between the particles and the membrane surface. The extent of particle deposition and subsequent membrane fouling depends on the interplay between double layer repulsion and permeation drag. When operating at small permeation rates, particle deposition may be prevented by the strong double layer repulsion, and no fouling will occur. In this case, membranes with a large negative zeta potential are desired. On the other hand, at the high permeation rates encountered in most operations of thin film composite RO and NF membranes, particles may deposit onto the membrane surface and onto previously retained particles because of the strong permeation drag. In this situation, fouling can be significant for waters containing measurable levels of suspended colloidal particles.

6.4 Low Ionic Strength When Particles and Membranes are Oppositely Charged

In this case, the initial deposition of particles onto the oppositely charged membrane surface is favorable. Because of the low ionic strength, a strong lateral double layer repulsion exists between retained particles, and the initial density of surface coverage is not too high (Adamczyk et al., 1994; Johnson and Elimelech, 1995). Under these conditions, a strong double layer repulsion also exists between retained particles and approaching suspended particles. In this case, the extent of colloidal

fouling is postulated to depend on the interplay between double layer repulsion and permeation drag. For RO membranes operating at high permeation rates, permeation drag may overcome double layer repulsion between approaching and retained particles, resulting in the formation of a fouling layer on the membrane surface. On the other hand, when operating at small permeation rates, double layer repulsion may overcome the opposing permeation drag, and fouling will beminimized.

7. BIBLIOGRAPHY

Abramson, H.A. (1934). *Electrokinetic Phenomena and Their Application to Biology and Medicine.* ACS Monograph Series, No. 66, Chemical Catalog Co., New York.

Adamczyk, Z., Siwek, B., Zembala, M., and Belouschek, P. (1994). "Kinetics of Localized Adsorption of Colloid Particles." *Advances in Colloid and Interface Science,* 48(4), 15 I-280.

American Water Works Association Membrane Technology Research Committee (1992). "Committee Report: Membrane Processes in Potable Water Treatment." *Journal of the American Water Works Association,* 84(1), 59-67.

Beckett, R. and Le, N.P. (1990). "The Role of Organic Matter and Ionic Composition in Determining the Surface Charge of Suspended Particles in Natural Waters." *Colloids and Surfaces,* 44, 35-49.

Berner, E.K. and Berner, R.A. (1987). *The Global Water Cycle,* Prentice-Hall, New Jersey.

Bonekamp, B.C., Hidalgo Alvarez, R.H., de las Nieves, F.J., and Bijsterbosch, B.H. (1987). "The Effect of Adsorbed Charged Polypeptides on the Electrophoretic Mobility of Positively and Negatively charged Polystyrene Latices, *Journal of Colloid and Interface, Science,* 118(2), 366-371.

Börner, M.; Jacobasch, H.-J., Simon, F., Churaev, N.V., Sergeeva, I.P, and Sobolev, V.D. (1994). "Zeta Potential Measurements with Fibre Plugs in 1: 1 Electrolyte Solutions." *Colloids and Surfaces A: Physicochemical and Engineering Aspects,* 85, 9- 17.

Cadotte, J.E. (1985). Evolution of Composite Reverse Osmosis Membranes, in Douglas R. Lloyd (Ed.) *Materials Science of Synthetic Membrane,* American Chemical Society, Washington D.C.

Causserand, C., Nyström, M. and Aimar, P. (1994). "Study of Streaming Potentials of Clean and Fouled Ultrafiltration Membranes." *Journal of Membrane Science,* 88, 21 l-222.

Chapman-Wilbert, Michelle. (1993). *The Desalting and Water Treatment Membrane Manual: A Guide to Membranesfor Municipal Water Treatment,* United States Department of the Interior Bureau of Reclamation.

Christoforou, C.C., Westermann-Clark, G.B., and Anderson, J.L. (1985). "The Streaming Potential and Inadequacies of the Helmholtz Equation." *Journal of Colloid and Interface Science,* 106(1), 1 - 11.

Cohen, R. and Radke, C. (199 1). "Streaming Potentials of Nonuniformly Charged Surfaces." *Journal of Colloid and Interface Science,* 141(2), 338-347.

Dunstan, D.E. (1992). "Electrophoretic Mobility of Hydrocarbon Particles in KC1 Solutions." *Langmuir,* 8(6), 1507- *1508.*

Dunstan, D.E. (1993). "Electrokinetics of Polystyrene Latices: The Role of the Hydrophobic Surface." *Journal of the Chemical Society-Faraday Transactions,* 89(3), 521-526.

Dunstan, D.E. and Saville, D.A. (1992). "Eiectrophoretic Mobility of Colloidal Alkane Particles in Electrolyte Solutions." *Journal of the Chemical Society-Faraday Transactions,* 88(14), 203 l-2033.

Edwards, M., Benjamin, M.M., and Ryan, J.N. (1995). "The Acidity of NOM and its Role in Sorption to Oxide Surfaces." Submitted.

Elimelech, M., Chen, W.H., and Waypa, J.J. (1994). "Measuring the Zeta (Electrokinetic) Potential of Reverse Osmosis Membranes by a Streaming Potential Analyzer." *Desalination,* 95, 269-286.

Elimelech, M., Gregory, J., Jia, X., and Williams, R.A. (1995). *Particle Deposition and Aggregation: Measurement, Modeling, and Simulation,* Butterworth-Heinemann, Oxford.

Elimelech, M. and O'Melia, C.R. (1990). "Effect of Electrolyte Type on the Electrophoretic Mobility of Polystyrene Latex Colloids." *Colloids and Surfaces, 44, 165-I 78.*

Fairbrother, F. And Mastin, M. *(1924). Journal of the Chemical Society,* 75, 23 18.

Glater, J., McCutchan, J.W., McCray, S.B., and Zachariah, M.R. (1981 a). "The Effect of Halogens on the Performance and Durability of RO Membranes." ACS Series, No. 153, 171-190.

Glater, J., McCutchan, J.W., McCray, S.B., and Zachariah, M.R. (1981 b). "Halogen Interactions with Typical RO Membranes." Water Reuse Symposium II, August 23-28, Washington, D.C., Vol. 2, 1399-1409:

Glater, J., Zachariah, M.R., McCray, S.B., and McCutchan, J.W. (1983). "Reverse Osmosis Membrane Sensitivity to Ozone and Halogen Disinfectants." *Desalination, 48,* 1- 16.

Glater, J., Hong, S-K., and Elimelech, M. (1994). "The Search for a Chlorine Resistant Reverse Osmosis Membrane." *Desalination,* 95, 325-345.

Goff, J.R. and Luner, P. (1984). "Measurement of Colloid Mobility by Laser Doppler Electrophoresis: The Effect of Salt Concentration on Particle Mobility." *Colloid and Interface Science,* 99, 468-483.

Goosens, J.W.S. and Zembrod, A. (1979). "Characterization of the Surface' of Polymer Latices by Photon Correlation Spectroscopy." *Colloid and Polymer Science,* 257, 437-438.

Hunter, R.J. (1981). *Zeta Potential in Colloid Science: Principles and Applications,* Academic Press, London.

Jacangelo, J.G., Patania, N.L., and Trussell, R.R. (1989). "Membranes in Water." *Civil Engineering, 68-* 71.

Jacobasch, H.-J., Bauböck, G., and Schurz, J. (1985). "Problems and Results of Zeta-Potential Measurements on Fibers." *Colloid and Polymer Science,* 263, 3-24.

Jacobasch, H.-J. and Schurz, J. (1988). "Characterization of Polymer Surfaces by Means of Electrokinetic Measurements." *Progress in Colloid and Polymer Science,* 77, 40-48.

Johnson, P.R. and Elimelech, M. (1995). "Dynamics of Colloid Deposition in Porous Media: Blocking Based on Random Sequential Adsorption." *Langmuir,* 1 1(3), 801-8 12.

Jordan, D.O. and Taylor, A.J. (1952). "The Electrophoretic Mobilities of Hydrocarbon Droplets in Water and Dilute Solutions of Ethyl Alcohol." *Transactions of Faraday Society,* 48, 346-355.

Kaneko, N. and Yamamoto, Y. (1976). "Membrane Potential in Reverse Osmosis Process." *Journal of Chemical Engineering of Japan,* 9(2), 158-160.

Kesting, R.E. (1985). *Synthetic Polymeric Membranes: A Structural Perspective, 2nd ed.*, John Wiley, New York.

Khedr, M.G.A., Abd el Haleem, S.M., and Baraka, A. (1985). "Selective Behaviour of Hyperfiltration Cellulose Acetate Membranes Part II. Streaming Potential." *Journal of Electroanalytical Chemistry,* 184, 161-169.

Litton, G.M. and Olson, T.M. (1994). "Colloid Deposition Kinetics with Surface-Active Agents: Evidence for Discrete Surface Charge Effects." *Journal of Colloid and Interface Science,* 165, 522-*525.* --

Loeb, S. (1980). "The Loeb-Sourirajan Membrane: How It Came About. in: *ACS Symposium Series of Synthetic Membranes*, 153, l-9.

McMurry, J. (1988). *Organic Chemistry,* Wadsworth, Inc., Belmont, CA.

Midmore, B.R. and Hunter, R.J. (1988). "The Effect of Electrolyte Concentration and Co-Ion Type on the Zeta Potential of Polystyrene Latexes." *Journal of Colloid and Interface Science,* 122, 52 l-529.

Morel, F.M.M. and Hering, J.G. (1993). *Principles and Applications of Aquatic Chemistry,* John Wiley & Sons, Inc., New York.

Morin, O.J. (1994). "Membrane Plants in North America." *Journal of the American Water Works Association,* 86(12), 42-54.

Mulder, M. (1991). *Basic Principles of Membrane Technology,* Kluwer Academic Publishers, The Netherlands.

Mukerjee, P. and Mysels, K.J. (197 1). *Critical Micelle Concentrations of Aqueous Surfactant Systems,* United States Department of Commerce National Bureau of Standards, Washington D.C., NSRDS-NBS 36.

Mysels, E.K. and Mysels, K.J. (1965). "Conductimetric Determination of the Critical Micelle Concentration of Surfactants in Salt Solutions." *Journal of Colloid Science, 20, 3* 15-32 1.

Nyström, M., Lindström, M., and Matthiasson, E. (1989). "Streaming Potential as a Tool in the Characterization of Ultrafiltration Membranes." *Colloids and Surfaces,-36, 297-312.*

Nyström, M., Pihlajamäki, A., and Ehsani, N. (1994). "Characterization of Ultrafiltration Membranes by Simultaneous Streaming Potential and Flux Measurements." *Journal of Membrane Science, 87,* 245-256.

Oldham, I.B., Young, F.J., and Osterle, J.F. (1963). "Streaming Potential in Small Capillaries." *Journal of Colloid Science, 18, 328-336.*

O'Melia, C.R. (1980). "Aquasols: The Behavior of Small Particles in Aquatic Systems." *Environmental Science and Technology,* 14(9), 1052-l 060.

Petersen, R.J. (1993). "Composite Reverse Osmosis and Nanofiltration Membranes." *Journal of Membrane Science,* 83, 81-150.

Potts, D.E., Ahlert, R.C., and Wang, S.S. (1981). "A Critical Review of Fouling of Reverse Osmosis Membranes." *Desalination,* 36, 235-264.

Privman, V., Frisch, H.L., Ryde, N., and Matijevic, E. (1991). "Particle Adhesion in Model Systems. Part 13: Theory of Multilayer Deposition." *Journal of Chemical Society Faraday Transactions,* 87(9), 1371-1375.

Rosen, M.J. (1989). *Surfactants and Interfacial Phenomena,* John Wiley & Sons, Inc., New York.

Sawyer, C.N., McCarty, P.L., and Parkin, G.F. (1994). *Chemistry for Environmental Engineering,* McGraw-Hill, Inc., New York.

Shaw, D.J. (1969). *Electrophoresis,* Academic Press, London.

Song, L. and Elimelech, M. (1993). "Dynamics of Colloid Deposition in Porous Media: Modeling the Role of Retained Particles." *Colloids and Surfaces A,* 73(6), *49-63.*

Song, L. and Elimelech, M. (1995). "Particle Deposition onto a Permeable Surface in Laminar Flow." *Journal of Colloid and Interface Science,* 173, 165- 180.

Stachurski, J. and Michalek, M. (1985). "The Zeta Potential of Emulsion Droplets of the Aliphatic Hydrocarbons in Aqueous Solutions." *Colloids and Surfaces,* 15, 255-259.

Stumm, W. (1992). *Chemistry of the Solid-Water Interface.* John Wiley & Sons, Inc., New York.

Stumm, W. and Morgan, J.J. (1981). *Aquatic Chemistry,* Wiley-Interscience, New York.

Tanny, G., Hoffer, E., and Kedem, 0. (197 1). "Streaming Potentials During Hyperfiltration." *Experentia Supplementurn,* 18, 619-630.

Tomaschke, E. (August 14, 1990). Interfacially Synthesized Reverse Osmosis Membrane Containing an Amine Salt and Processes for Preparing the Same, United States Patent 4,948,507.

Thorn, K.A., Folan, D.W., and MacCarthy, P. (1989). "Characterization of the International Humic Substances Society Standard and Reference Fulvic and Humic Acids by-Solution State Carbon- 13 (^{13}C) and Hydrogen-l (H) Nuclear Magnetic Resonance Spectrometry." Water Resources Investigations Report 89-4196, U.S. Geological Survey, Denver.

Tipping, E. and Higgins, D.C. (1982). "The Effect of Adsorbed Humic Substances on the Colloid Stability of Haemitite Particles." *Colloids and Surfaces,* 5(2), *85-92.*

van den Hoven, Th.J.J. and Bijsterbosch, B.H. (1987). "Streaming Currents, Streaming Potentials and Conductances of Concentrated Dispersions of Negatively-Charged, Monodisperse Polystyrene Particles. Effect of Adsorbed Tetraalkylammonium Ions." *Colloids and Surfaces, 22, 187-205.*

van der Linde, A.J. and Bijsterbosch, B.H. (1990). "Does the Maximum in the Zeta Potential of Monodisperse Polystyrene Particles Really Exist? An Electrokinetic Study." *Croatica Chemica Acta,* 63(3), *455-465.*

van der Put, A.G. and Bijsterbosch, B.H. (1983). "Electrokinetic Measurements on Concentrated Polystyrene Dispersions and Their Theoretical Interpretation." *Journal of Colloid and Interface Science,* 92(2), *499-507.*

Voeglti, L.P. and Zukoski, C.F. (1991). "Adsorption of Ionic Species to the Surface of Polystyrene Latexes." *Journal of Colloid and Interface Science,* 141, 92- 108.

Waypa, J.J., Wilkie, J.A., and Elimelech, M. "Removal of Arsenic from Water by Membrane Processes.:' *Proceedings of the 199.5 AWWA Annual Conference,* Anaheim, CA, June 18-22, 1995.

Westall, J. and Hohl, H. (1980). "A Comparison of Electrostatic Models for the Oxide Solution Interface." *Advances in Colloid and Interface Science,* 12,265.

Yoo, R.S., Brown, D.R., Pardini, R.J., and Bentson, G.D. (1995). "Microfiltration: A Case Study." *Journal of the American Water Works Association,* 87(3), *38-49.*

Zhu, X. and Elimelech, M. (in press). "Fouling of Reverse Osmosis Membranes by Aluminum Oxide Colloids." *Journal of Environmental Engineering.*

APPENDIX

Data Used to Construct Figures 11 through 30

Figure 11						LPPN__AB	
0.001 M NaCl						LPPN__A_	
4.9	0.4	-3.7	-6.5	-9.0	-10.3	-12.7	-14.1
5.6	1.1	-3.4	-6.1	-9.0	-11.0	-13.1	-14.5
4.9	0.7	-3.4	-6.5	-8.7	-10.6	-12.7	-14.1
5.7	1.1	-3.0	-6.1	-9.0	-11.3	-13.1	-14.5
4.9	0.7	-3.4	-6.5	-8.7	-11.0	-12.7	-14.1
5.7	1.4	-3.0	-6.2	-8.7	-11.3	-13.5	-14.5
5.3	0.9	-3.3	-6.3	-8.8	-10.9	-13.0	-14.3
0.01 M NaCl						LPPN__B_	
4.2	1.7	-3.4	-6.9	-8.6	-12.2	-15.7	-14.2
6.2	3.5	-1.7	-5.2	-8.6	-12.1	-15.7	*-16.0
4.2	1.7	-3.4	-6.9	-8.6	-12.1	-16.7	-14.3
6.2	1.7	-1.7	-5.2	-8.6	-12.1	-13.9	-14.3
4.2	0.0	-3.4	-6.9	-8.6	-12.1	-14.0	-14.3
6.2	0.0	-1.7	-5.2	-8.6	-12.1	-14.0	-14.3
5.2	1.4	-2.6	-6.0	-8.6	-12.1	-15.0	-14.3
* denotes a stray value that has been omitted							

Figure 12						HRPN__AB	
0.001 M NaCl						HRPN__A_	
-0.9	-1.5	-3.3	-5.1	-5.9	-6.7	-6.9	-7.7
-0.9	-1.5	-2.9	-5.1	-5.4	-6.2	-7.0	-7.7
0.0	-1.0	-3.4	-5.1	-5.9	-6.7	-7.0	-7.1
0.0	-1.0	-2.9	-4.6	-5.9	-6.2	-7.0	-7.7
0.0	-1.0	-2.9	-5.1	-5.9	-6.2	-7.0	-7.1
0.0	-1.5	-2.9	-4.6	-5.4	-6.2	-7.0	-7.7
-0.3	-1.2	-3.0	-4.9	-5.7	-6.4	-7.0	-7.5
0.01 M NaCl						HRPN__B_	
-2.3	-3.7	-3.7	-5.7	-7.7	-7.8	-9.9	*-10.2
2.3	-3.7	-3.7	-5.7	-7.6	-7.8	-9.9	-12.2
-2.3	-3.7	-3.7	-5.7	-7.6	-7.8	-9.9	-12.2
2.3	-3.8	-3.7	-5.7	-7.6	-7.8	-9.9	-12.2
2.3	-1.9	-3.7	-5.7	-7.6	-7.8	-9.9	-12.2
0.0	-1.9	-3.7	-5.7	-7.6	-7.8	*-7.9	-12.2
0.4	-3.1	-3.7	-5.7	-7.6	-7.8	-9.9	-12.2
* denotes a stray value that has been omitted							

Figure 13						NFPN AB	
0.001 M NaCl		-1.9				NFPN A	
6.0	-0.8	-1.9	-7.5 -7.5	-13.3	-17.3 -17.3	*-19.4	-23.5 -21.6
6.0	-0.8						
6.0	-0.8	-1.9	-7.51	-13.31	-17.3	-19.41	-21.61
6.0	0.0	-1.9	-7.5	-13.3	-17.3	-19.4	-23.5
6.0	0.0	0.0	-7.5	-13.3	-17.3	-19.4	-21.6
6.0	0.0	0.0	-7.5	-13.3	-17.3	-19.4	-23.5
6.0	-0.4	-1.3	-7.5	-13.3	-17.3	-19.4	-22.6
0.01 M NaCl						NFPN B	
7.0	7.4	3.3	-6.6	-13.2	-16.6	-20.0	-23.5
7.0	3.7	3.3	-6.6	-13.2	-16.6	-20.0	-23.5
7.0	7.4	-3.3	-6.6	-13.2	-16.6	-20.0	-23.5
7.0	3.7	0.0	-6.6	-13.2	-16.6	-20.0	-23.5
7.0	7.4	0.0	-6.6	-13.2	-16.6	-20.0	-23.5
7.0	3.7	0.0	-6.6	-13.2	-16.6	-20.0	-23.5
7.0	5.5	0.6	-6.61	-13.21	-16.6	-20.01	-23.5
* denotes a strav valuethathas been omitted							

Figure 14						CEPN AB	
0.001 M NaCl						CEPN A	
7.1	0.81	-3.5	-6.5	-12.7	-15.8	-17.1	-16.6
14.1	0.8	-4.2	-6.9	-12.3	-14.7	-15.61	-15.4
7.1	0.8	-3.19	-6.5	-13.0	-15.0	-17.1	-16.6
14.1	0.8		-6.9				-15.4
7.1	*1.7	-3.1	-6.5	-13.0	-15.41	-16.7	-16.61
14.1	0.8	3.9	-6.9	-12.3	-14.71	-15.6	-150
7.61	0.8	-3.61	-6.71	-12.61	-15.11	-16.31	-15.9
0.01 M NaCl						CEPN B	
9.3	2.2~	-1.8	-7.0	-12.2	-14.0,	-17.51	-16.0 -15.0
9.3	2.2,	-1.81	-7.01	-10.4	-14.0	-15.71	-14.2 -16.8
9.3	2.2~	-1.8)	-7.0	-12.2	-15.7'		-16.0 -16.8
0.0	2.2'	-1.8	-7.0	-10.4	-14.0,	-15.7	-14.2' -15.0
0.0	2.2	-1.8	-7.0	-12.2	-15.7	-15.7; '15.9~	-16.8
	*0.0			-104	-122'	15.7	-14 2 -16.8
4.6	2.2	-1.8	-7.7.0	-11.3	-14.3	-16.3	----- -15.1; -16.2
* denotes a stray value that has been omitted							

Figure 15						LPPC__AB	
0.0001 M CaCl2						LPPC__A_	
7.7	2.5	-0.5	-4.1	-6.3	-9.4	-10.2	-11.3
8.9	3.5	-0.2	-4.6	-7.1	-9.7	-10.8	-11.3
7.7	3.0	-0.2	-4.1	-6.6	-9.5	-10.3	-11.0
-0.5	3.5)		-4.6	-7.1	-9.7	-10.8	-11.3
8.3	3.0	0.0	-4.1	-6.6	-9.5	-10.6	-11.0
8.9	3.5	0.0	-4.6	-7.2	-9.8	-10.6	-11.3
8.4	3.2	-0.2	-4.3	-6.8	-9.6	-10.5	-11.2
0.0001 M CaCl2						LPPC__B_	
5.7	3.4	0.5	-2.2	-5.0	-6.8	-7.5	-7.4
8.6	4.0	0.5	-2.2	*-5.6	-6.8	-7.5	-7.5
5.7	3.4	1.1	-2.2	-5.0	-6.8	-7.5	-7.5
8.6	4.0	1.1	-2.2	-5.0	-6.8	-7.5	-7.5
6.7	3.4	0.0	-2.2	-5.0	-6.8	*-7.0	-7.5
8.6	4.6	0.0	-2.2	-5.0	-6.8	-7.5	-7.5
7.3	3.0	0.5	-2.2	-5.0	-6.8	-7.0	-7.5

* denotes a stray value that has been omitted

Figure 16						LPPCN_AB	
O-0001 M CaCl2						LPPCN_A_	
4.4	2.0	-3.9	-9.8	-13.7;	*-11.8	-13.8:	-16.2
4.4	5.9	-2.0	-7.8	-12.3	-13.7	-13.81	-16.2
4.4'	2.0	-3.9	-9.8	-13.7	-13.7	-13.8	-16.3
4.4	4.0	-2.0	-7.8	-11.7,	-13.7	*-11.9	-16.2
4.4	2.0	-3.9	-9.8	-13.7'	-13.7	-13.8	-16.3
4.4	4.0	-3.9	-7.8	-11.8	-13.7	-13.9	-16.3
4.4,	3.3	-3.3	-8.8	-12.8	-13.7	-13.8)	-16.3
0.001 M CaCl2						LPPCN_B_	
4.4	1.8	-5.3	-8.9	-10.71	-12.5	-14.4	-14.8
4.4	1.8,	-1.8	-7.1	*-8.9	-12.5	-14.4	-14.8
4.4	1.8	-3.5	-8.9	-10.7	-12.5	-14.3:	-14.8
4.4	0.0	-1.8	-7.1	-10.7	-12.5	-14.3	-14.8
4.4	0.0	-3.5	-7.1	-10.7	-12.5	-14.4	-14.8
4.4	0.0	-1.8	-7.1	-10.7	-12.5	-14.4	-14.8
4.4	0.91	-2.9	-7.7	-10.7	-12.5	-14.4'	-14.8

* denotes a stray value that has been omitted

Figure 17					HRPCN_AB		
0.0001 MCaCl2						HRPCN_A	
2.2	-3.6	-5.4	-7.3	-7.4	-11.3:	-9.5	-10.0
2.2	-3.6	-5.4	-7.3	-7.4	-9.4	-9.5	-8.0
2.2	-3.6	-5.4	-7.3	-9.3	-11.3	-7.6	-10.0
0.0	-3.6	-5.4	-7.3	-7.4	-9.4	-7.6	-8.0
0.0	-3.6	-5.4	-7.3	-9.3	-9.4	-9.5	-10.0
0.0	-3.6	-5.4	-7.3	-7.4	-9.4	-9.5	-8.0
1.1	-3.6	-5.4	-7.3	-8.0	-10.0	-8.9	-9.0
0.001 MCaCl2						HRPCN_B	
2.2	2.1	-4.1	-6.2	-6.3	-8.5	-8.6	-6.6
2.5	2.1	-4.1	-6.21	-6.3	-8.6	-8.6	-6.6
2.5'	0.0	-4.1	-6.2	-6.3	-8.5	-8.6	-6.6
0.0	0.0	-4.1	-6.2	-6.3	-8.6	-6.5	-6.6
0.0	0.0	-4.1	-6.3	-6.3	-8.5	-8.6	-6.6
0.0	0.0	-4.1	-6.2	-6.3	-8.5	-8.6	-6.6
1.2	0.7	-4.1	-6.2	-6.3	-8.6	-8.6	-6.6
* denotes a stray value that has been omitted							

Figure 18					NFPCN_AB		
0.0001 M CaCl2						NFPCN_A	
7.7	3.7	-6.6	-9.8	-16.5	-16.6	-16.6	-20.1
7.7	3.7	-6.6	-9.8	-13.2	-16.6	-16.6	-20.2
7.7	3.7	-3.3	-9.8	-13.2	-16.6	-19.9	-20.2
0.0	0.0	-6.6	-9.8	-13.2	-16.6	-16.6	-20.2
0.0	0.0	-3.3	-9.8	-16.5	-16.7	-20.0	*-16.8
0.0	0.0	-6.6	-9.8	-13 2	-16.71	-200	-202
3.8,	1.8	-5.5	-9.8	-14.3	-16.6	-18.3	-20.2
0.001 M CaC12						INFPCN_B	
7.8	0.0	3.5	-3.5	-10.6	-106	-14.2	-17.8
7.8	0.0	3.5	-3.5	-10.6,	-14.1:	-17.7	-17.9
7.8	0.0	0.0	-3.5	-14.1~	-10.6	-14.2~	-17.8
7.8	0.0	0.0	-3.5)	-10.6;	-14.1	-17.71	-17.8
7.8	0.0	0.0	-3.5;	-10.6	-10.6	-14.21	-14.3
*0.0	0.0	0.0	-3.5	-10.6	-14.1	-17.7	-14.3
7.8	0.0	1.2	-3.51	-10.6	---- -12.4,	-15.9	-16.7
* denotes a stray value that has been omitted							

Figure 19						CEPCN_AB	
0.0001 M CaCl2						CEPCN_A_	
8.1	-2.1	-3.6	-6.9;	-10.4	-12.1	-13.9	-14.1
8.1	2.1	-1.8	-5.2	-8.6	-12.1	-13.9	-14.1
8.1	2.1	-3.6	-6.9	-10.4	-12.1	-13.9	-14.1
0.0	2.1	-1.8	-5.2	-8.6	-12.1	-13.9	-14.1
0.0	0.0	-3.6	-6.9	-10.4	-12.1	-13.9	-14.1
0.0	0.0	-1.8	-5.2	-8.7	-12.1	-13.9	-14.1
4.0	0.7	-2.7	-6.0	-9.5	-12.1	-13.9	-14.1
0.001 M CaCl2						CEPCN_B_	
8.0	2.4	-2.0	-5.9	-7.8	-9.8	-9.8	-9.9
8.0	2.4	2.0	-2.0	-3.9	-5.9	-7.9	-7.9
8.0	2.4	-3.9	-5.9	-7.8	-9.8	-9.8	-9.9
0.0	0.0	-3.9	-2.0	-3.9	-5.9	-7.8	-7.9
0.0	0.0	0.0	-5.9	-7.8	-9.8	-9.8	-9.9
0.0	0.0	0.0	-2.0	-3.9	-5.9	-7.9	-7.9
4.0	1.2	-2.0	-3.9	-5.9	-7.8	-8.8	-8.9

Figure 20						LPPSN_AB	
0.0001 M Na2SO4						LPPSN_A_	
4.4	3.6	-3.5	-8.8	-10.6	-10.7	-12.4	-12.9
6.6	5.4	-3.5	-8.8	-10.6	-12.4	-14.2	-14.7
4.4	3.6	-3.5	-8.8	-10.61	-10.7	-14.2	-12.9
6.6	3.6	-3.5'	-8.0'	-12.3,	-12.4	-14.2	-14.7
4.4	1.8	-3.5	-8.8	-12.3;	-12.4,	-12.4	-12.9
6.6	3.6'	-3.5	-8.8'	-12.3	-12.4	-142	-14.7
5.5	3.6	-3.5	-8.8	-11.51	-11.8	-13.6	-13.8
0.001 M Na2SO4						LPPSN_B_	
4.8	2.0,	-4.0	-7.9	-10.0,	-14.1	-12.1	-14.5
4.8	4.1	-4.0	-8.0	-12.0	-14.01	-14.1	-16.6
4.8,	2.0	-4.0	-8.0	-10.0	*-12.1	-14.11	-14.5
4.8'	4.1	-4.0	-8.0	-10.01	-14.1;	-16.1'	-16.6
4.8	2.01	-4.01	-8.0	-10.0	-14.1,	-14.1	-14.5
*2.4	4.1	-4.0	-8.0	-121.	-14 . 11	-16 . 1	-16.6
- -4.8	3.1	-4.0	-8.0	-10.7	-14.11	14.4;	-15.6

* denotes a strav value that has been omitted

Figure 21						HRPSN_A_		
0.001 M CaCl2						HRPSN_A_		
40.8	*-7.2	*-4.9	*-4.2	-8.4	-14.1	-14.1	-21.2	-21.3
-20.4	0.0	-2.5	-6.3,	-8.4	-7.1	7.01	-7.1	-7.1
0.0	0.0	-2.5	-6.3	-8.4	-14.1	-14.1	-21.2	-14.2
0.0	0.0	-2.5	-6.3;	-8.4	-7.1	7.0	-7.1	-14.2
0.0	0.0	-2.5	-6.3	-8.4	-14.1	-14.1	-21.2	-21.3
0.0	0.0	-2.5	-6.3	-8.4	-7.1	7.0	-7.1	-7.1
3.4	0.0	-2.5	-6.3	-8.4	-10.6	-10.6	2	1 -14.2
* denotes a strav value that has been omitted								

Figure 22					NFPSN_AB		
0.0001 M CaCl2						NFPSN_A_	
7.8	3.7	*-3.4	-3.4	-10.2	-10.3	-17.3	-20.9
7.8	7.4	0.0	-6.8	-13.6	-13.7	-17.3	-24.4
7.8	3.7	0.0	-6.8	-6.8	-10.3	-17.3	-20.9
7.8	3.7	0.0	-6.8	-10.2	-13.7	*-20.8	-24.4
7.8	3.7	0.0	-3.4	-6.8	-10.3	-17.3	-20.9
7.8	0.0	0.0	-6.8	-10.2	-13.7	-17.3	-24.4
7.8	1.8	0.0	-5.6	-9.7	-12.0	-17.3	-22.7
0.001 M CaCl2						NFPSN_B_	
8.2	4.0	-3.7	-14.8	-7.4	-11.2	-18.9	-15.2
8.2	4.0	-3.7	-14.8	-14.9	-11.2	-18.9	-19.0
8.2	4.0	0.0	-14.8	-11.1	-11.2	-15.1	-15.2
8.2	4.0	0.0	-14.8	-11.2	*-14.9	-18.8	-15.2
8.2	4.0	0.0	-14.8	-11.1	-11.2	-15.1	-11.4
*0.0	*0.0	0.0	*-18.5	-11.1	-11.2	-18.9	-15.2
8.2	4.0	-1.2	-14.8	-11.2	-11.2	-17.6	-15.2
* denotes a stray value that has been omitted							

Figure 23						CEPSN_AB	
0.0001 M CaCl2						CEPSN_A_	
8.7	2.1	-1.7	-6.8	-10.1	-13.5	-13.6	-15.3
8.7	2.1	-1.7	-6.7	-13.5	-15.2	-17.0	-17.0
0.0	0.0	-1.7	-6.8	-10.2	-13.5	-13.6	-15.3
0.0	0.0	-1.7	-6.8	-13.5	-15.2	-17.0	-16.9
0.0	0.0	-1.7	-6.8	-10.1	-13.5	-13.6	-15.3
0.0	0.0	-1.7	-6.8	-13.5	-15.2	-17.0	-16.9
4.4	0.7	-1.7	-6.8	-11.8	-14.3	-15.3	-16.1
0.001 M CaCl2						CEPSN_B_	
-17.1	2.4	-2.1	-6.1	-10.1	-12.1	-14.2	-14.3
-18.8	2.4	-2.1	-8.1	-12.2	-14.2	-16.2	-16.4
-17.1	0.0	-2.1	-6.1	-10.1	-10.1	-12.2	-14.3
-18.8	0.0	-2.1	-8.1	-12.2	-14.2	-14.2	-16.4
-17.1	0.0	-2.1	-6.1	-10.1	-10.1	-12.2	-14.3
-18.8	0.0	-2.1	-8.1	-12.2	-14.2	-14.2	-16.4
-17.9	0.8	-2.1	-7.1	-11.2	-12.5	-13.9	-15.3

Figure 24						LPPHN_AB	
no humic acid						LPPN__B_	
4.2	1.7	-3.4	-6.9	-8.6	-12.2	-15.7	-14.2
6.2	3.5	-1.7	-5.2	-8.6	-12.1	-15.7	*-16.0
4.2	1.7	-3.4	-6.9	-8.6	-12.1	-16.7	-14.3
6.2	1.7	-1.7	-5.2	-8.6	-12.1	-13.9	-14.3
4.2	0.0	-3.4	-6.9	-8.6	-12.1	-14.0	-14.3
6.2	0.0	-1.7	-5.2	-8.6	-12.11	-14.61	-14.3
5.2	1.4	-2.6	-6.0	-8.6	-12.1	-15.0	-14.3
1 mg/l humic acid						LPPHN_A_	
-3.8	-7.5	-10.4	-14.8	-16.3	-16.4	-16.4	-15.3
-3.8	-7.5	-10.4	-16.2	-17.8	-19.3	-18.0	-18.3
-3.8	-7.5	-10.4	-14.8	-16.3	-16.3	-16.4	-15.3
-3.8	-7.6	-10.4	-16.2	-17.8	-17.8	-18.0	-18.4
-3.8	-7.5	-10.4	-14.8	-16.3	-16.3	-16.4	-15.4
*-5.7	-7.6	*-11.9	-16.3	-17.8	-17.8	-17.9	-18.4
-3.8	-7.5	-10.4	-15.5	-17.1	-17.3	-17.2	-16.9
10 ma/l humic acid						LPPHN B	
-4.1	-8.4	-11.5	-14.8	-11.4	-14.9,	-14.9	*-13.5
-4.1	-8.4	-13.2	-14.8	-13.1	-16.6	-16.61	-15.3
-6.2;	-8.41	-13.21	'-13.21	-14.8	-14.9,	-15.0~	-15.3
-6.2	-10.1	-13.2	-14.8	-14.8	-16.61	-16.6'	-15.3
-6.2	-10.1	-13.2	-14.8	-14.9	-14.9	-14.9'	-15.3
-4.1	-8.4	-13.2	-14.8	-14.9	-16.6	-16.6	-15.3
-5.2	-9.0	-13.2	-14.8	-14.9	-15.7	-15.8	-15.3
* denotes a strav value that has been omitted							

Figure 25						NFPHN_AB	
no humic acid						NFPN__B_	
7.0	7.4	3.3	-6.6	-13.2	-16.6	-20.0	-23.5
7.0	3.7	3.3	-6.6	-13.2	-16.6	-20.0	-23.5
7.0	7.4	-3.3	-6.6	-13.2	-16.6	-20.0	-23.5
7.0	3.7	0.0	-6.6	-13.2	-16.6	-20.0	-23.5
7.0	7.4	0.0	-6.6	-13.2	-16.6	-20.0	-23.5
7.0	3.7	0.0	-6.6	-13.2	-16.6	-20.0	-23.5
7.0	5.5	0.6	-6.6	-13.2	-16.6	-20.0	-23.5
0.2 mg/l humic acid						NFPHN_A_	
0.0	-6.2	-9.8	-16.2	-19.4	-19.4	-22.7	-19.4
0.0	-6.2	-9.8	-16.2	-16.2	-19.4	-19.5	-19.5
0.0	-6.2	-9.8	-16.2	-19.4	-19.4	-22.7	-19.5
0.0	-6.2	-9.7	-12.9	-16.2	-19.4	-19.5	-19.4
0.0	-6.2	-9.7	-16.2	-19.4	-19.4	-22.7	-19.4
0.0	-6.2	*-6.5	-12 9	-19.4	-19.4	.-19.5	-19.4
0.0	-6.2	-9.8	-15.1	-18.3	-19.4	-21.1	-19.4
2 mg/l humic acid						NFPHN_B_	
-7.8	-7.8	-9.6	-15.7	-18.8	-22.0	-22.0'	-22.1
--- -7.8	-7.8	-9.6	-12.6	-18.8	-18.9	-22.0	-22.1
-7.8	-7.8	-9.6	-15.7	-18.8	-22.01	-22.0	-22.1
0.0	-7.8	-9.6	-12.5	-18.8	-18.9	-22.01	-19.0
0.01	-7.81	-9.6	-15.7	-18.8	-22.0'	-22.0	-22.1
0.0	-7.8	-9.6	-12 6	-18.8	-18.9	-18.81	-19.0
-3.91	-7.8	-9.6	-14.1	-18.8	-20.5	-22.0'	-21 .I
. denotes a stray value that has been omitted							

Figure 26						CEPHN_AB		
no humic acid						CEPN__B_		
9.3	2.2	-1.8	-7.0	-12.2	-14.0	-17.5	-16.0	-15.0
9.3	2.2	-1.8	-7.0	-10.4	-14.0	-15.7	-14.2	-16.8
9.3	2.2	-1.8	-7.0	-12.2	-15.7	-17.5	-16.0	-16.8
0.0	2.2	-1.8	-7.0	-10.4	-14.0	-15.7	-14.2	-15.0
0.0	2.2	-1.8	-7.0	-12.2	-15.7	-15.7	-15.9	-16.8
0.0	*0.0	-1.8	-7.0	-10.4	-12.2	-15.7	-14.2	-16.8
4.6	2.2	-1.8	-7.0	-11.3	-14.3	-16.3	-15.1	-16.2
0.2 mg/l humic acid						CEPHN_A_		
0.0	-6.2	-8.3	-12.3	-16.5	-16.5	-16.4	-16.5	
0.0	-6.2	-4.2	-8.2	-12.3	-12.4	-12.3	-12.4	
0.0	-6.2	-8.3	-12.3	-16.5	-16.5	-16.4	-16.5	
0.0	-6.2	-4.2	-8.2	-12.3	-12.4	-12.3	-8.3	
0.0	-6.2	-8.3	-12.4	-16.5	-16.5	-16.4	-12.4	
0.0	*-4.1	-4.2	-8.3	-12.3	-12.4	*-8.2	-8.3	
0.0	-6.2	-6.3	-10.3	-14.4	-14.4	-14.8	-12.4	
2 mg/l humic acid						CEPHN_B_		
-8.2	-10.2	-13.3	-16.5	-19.8	-19.8	*-19.8	-16.5	
-8.2	-8.1	-13.3	*-9.9	-13.2	-16.5	-13.2	-13.2	
-8.2	-10.2	-13.3	-16.5	-19.8	-19.8	-16.5	-16.5	
-8.2	-8.1	-13.3	-13.2	-13.2	-13.2	-13.2	-13.2	
-8.2	-10.2	-13.3	-16.5	-19.8	-19.8	-16.6	-16.5	
-8.2	-8.1	*-10.0	-13.2	-13.2	-13.2	-13.2	-13.2	
-8.2	-9.1	-13.3	-15.2	-16.5	-17.0	-14.5	-14.9	
* denotes a stray value that has been omitted								

Figure 27						LPPDN_AB	
no SDS						LPPN__B_	
4.2	1.7	-3.4	-6.9	-8.6	-12.2	-15.7	-14.2
6.2	3.5	-1.7	-5.2	-8.6	-12.1	-15.7	*-16.0
4.2	1.7	-3.4	-6.9	-8.6	-12.1	-16.7	-14.3
6.2	1.7	-1.7	-5.2	-8.6	-12.1	-13.9	-14.3
4.2	0.0	-3.4	-6.9	-8.6	-12.1	-14.0	-14.3
6.2	0.0	-1.7	-5.2	-8.6	-12.1	-14.0	-14.3
5.2	1.4	-2.6	-6.0	-8.6	-12.1	-15.0	-14.3
0.00001 M SDS						LPPDN_A_	
2.0	-1.6	*-6.4	-12.8	-12.8	-14.3	-17.8	-16.9
2.0	-1.6	-8.0	-12.8	-12.8	-17.6	-19.4	-18.6
2.0	0.0	-8.0	-12.8	-12.8	-17.6	-17.8	-16.9
2.0	0.0	-8.0	-12.8	-14.4	-19.3	-17.8	-18.5
0.0	0.0	-8.0	-12.8	-14.4	-17.7	-16.2	-16.8
0.0	0.0	-8.0	-12.8	-16.1	-17.7	-19.4	-18.5
1.3	-0.5	-8.0	-12.8	-13.9	-17.4	-18.1	-17.7
0.0001 M SDS						LPPDN_B_	
-14.3	-14.8	-19.4	-21.0	-21.0	-22.7	-21.3	-20.6
-14.3	-14.8	-19.4	-20.9	-22.7	-22.6	-23.0	-24.0
-14.3	-14.9	-19.3	-20.9	-21.0	-21.1	-21.3	-20.6
-14.3	-14.8	-19.4	-20.9	-21.0	-22.6	-22.9	-24.0
-14.3	-14.8	-19.4	-20.9	-21.1	-21.1	-21.3	-20.6
-14.3	-14.8	-19.4	-20.9	-21.0	-22.6	-22.9	-24.1
-14.3	-14.8	-19.4	-20.9	-21.3	-22.1	-22.1	-22.3
* denotes a stray mark that has been omitted							

Figure 28						CEPDN_AB		
no SDS						CEPN__B_		
9.3	2.2	-1.8	-7.0	-12.2	-14.0	-17.5	-16.0	-15.0
9.3	2.2	-1.8	-7.0	-10.4	-14.0	-15.7	-14.2	-16.8
9.3	2.21	-1.81	-7.01	-12.21	-15.7	-17.5	-16.0	-16.8
0.0	2.2	-1.8	-7.0	-10.4	-14.0	-15.7	-14.2	-15.0
0.0	2.2	-1.8	-7.0	-12.2	-15.7	-15.7	-15.9	-16.8
0.0	*0.0	-1.8	-7.0	-10.4	-12.2	-15.7	-14.2	-16.8
4.6	2.2	-1.8	-7.0	-11.3	-14.3	-16.3	-15.1	-16.2
0.00001 M SDS						CEPDN_A_		
-9.3	-4.1	-7.2	-10.7	-17.7	-17.7	-17.9	-18.0	
-9.3	-4.1	-3.6	-7.1	-10.6	-14.2	-17.8	-18.0	
0.0	-4.1	-7.2	-10.7	-17.7	-17.8	-17.9	-18.0	
0.0	0.0	-3.6	-7.1	-10.6	-14.2	-17.9	-18.0	
0.0	0.0	-7.2	-10.7	-17.8	-17.8	-17.8	-18.0	
0.0	0.0	-3.6	-7.1	-10.6	-14.2	-17.8	-18.0	
-3.1	-2.0	-5.4	-8.9	-14.2	-16.0	-17.8	-18.0	
0.0001 M SDS						CEPDN_B_		
-18.81	-12.01	-14.41	-10.6	-10.71	-7.1	-3.6	-32.4	
-18.8	-12.0	-14.4	-21.3	-28.5	-28.6	-28.6	-32.4	
-18.8	-12.01	-14.41	-10.61	-10.7;	-7.1	-28.6	-32.4	
-18.8	-12.01	-14.41	-21.31	-25.01	-28.61	-28.6	0.0	
-18.8	-12.0	-14.4	-14.2	-10.7	-7.1	0.0	0.0	
-18.8	-12.01	-14.4	-20.3	-25.0	-28.6	0.0	0.0	
-18.8	-12.01	-14.4;	-16.5	-18.41	-17.91	-14.9	-16.2	
. denotes a stray value that has been omitted								

Figure 29						HRCLENAC	
uncleaned (old)						HRPN_B	
-2.3	-3.7	-3.7	-5.7	-7.7	-7.8	-9.9	*-10.2
2.3	-3.7	-3.7	-5.7	-7.6	-7.8	-9.9	-12.2
-2.3	-3.7	-3.7	-5.7	-7.6	-7.8	-9.9	-12.2
2.3	-3.8	-3.7	-5.7	-7.6	-7.8	-9.9	-12.2
2.3	-1.9	-3.7	-5.7	-7.6	-7.8	-9.9	-12.2
Q&i-	-1.9	-3.7	-5.7	-7.6	-7.8	*-7.9	-12.2
0.4	-3.1	-3.7	-5.7	-7.6	-7.8	-9.9	-12.2
uncleaned (new)						HRPN_C_	
0.0	-2.2	-7.2	-3.6	-3.6	-3.6	-3.6	-3.6
0.0	-2.2	-3.6	-3.6	-3.6	-7.2	-3.6	-3.6
0.0	-2.2	-3.6	-3.6	-3.6	-3.6	-3.6	-3.6
0.0	0.0	-3.6	0.0	0.0	-7.2	-3.6	-3.6
0.0	0.0	0.0	0.0	0.0	-3.6	*-7.2	0.0
0.0	0.0	0.0	0.0	0.0	0.0	-3.6	0.0
0.0	-1.1	-3.0	-1.8	-1.8	-4.2	-3.6	-2.4
DI cleaned						HRCLENA_	
0.0	-4.5	-4.1	-8.1	-8.1	-8.1	-12.3	-12.4
0.0	-4.5	-4.1	-4.1	-8.1	-8.1	-8.2	-8.3
0.0	-4.5	-4.1	-8.1	-8.1	-12.2	-12.3	-12.4
0.0	0.0	-4.1	-4.1	-8.1	-8.1	-8.2	-8.3
0.0	0.0	-4.1	-8.11	-8.1	-12.2	-12.21	-12.4
0.0	0.0	-4.1	-8.1	-8.1	-8.1	-8.1	-8.3
0.0	-2.2	-4.1	-6.8	-8.1	-9.5	-10.2	-10.3
acid cleaned						HRCLENB_	
0.0	-2.4	-4.31	-6.4	-6.4	-8.5	-8.6	
0.0,	-2.4,	-2.2	-4.3	-6.4	-6.4	-6.4	
0.0	-2.4	-4.3	-6.4	-6.4'	-8.5	-8.6	
0.0	0.0	-2.2	-4.3	-6.4	-6.4	-6.4	
0.0	0.0	-4.3	-6.4	-6.4	-8.5	-8.6	
0.0	0.0	-2.2	-4.2	-6.4	-6.4	-6.4	
0.0	-1.2	-3.2	-5.3	-6.4	-7.5	-7.5	
base cleaned						HRCLENC_	
0.0	0.0	-3.8	-3.8	-7.5	-7.5	-7.6	-7.6
0.0	0.0	-1.9	-3.8	-3.8	-5.7	-5.7	-5.7
0.0	0.0	-3.8	*-5.7	-5.6	-7.6	-7.6	-7.6
0.0	0.0	-1.9	-3.8	-5.6	-5.7	-5.7	-5.7
0.0	0.0	-3.8	-3.8	-5.6	-7.5	-7.6	-7.6
0.0	0.0	-1.9	-3.8	-5.6	-5.7	-5.7	-5.7
0.0	0.0	-2.9	-3.8	-5.6	-6.6	-6.6	-6.7

* denotes a stray value that has been omitted

Figure 30

CECLENAF

uncleaned

CEPN__B_

9.3	2.2	-1.8	-7.0	-12.2	-14.0	-17.5	-16.0
9.3	2.2	-1.8	-7.0	-10.4	-14.0	-15.7	-14.2
9.3	2.2	-1.8	-7.0	-12.2	-15.7	-17.5	-16.0
0.0	2.2	-1.8	-7.0	-10.4	-14.0	-15.7	-14.2
0.0	2.2	-1.8	-7.0	-12.2	-15.7	-15.7	-15.9
0.0	*0.0	-1.8	-7.0	-10.4	-12.2	-15.7	-14.2
4.6	2.2	-1.8	-7.0	-11.3	-14.3	-16.3	-15.1

DI cleaned-

CECLENA_

8.4	4.1	-7.2	-10.8	-14.5	-14.5	-18.1	-18.1
8.4	4.1	-3.6	-3.6	-10.8	-10.81	-10.9	-14.5
8.4	4.1	-7.2	-10.8	-14.5	-14.5	-18.1	-18.2
8.4	0.0	-3.6	-3.6	-10.8	-10.9	-10.9	-10.9
8.4	0.01	-3.6	-10.8	-14.51	-14.51	-18.1	-18.21
*0.0	0.0	-3.6	-3.6	-10.81	-10.9	-10.9	-10.9
8.4	2.0	-4.8	-7.21	-12.61	-12.7	-14.51	-15.1

DI cleaned (6 hours)

CECLENB_

-8.7'	0.0	0.0	0.0	-4.8	-4.8	-4.8	-4.8
-8.7	0.0	0.0	0.0	-4.8	-4.8	-4.8	-4.8
0.01	0.0	0.0	0.0	-4.8	-4.8	-4.8	-4.8
0.0	o.oi	0.0	0.0	0.01	-4.8;	-4.8	0.0
0.0	0.0	0.0	0.0	0.0	-4.8	-4.8	0.0
0.0	0.0	0.0	0.0	0.0	-4.8	-4.8	0.0
-2.9	0.0	0.0	0.0	-2.4	-4.8	-4.8	-2.41

DI cleaned (0 hours)

CECLENC_

7.7	3.5	-3.1	-6.5	-13.0	-13.1	-13.1	-13.31
7.7	3.5	-3.1	-3.3	-9.8	-13.1,	-13.1	-13.3
7.71	3.5	-3.1	-6.5	-13.0	-13.1	-13.1	-13.3
0.0	0.0	0.0	-3.3	-9.8	-13.1	-13.1	-13.3
0.0	0.0	0.0	-6.5	-9.8	-13.11	-13.11	-13.3
0.0	0.0	0.0	-3.3	-9.8	-13.1	-13.1'	-133
3.8	1.8	-1.6	-4.9	-10.8'	-13.1	-13.1	-13.3

Figure 30 (continued)

CECLENAF

acid cleaned

CECLEND_

8.8;	3.8~	-3.4	-6.6	-13.3	-13.3;	-16.7'
8.8	3.8;	-3.4	-3.31	-10.0	-10.0	-10.0
8.8	3.8	-3.4	-6.61	-13.31	-13.31	-16.7'
0.0	0.0	-3.4	-3.3	-10.01	-10.0	-13.3'

0.0	0.0	0.0,	-6.6	-13.3	-13.3	-16.6	
0.0	0.0	0.0	-3.3;	-10.0	-10.0	-13.3	
4.4	1.9	-2.3	-5.0	-11.6	-11.61	-14.4	
base cleaned						CECLENE_	
8.4	3.9	3.5	-3.4	3.4	3.4	-3.4	-6.8
8.4	7.8	3.5	3.41	-3.4	3.4	-3.4	-3.4
8.4	3.9)	3.5	3.41	-3.4	3.4	-6.8	-6.9
0.0	7.8	0.0	3.4	0.0	3.4	-3.4	-3.4
0.0	3.9:	0.01	0.0	0.0	0.0	-6.9	0.0
0.0	7.8	0.0	0.0	0.0	0.0	-3.4	0.0
4.2	5.8	1.8;	1.1'	-0.6	-2.3	-4.6	-3.4
base cleaned (repeat)						CECLENF_	
7.0	3.6	-3.2	-6.2	-9.4	-12.5	-12.6	-12.6
7.8	3.6	3.2	-6.3	-6.3	-6.3	-9.4	-9.5
7.0	3.6	-3.2	-6.3	-9.4	-12.5	-12.6'	-12.6
0.0	0.0	3.2	0.0	-3.1	-6.3	-9.4	-9.5
0.0	0.0	-3.2	0.0	-9.4	-9.4	-12.5	-12.6
0.0	0.0	3.3'	0.0	-6.3	-6.3	-9.4	-9.4
3.9	1.8	0.0;	-3.1'	-7.3	-8.9	-11.0	-11.0
* denotes a strav value that has been omitted							

Mission

The mission of the Bureau of Reclamation is to manage, develop, and protect water and related resources in an environmentally and economically sound manner in the interest of the American Public.